University of Notre Dame

2017 - 2018

Notre Dame Rocketry Team

Critical Design Report

NASA Student Launch 2018

Deployable Rover and Air Braking System Payloads

Submitted January 12, 2017

365 Fitzpatrick Hall of Engineering

Notre Dame, IN 46556

Table of Contents

1 Summary of CDR Report

1.1 Team Summary

Team Name:	Notre Dame Rocketry Team
	365 Fitzpatrick Hall of Engineering
	Notre Dame, IN 46556
NAR Mentor:	Dave Brunsting, NAR/TAR Level 2
	dacsmema@gmail.com or (269) 838 - 4275
NAR/TRA Section:	TRA #12340, Michiana Rocketry

1.2 Launch Vehicle Summary

1.2.1 Size and Mass

A summary of the launch vehicle size and mass are shown in Table XX below. These parameters were established using CREO and OpenRocket models of the launch vehicle. The chosen variable diameter design allows room for the rover payload without adding the excess weight that a single larger diameter design would while still maximizing the effectiveness of the air braking system. It was determined that a length of 124.5 inches was necessary to adequately fit the propulsion system, recovery system, and both payloads.

Table 1. Launch Vehicle Size and Mass Parameters

Property	Dimension
Length (in)	128
Fore Outer Diameter (in)	7.675
Fore Inner Diameter (in)	7.515
Aft Outer Diameter (in)	5.54
Aft Inner Diameter (in)	5.38
Number of Fins	4
Fin Span (in)	7.2
Loaded Weight (oz)	773
Weight without Motor (oz)	622

1.2.2 Final Motor Choice

The Cesaroni L1395-BS (blue streak) has been selected as the final motor choice. Important parameters for this motor are shown below in Table 2. With the current vehicle mass and size, OpenRocket is predicting an altitude for this motor of 5513 feet when in 10 mph winds and standard atmospheric conditions. This is well above the target altitude, but within the altitude range for the Air Braking System to lower the vehicle to the desired 5280 feet. This higher apogee also allows for any unforeseen increases in weight or drag during construction. If the weight does not change, ballast can be added to lower the projected altitude to a more manageable amount for the Air Braking System.

Table 2. Cesaroni L1395-BS Motor Characteristics

Property	Dimension
Peak Thrust (lbf)	400.5
Average Thrust (lbf)	314
Total Impulse (lbf*s)	1101

1.2.3 Rail Size

The launch pad's rail, the main interface between the rocket and the ground, will be 12-feet long and 1.5 inch wide. Simulations with this rail length and the selected motor show an off rail velocity of 69.4 ft/s, which is safely above the minimum required velocity of 52 ft/s. The body tube will be attached to the rail by two large rail buttons (0.63 inch diameter), which will be located at the rear end of the rocket and screwed into small wooden blocks attached directly to the fin can of the launch vehicle. These blocks will extend 1.3 inches from the fin can to keep the variable diameter portion of the launch vehicle separated from the launch rail during take-off. The drag tabs of the Air Braking System will not deploy until after burnout and thus will not affect the location of the rain buttons.

1.2.4 Recovery Subsystem

The recovery subsystem is a dual deployment system consisting of a drogue parachute to be released at apogee and a main parachute to be released at 600 feet above ground level. When the charges are detonated, the rocket will separate into three tethered sections. The deployment of these black powder charges will be controlled by a system of redundant altimeters to ensure accuracy. A GPS module will track the vehicle so recovery can be made easier.

1.3 Payload Summary

The deployable rover payload will contain an autonomously driven rover that is deployed via ejection charges and controlled by a ground station upon safe landing. The rover will detect the sections of the rocket and any other obstacles via a LiDAR sensor, Bluetooth chips and GPS. The rover will drive at least five feet away from the rocket and deploy two sets of folded solar panels. The solar panels will be actuated via a servomotor. During the flight of the rocket, the rover will be secured to prevent any motion that could alter the flight path of the rocket. The

servomotor that controls the solar panels will also be used to secure the rover by pinning it in place using the solar panel racks.

The purpose of the air braking system is to alter the flight of the rocket and bring it to an apogee of 5280 feet. The system is comprised of three overarching components, an aerodynamic component, a mechanical component, and an electronic component. Each of these three components are composed of different parts and interact with the others to achieve the required apogee. The vehicle design team has selected a motor that will overshoot the target apogee if the flight is unaltered and the air braking system will induce an additional drag force on the rocket to reduce the predicted unaltered apogee to the target apogee. The entire system fits inside the coupler between the fin can and the main body tube, with the aerodynamic component exterior to the rocket body and placed just forward of the fins.

2 Changes Made Since PDR

2.1 Vehicle Criteria

There have been a few design changes made to the launch vehicle since the Preliminary Design Review.

First, the length of the recovery payload body tube has been increased to 48 inches. This increase is due to size constraints set by the large 12 inch parachute, and the need for a longer packing length in the body tube, in which it is stored.

Second, the weight of the rocket has decreased from 40.4 lbs to 38.81 lbs. This decrease is due to the finalization of weights in the individual payloads. All payloads were under the weights allotted to them at the beginning of the design phase, and this change is weight is welcome, as it allows for a firm finalization of the motor. If needed, ballast will be used in order to control predicted un-braked apogee. The change in weight also changed the predicted stability in powered flight from 3.07 to 2.71. This decrease is also welcome, as it decreases the impact of wind gusts on the flight while maintaining a comfortable cushion above the competition stability requirement of 2.0.

Finally, in depth computation fluid dynamic analysis of the structure of the rocket was downgraded on the team's list of priorities. Initial CFD analysis, subsequent wind tunnel testing, and subscale flights led the team to believe that a more detailed CFD analysis was not as crucial as initially thought. While the process is still underway, it will only be completed if time permits.

2.2 Recovery Criteria

Since PDR, no major changes have been made to the Recovery System. All major components have been purchased and shipped, allowing construction and testing to begin

promptly following CDR. Small hardware items such as screws and electrical connectors will be purchased on an as-needed basis since unforeseen construction constraints and breakthroughs are expected. Since the essential concept of the CRAM v4 follows in the footsteps of previous version, but with significant material and redundancy improvements, no major obstacles are expected going forward.

2.3 Deployable Rover Criteria

Since the PDR the most significant change has been the replacing the material of the body of the rover. Initially the body was going to be machined from a block of aluminum, but in the interest of weight, cost and ease of manufacturing, High-Density Polyethylene (HDPE) will instead be used. The techno router available in the workshop located in Stinson 214 will be used to customize the block of HDPE into the desired design. This material will be strong enough to handle the loads placed on the rover while also reducing the weight of the payload.

Another change is the power source of the payload. The rover will now use six IMREN 18650 3000 mAh High Drain Batteries. This new battery was chosen over the initially selected battery, the Tracer 12V 8Ah Lithium Polymer Battery Pack, in order to reduce the weight of the rover and therefore the entire payload. The new batteries are also smaller and in turn fit on the rover in a more practical manner.

Further consideration into the deployment of the rover led to the addition of spring-loaded ramps at the end of the four tracks inside the body tube of the rocket. These ramps will prevent the rover from bottoming out while driving out of the body tube.

A final change since the PDR is the addition of Bluetooth chips throughout the rocket in order to provide a more robust method of locating each section of the rocket once the rover is driving on the launch field. The payload will still use the GPS as discussed in the PDR.

2.4 Air Braking System Criteria

There have been no changes made to the payload criteria. The goal of the system is to control the reduction in apogee of the rocket to hit a target of 5280 feet. It will do this without inducing any destabilizing forces or moments that could negatively affect the flight of the rocket or cause a crash. It will also be reusable upon landing, meaning it will not malfunction or break during the rocket's flight and landing.

2.5 Project Plan Criteria

The project plan has been improved in terms of the testing and requirements compliance. Verifications have been specified and described in further detail than in the preliminary design report. The testing and verification plans have been specified in each sub-team's sections. While each sub-team has remained in very close proximity to their given budgets, the travel budget has highly increased due to a new travel policy implemented this year by the University of Notre

Dame. For this reason, the Notre Dame Rocketry Team is currently working with the university administration to fully fund the travel costs. Scheduling has remained the same as that of the preliminary design report, as this year the team is following a stricter schedule so as to allow extra time for testing prior to the competition launch.

3 Vehicle Criteria

3.1 Design and Verification of Launch Vehicle

3.1.1 Mission Statement

The mission is to successfully design, construct and launch a rocket carrying a deployable rover to exactly an altitude of 5,280 feet above ground level. An air braking system consisting of four drag tabs deployed at various altitudes depending on flight conditions will ensure success in meeting the altitude requirement. The rover contained in a section directly below the nose cone will deploy upon landing. The recovery systems will allow the rocket to separate into three sections and deploy both a drogue and a main parachute to secure a safe descent. The vehicle and its payloads must be reusable on the same day without need for repairs or modifications. The team also will make an impact on the local community of South Bend and Notre Dame through educational events and media presence.

3.1.2 Mission Success Criteria

Several conditions must be met for the mission to be considered a success. The following criteria have remained constant, and are the team's main design drivers throughout this process and will be considered in all future design changes and verification models.

The dominant criteria for a successful mission are:

1. *Altitude*: The vehicle must reach an apogee of as close to 5280 feet as possible. Success of this criterion will be determined based on readings from an altimeter onboard the rocket. A desirable range is 5280 ± 100 feet, or 5180-5380 feet.

2. *Stability*: The rocket must maintain an acceptable degree of stability, minimum of 2, for the duration of its flight. Stability is determined theoretically with OpenRocket and RockSim models.

3. *Structural Integrity*: The vehicle must remain intact for the duration of its flight. Each component of the rocket from the motor retention and the internal bulkheads to the drag

tabs on the air braking system and the onboard rover must survive the flight without compromise.

4. *Recovery*: The vehicle must be reusable upon recovery without requiring repairs. Success in recoverability is predicted by the kinetic energy of each section upon landing based on simulation data. Recoverability of the rocket will be determined based on the condition of each component after the rocket lands.

5. *Rover Payload*: The rover payload must safely deploy from the internal structure of the launch vehicle when remotely triggered after landing, move 5 feet away from all rocket components, and deploy a set of foldable solar cell panels. Success of the rover payload is determined by GPS coordinates before and after movement and by the level of solar charge on the panels.

Air Braking System: The air braking system must successfully deploy its four drag tabs based on conditions of flight in order to slow the rocket to reach the goal apogee. Success of the air braking system will be determined based on the difference between the apogee of the rocket and the onboard computers logging servo motor actions.

3.1.3 Mission Requirements and Verifications

Requirement:	Requirement will be met by:	Method of Verification:
The launch vehicle will hit an apogee of 5280 feet.	-Making a motor choice that provides the launch vehicle with enough thrust to overcome its mass. -Constructing a launch vehicle that minimizes drag by utilizing a smooth surface	-The Subscale Test on Dec. 2nd provided initial comparisons for predictive programs and actual results -Full Scale Tests in Feb. 2018 will verify predictions as well as effect of the Air Braking System on the vehicle's apogee.
The launch vehicle shall carry one commercially available, barometric altimeter.	-Attaching the altimeter to the launch vehicle within the recovery system.	-The recovery sub-team lead has ensured that the recovery system of the launch vehicle

		includes a barometric altimeter.
The launch vehicle shall be recoverable and reusable.	-Ensuring with extensive testing that each sub-system (the recovery system especially) performs both individually and integrated with every other system. -Designing the vehicle to launch safely more than once.	-The tests outlined Section 3.6 will verify the performance of each sub-system individually. -Full Scale Tests will verify the performance of the vehicle as a whole; an evaluation of the vehicle following these tests will verify its ability to launch again successfully.
All recovery electronics shall be powered by commercially available batteries.	-Ensuring that the recovery system is designed to include only commercially available batteries.	-Vehicle has been designed to include the appropriate batteries.
The launch shall be limited to a single stage and four (4) independent sections	-Ensuring that the launch vehicle only requires one launch stage and that it includes the necessary amount of sections.	-The motor has been chosen so that the vehicle reaches apogee with only one stage. -The launch vehicle has been designed to have three (3) independent sections. -The launch vehicle used during the Full Scale Tests will be confirmed as having three (3) independent sections.
The launch vehicle shall be capable of being prepared for launch in 4 hours.	-Integrating all of the vehicle's subsystems in such a way that allows for assembly within the required time.	-Procedural checklists have been created to streamline the vehicle assembly process with minimal error -During the Full Scale Tests in Feb. 2018, the team will assemble the launch vehicle and have it prepared for launch within the proper time frame.

The launch vehicle shall be launched using a 12-volt direct firing system.	-Ensuring that the vehicle design includes the required 12-volt direct firing system.	-During the Full Scale Tests in Feb. 2018, the team will use the required firing system to launch the vehicle.
The launch vehicle shall require no special ground equipment to initiate launch.	-Designing the launch vehicle to successfully launch without the aid of any special equipment.	-The vehicle has been designed to launch using only the required igniter and supplied firing system -During the Full Scale Tests in Feb. 2018, the team will launch the vehicle without utilizing any special equipment.
The launch vehicle shall use a commercially available motor.	-Choosing a motor in alignment with the NAR and TRA regulations. -Staying in contact with the team's mentor regarding any updates to motor choices as the vehicle design changes.	-A commercially available motor has been chosen that aligns with NAR and TAR regulations. -The teams mentor has been contacted about motor and design choices. -During the Full Scale Tests in Feb. 2018 and on the day of the competition, the mentor of the team will handle all motors.
The minimum velocity off the rail shall not be below 52 ft/s.	-Selecting a motor with the right impulse to achieve the required velocity. -Meticulously calculating interruption angles for rail buttons to ensure that the launch vehicle's interaction with the launch pad is smooth and uninterrupted.	-Simulations using OpenRocket and RocketSim have verified that the rocket will have an off-rail velocity greater than 52ft/s. -Full Scale Tests in Feb. 2018 will in turn verify the accuracy of the above simulations and confirm the velocity.
The team shall launch and recover a subscale.	-The team will construct and launch a subscale, the specifications and materials	-Subscale successfully launched and recovered on Dec. 2nd.

	of which are outlined in Section 3.2.1 and Section 3.1.7.2.2, respectively.	
The launch vehicle shall have a static stability of at least 2.0 at rail exit.	-Placing the Air Braking System slightly above the center of pressure so that the deployment of tabs in flight does not cause over-stability when deployed -Ensuring that necessary ballasts are spread across the launch vehicle so as not to affect the stability margin	-The pre and post burnout positions of the Center of Gravity and Center of Pressure have been predicted using OpenRocket and Rocksim. - Full Scale Tests in Feb. 2018 will verify the accuracy of the simulations and ensure that the vehicle achieves the proper stability margin.
The launch vehicle shall have a sufficient thrust-to-weight ratio to achieve required apogee.	-Choosing a motor that provides the proper amount of thrust to overcome the weight of the launch vehicle.	-OpenRocket and RockSim simulations have verified the thrust-to-weight ratio provided by the motor choice. -Full Scale Tests in Feb. 2018 will verify the accuracy of these simulations in reaching the required apogee.
The launch vehicle shall contain a remotely activated rover which will autonomously travel five feet and deploy a set of foldable solar panels.	-Designing, constructing, and deploying the Rover Payload system, the specifications of which are included in section 5.1	-Full Scale Tests in Feb. 2018 will verify the ability of the Rover Payload system to deploy successfully.
Payload affecting flight shall be verified before launch at competitions	- Confirming the effect of Air Braking System's tabs on flight path compared to lack thereof - Confirming the structural strength of Payload Integration - Confirming the efficacy of Payload in a practical sense	- Subscale Flight successfully completed on Dec. 2nd, significant decrease in apogee linked to Air Braking Tabs. - FEM Analysis and Load analysis. - Full Scale Flights in Feb. 2018.

Launch Vehicle's subsystems shall have finished the design phase; Subscale will have been launched by CDR	- Ensuring each subsystem fits in with the overall system and can be edited at short notice. - Designing and launching a subscale that will verify the accuracy of our software prediction for confidence.	-Subscale successfully launched on Dec. 2nd, verifying prediction programs. -Launch Vehicle Subsystems finishing design phase, beginning production in Jan. 2018.

KEY: Not started; In Progress; Finished

3.1.4 System Level Design Review

3.1.4.1 Vehicle Description

The launch vehicle will have the capability of carrying two experimental payloads to an altitude of 5380 ± 100 feet. This exceeds the mission requirement of 5280 feet because one of the experimental payloads consists of an Air Braking System that is designed to reduce the rocket's apogee by up to 250 feet through the use of four flat plates extending from the body tube and into the flow path. The purpose of the tabs is to increase the drag force on the launch vehicle to lower apogee to the mission requirement. The other aforementioned payload will consist of a Deployable Rover held in the fore section of the launch vehicle. Further discussion of the payloads will follow in subsequent sections of the report.

The safe recovery of the launch vehicle will be achieved through a two-stage recovery system. Upon reaching an apogee of 5280 feet through the help of the Air Braking System, the rocket will separate into two tethered sections under a drogue parachute. Subsequently, at an altitude of 650 feet, the aft section of the rocket will separate into an additional two tethered sections under the main parachute. This will ensure that the launch vehicle remains within the recovery area for the competition and that the three individual sections of the launch vehicle will not exceed the maximum kinetic energy of 75 ft-lbf.

The final design of the rocket will have a length of 128 inches and a weight of 48.3 lbs. It will be propelled by a Cesaroni L1395 solid fuel motor.

3.1.4.2 Overview of Vehicle Design

The launch vehicle will have a variable diameter, beginning at 7.675 inches aft of the nose cone and transitioning to a diameter of 5.5 inches aft of a transition section 4 inches long. The rocket will weight approximately 892 ounces. Attached to the fin can, there are 4 trapezoidal

fins with root and tips chords of 7 inches and a height of 7.5 inches. At launch, the rocket will have a stability margin of 2.71 calibers. These values are shown in Tables 3 and 4 below.

The rocket consists of six subsections: the nose cone, the Deployable Rover payload Bay, the Transition Section, the parachute bay, the Air Braking Payload (ABP), and the fin can. The nose cone, made of polypropylene, is 22 inches long. The Deployable Rover Payload Bay contains all of the components necessary for rover deployment, including altimeters and accelerometers. The transition section allows for the connection of the Deployable Rover Payload bay and the parachute bay, which contains the Compact Removable Avionics Module (CRAM) and both the main and drogue parachutes. The ABP contains four tabs and a gear system used to extend them. The fin can contains the motor and the four main fins.

The five subsections of the rocket fall into three main sections based on how they separate during the descent of the rocket. At apogee, Section I separates from Section II and the drogue is ejected. At 650 feet above ground level, Section II separates from Section III and the main parachute is deployed. Section I contains the nose cone, the Deployable Rover Payload Bay, and the transition section. Section II is the parachute bay, and Section II is made up of the ABP and fin can. Figure 1 shows the sections and subsections. Figures 2 and 3 contain more detailed CAD drawings of the rocket.
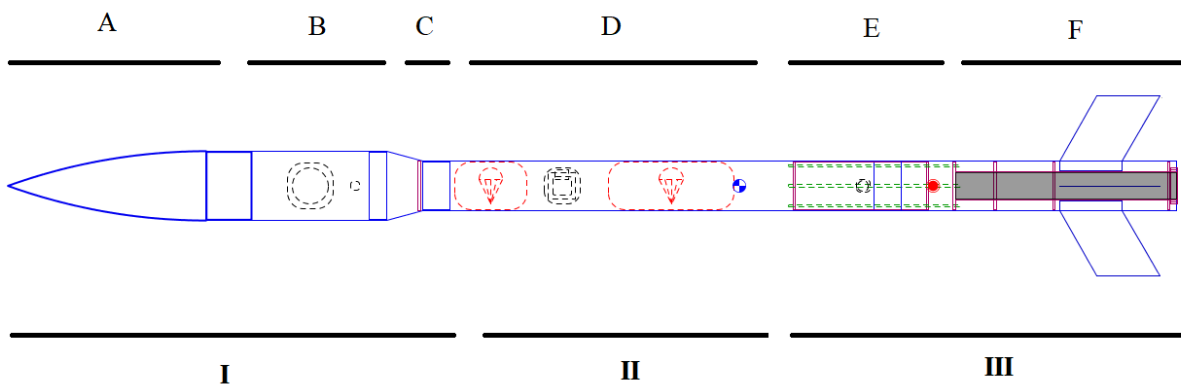
Figure 1.Vehicle Sections and Subsections
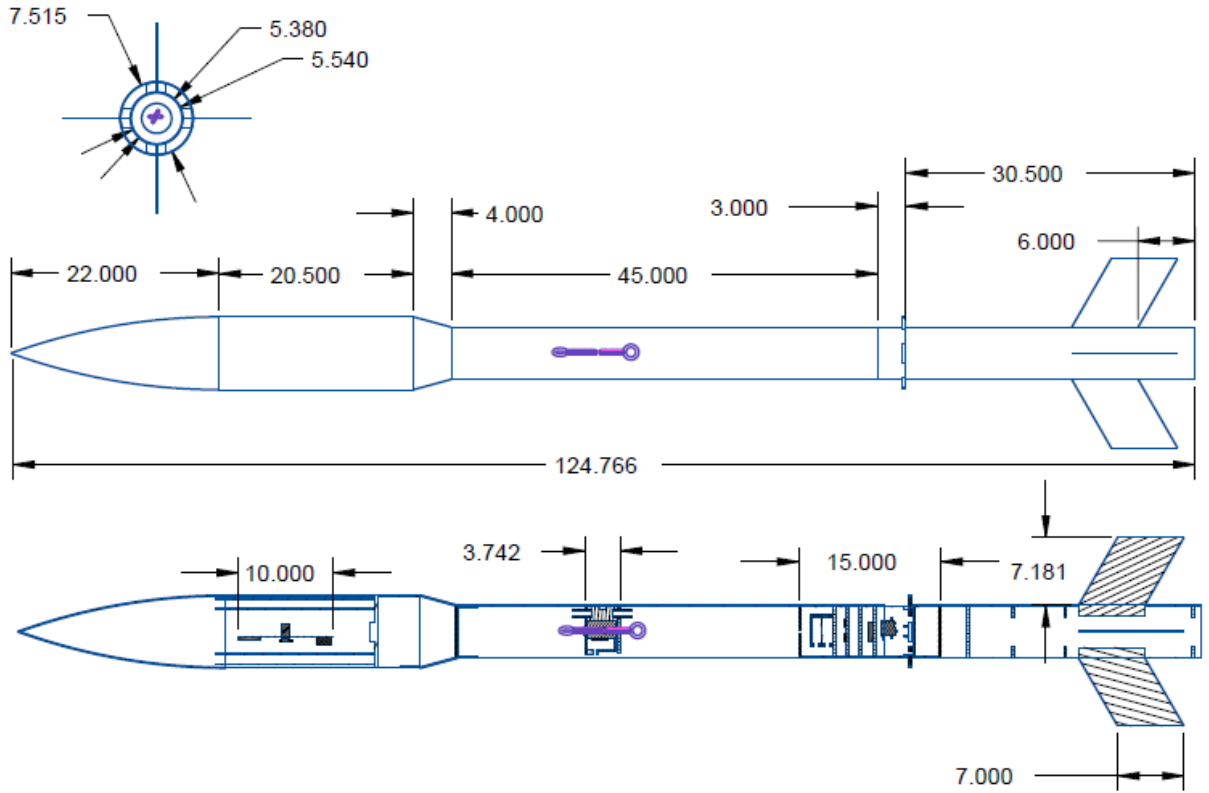
Figure 2. Final Launch Vehicle Design. Dimensions in inches.

Item	Qty	Description
1	1	NOSE_CONE
2	1	ROVER_COUPLER
3	1	ROVER_PAYLOAD
4	1	TRANSITION
5	4	BULKHEAD
6	1	RECOVERY_TUBE
7	1	CRAM
8	1	ABP_COUPLER
9	4	TIE_ROD
10	1	ABP_PAYLOAD
11	1	FIN_CAN
12	4	FIN
13	3	CENTERING_RING

Notre Dame Rocketry Team	**Project: CDR**	**Drawn By: Joseph Gonzales**	
Year: 2017-2018	**Title: Exploded CDR Model**	Date: 12/12/17	Scale: 0.09
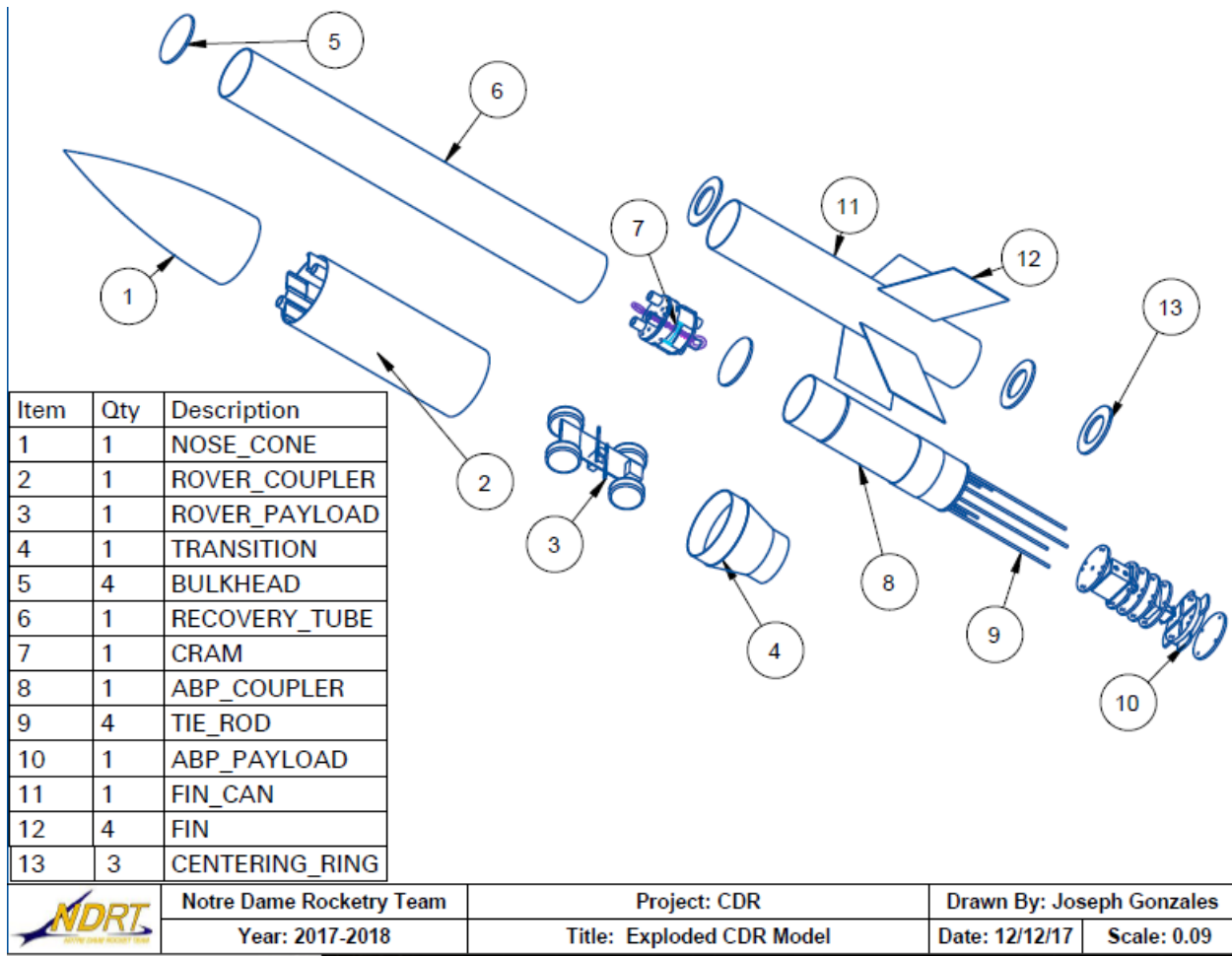
Figure 3. Launch Vehicle-Exploded Model.

Table 3. Launch Vehicle Dimensions.

Property	Value
Total Length (in)	125
Diameter, Nose Cone to Transition (in)	7.675
Diameter aft of Transition (in)	5.5
Number of Fins	4
Tip/Chord Length (in)	7

Fin Height (in)	7.5
Fin Width (in)	0.125
Weight with Motor (lbs)	48.31
Weight Without Motor (lbs)	38.81
Stability Margin with Motors	2.71
Stability Margin without Motors	3.85

Table 4. Description of Launch Vehicle Sections and Sub-Sections.

Section	Sub-Section	Label	Composed of	Description
I	Nose Cone	A	Hollow nose cone, 22 inch in height and 7.675 inch diameter, made of polypropylene	Connected to the deployable rover payload bay below
	Deployable Rover Payload Bay	B	20 inch long fiberglass body tube	Holds Deployable Rover Payload
	Transition Section	C	4 inch long fiberglass	Connects Deployable Rover Payload and Parachute Bay below
II	Parachute Bay	D	50 inch long carbon fiber body tube	Holds CRAM (Compact Removable Avionics Module), as well as main and drogue parachute
III	Air Braking	E	15 inch long carbon fiber coupler	Holds tabs used for changing apogee of

	Payload Bay			rocket during flight
	Fin Can and Motor Mount	F	30.5 inch long carbon fiber tube and carbon fiber fins	Holds motor and motor mount and carbon fiber fins

3.1.5   Component Design Review

3.1.5.1   Nose Cone

The full-scale launch vehicle will use a polypropylene nosecone purchased from Apogee Rockets. The team has used polypropylene nosecones in the past to great success. Polypropylene is strong enough to withstand any forces during landing or the rover deployment, and is both lightweight and inexpensive. Other materials that were considered were carbon fiber and fiberglass. Both are stronger than polypropylene, but given that the material properties of the nosecone are not critical to the launch vehicle design, the cheaper option was chosen and carbon fiber and fiberglass were neglected. The option of the team fabricating our own nosecone was considered, but given the increased chance of manufacturing error for little to no benefit, this option was quickly disregarded. Given that the nosecone is being purchased rather than fabricated by the team, the selection of a nosecone was also limited by the options found from commercial vendors. Fiberglass nosecones were found in the proper size, but were disregarded due to the reasons stated above.

The final option chosen for the launch vehicle and purchased from Apogee Rockets is the PNC-7.51". This nosecone has an outer diameter at the shoulder of 7.51 inches, which matches the inner diameter of the body tube section that houses the Rover Payload. The overall length of the nosecone is 22 inches, with a shoulder length of 5 inches. The weight of the nosecone is 30.66 ounces. This nosecone features an ogive shape, which is consistent with nosecones used in years previous. The main benefits of the ogive shape come with ease of construction.

Mounted in the nosecone will be two fiberglass bulkheads. These bulkheads will be used to eject the nosecone for deployment of the Rover Payload. One will be placed roughly halfway up the length of the nose cone, while the other will be placed at the top of the shoulder. As discussed later in Section 5.1, the bulkhead at the top of the shoulder will integrate with the Rover Payload to the nosecone and therefore allow proper deployment. These bulkheads will be attached using epoxy. The nosecone will be secured during flight with a series of shear pins. Black powder charges will be used to eject the nosecone once the launch vehicle has landed. Figures 4 and 5 below show CAD drawings and isometric views of the nosecone.

	Notre Dame Rocketry Team	Project: CDR	Drawn By: George Porter	
NDRT	Year: 2017-2018	Title: Nose Cone (Isometric)	Date: 1/2/18	Scale: 0.35
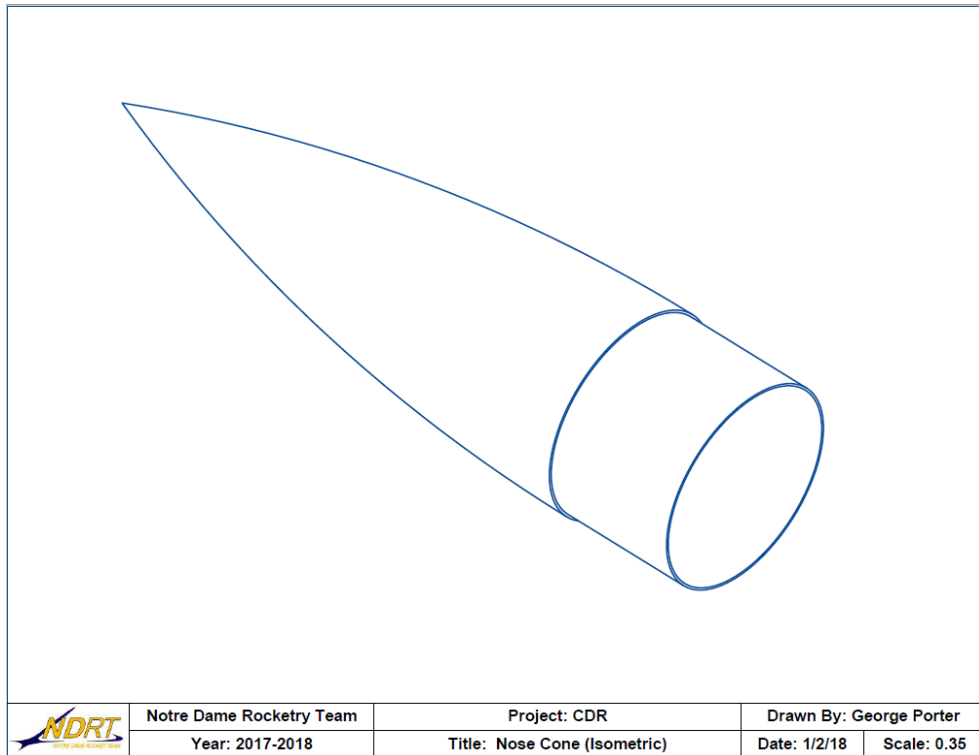
Figure 4. Isometric view of full-scale nosecone. Dimensions in inches.

	Notre Dame Rocketry Team	Project: CDR	Drawn By: George Porter	
NDRT	Year: 2017-2018	Title: Nose Cone (AS PURCHASED)	Date: 1/2/18	Scale: 0.25
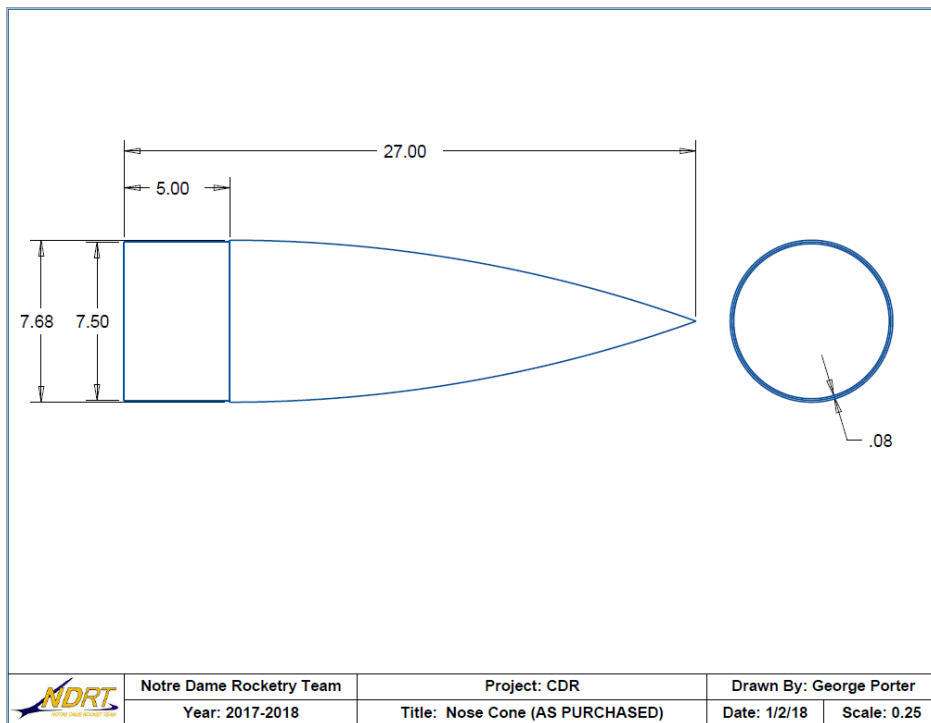
Figure 5. Side and bottom views of full-scale nosecone as purchased. Dimensions in inches.

The dimensions of the nosecone are shown below in Table 5.

Table 5. Dimensions of Nose Cone.

Property	Value
Length (in)	22
Shoulder Length (in)	5
Weight (oz)	30.66
Outer Diameter (in)	7.675
Inner Diameter (in)	7.51

3.1.5.2 Airframe

The airframe of the launch vehicle will consist of both carbon fiber and fiberglass body tubes and couplers. Carbon fiber tubing was used in the previous year and was shown to be a versatile material. It provides additional structural support compared to materials such as phenolic without sacrificing weight. This increase in strength properties makes it worth the additional cost and difficulties in manufacturing. Carbon fiber body tubes are commercially available and the team has access to facilities capable of modifying the tubes to fit the design.

However, carbon fiber shields radio frequencies, and the Rover Payload requires direct communication with a ground station after landing. For this reason, Section I of the launch vehicle will be constructed out of fiberglass tubing to allow transmission of signals to the rover. This section consists of the Rover Payload Bay with an outer diameter of 7.675 inches to allow more space to fully develop the rover, and the Transition Section to taper the main body down to 5.54 inches to conserve weight.

This transition section will consist of a 4 inch tapered section for a smooth reduction of 2 inches of body tube diameter, as well as two 3 inch shoulder couplers. This component will be made of fiberglass and is commercially available. This reduces the risk of improperly manufacturing the part in house and further ensures that no signals are inhibited from reaching the Rover Payload. A CAD model of the transition section is shown in Figure 6.
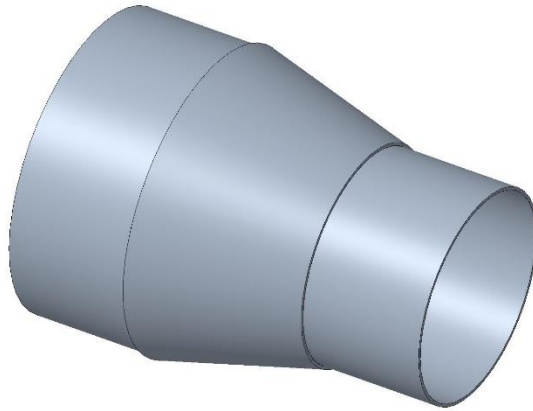
Figure 6. Transition Section CAD Model.

In order for the Air Braking System to function properly and be able to reduce apogee by 250 feet, the transition in the airframe diameter cannot induce major turbulence or flow separation at the location of the air braking tabs. Preliminary analysis of the flow field was conducted during PDR using ANSYS Fluent for the maximum simulated velocity of the rocket (200 m/s) using a body tube transition from 8 inches down to 5.5 inches. It was determined that this large transition would not cause significant boundary layer growth or flow separation at the location of the air braking tabs. For this reason, further and more developed CFD analysis of the flow field was deemed unnecessary. The final design of the Deployable Rover payload would only need a 7.675 inch diameter body tube and therefore would reduce the boundary layer growth seen in the preliminary analysis. It was determined that developing a more in depth model for a more comprehensive flow field analysis would be an inefficient use of resources and that the work done for PDR was sufficient to validate the use of the transition.

The overall integrity of the airframe will ultimately be verified through full scale testing. The materials chosen are historically reliable and will be further validated throughout construction of the rocket that will be flown at competition. The design presented in this report has been simulated using OpenRocket and RockSim software for a variety of flight conditions. The simulations tested the effects of mass distribution on the center of gravity, calculated the center or pressure, and predicted an apogee for the launch vehicle. Additionally, they allowed for different airframe finishes and ballast locations. After a full-scale flight test, the accuracy of these simulations will be verified to ensure better predictions for future flights.

Ultimately, the integrity of the airframe will be ensured through thorough construction techniques to maximize strength. Additional care will be taken when attaching the load bearing bulkheads and integrating the payload bays. The airframe will then be verified after the full-scale flight to further ensure that the carbon fiber and fiberglass supported the rocket in flight.

3.1.5.3 Fins

Several fin configurations were considered for our rocket's main fins, with a final decision being made following the Subscale Launch. The configurations varied in the shape, number, and construction material of the fins. The final configuration consists of four parallelogram-shaped fins, each made of carbon fiber.

A parallelogram fin shape was chosen due to its abundance of advantages. Foremost, this fin shape has a high effectivity at low Reynolds Numbers, which allows the fins to effectively straighten out the flight of the rocket. Additionally, with this shape, the velocity that would cause flutter in the fins exceeds the maximum velocity of the rocket. This is confirmed by the fact that the same fin design was used last year, and the fins did not experience flutter during the Full Scale Launch. A MATLAB program built on the following equations also proves that the flutter speed and the divergence speed won't be reached during the flight.

$$\frac{1}{2}\rho U^2|_{\text{flutter}} = \frac{[-E \pm (E^2 - 4DF)^{1/2}]}{2D}, \tag{4-66}$$

$$U_{\text{diverge}} = \left[\frac{k_\theta}{\pi\rho ca}\right]^{1/2}. \tag{4-53}$$

Conveniently, this fin shape is easy to make and replicate and, because all of the fins have the same airfoil shape, there is no drag that would arise from asymmetrical fin shapes. Carbon fiber was chosen for the construction material of the fins this year due to its light weight and strength, which increases apogee while sustaining structural robustness. In order to maintain flight in the vertical direction, fins were chosen that maximize stability and minimize drag and flutter, thereby also maximizing apogee. Furthermore, with this fin configuration, the team can quickly adjust the apogee of the rocket, if necessary, by increasing or decreasing the height of the fins. The fin is shown in 7.

The stability, structural integrity, and strength of the fins will continued to be tested through Finite Element Analysis and Fluid Analysis. Simulations will continue to be run to further confirm the apogee of the rocket achieved with this fin configuration. The team is confident in the choice of this configuration, because, as previously mentioned, the same configuration was used in last year's launch vehicle, with satisfactory results in its stability and apogee.
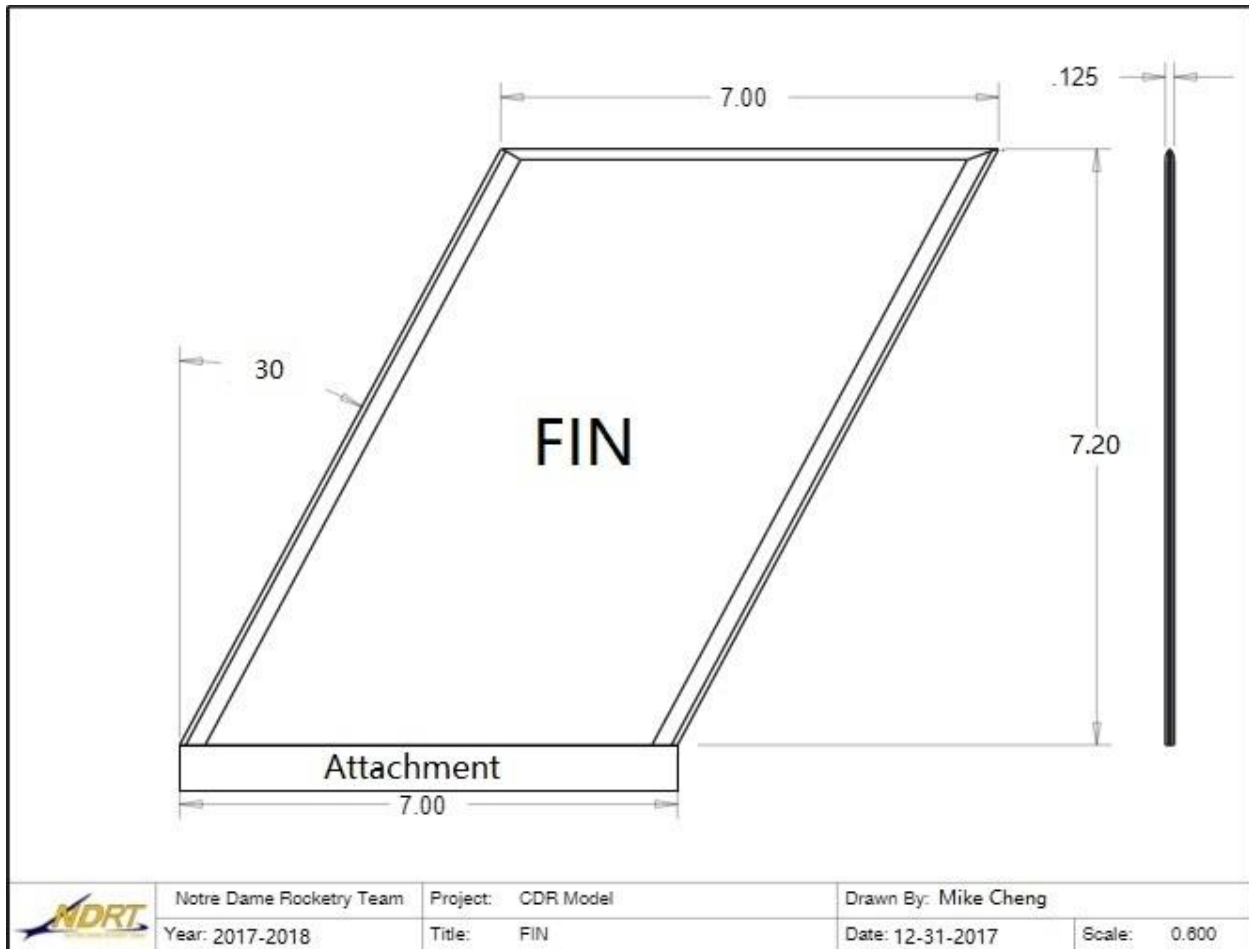
Figure 7. Final Fin Design. Dimensions in inches.

The fins will be ordered as carbon fiber plates. The fins will be cut appropriately, and the edges will be sanded to reflect airfoils in order to decrease drag. The edges of the fins will be lightly epoxied so that they do not dull. Rocketpoxy will be used to attach the fins to the body tube. A slim rectangle, 1.10 inches in width, is extruded from one end of each fin for ease of attachment. Fin alignment will be performed by the alignment mechanism used in past years. The mechanism consists of two circular plywood plates that are laser cut so that fin holes are exactly 90 degrees from one another. During construction, the plates are placed at each end of the fins for stabilization while the epoxy dries overnight. The laser cutting process ensures perfect angles so that misalignment may be avoided. Table 6 shows a summary of the fin dimensions.

Table 6. Summary of Fin Dimensions.

Characteristic	Value
Number	4
Root Chord (in)	7
Tip Chord (in)	7
Thickness (in)	0.125
Height/Span (in)	7.2
Sweep Angle (degrees)	30

3.1.5.4 Couplers

Couplers were selected in order to allow the rocket to easily be separated into various payloads both for construction purposes and during parachute deployment. Access doors had been considered in previous designs, but were abandoned due to possible disturbance of the flow profile and their limited ability to allow for parachute deployment during flight. Couplers were decided upon because of their convenience and lightweight, simple design.

There will be a coupler built into the transition section of the rocket, which connects the rover tube with the body tube. This coupler will be manufactured with the transition section out of fiberglass in order to minimize cost and potential errors in manufacturing. Additional couplers will connect the Air Braking Payload to both the main body tube and the engine mount. These will be constructed out of 0.08 inch thick carbon fiber. Carbon fiber was selected over Kraft Phenolic tubing as it is much sturdier, and would interface better with the rest of the rocket. The outer diameter of every coupler will be designed to be as close as possible to the inner diameter of the tubes they are connecting. This will allow for a tight fit to hold the rocket together, as well as provide extra stability for the body tubes during flight.

The transition section with couplers can be seen in Figures 8 and 10. The couplers connecting the Air Braking Payload to the engine mount are seen in Figures 9 and 11.
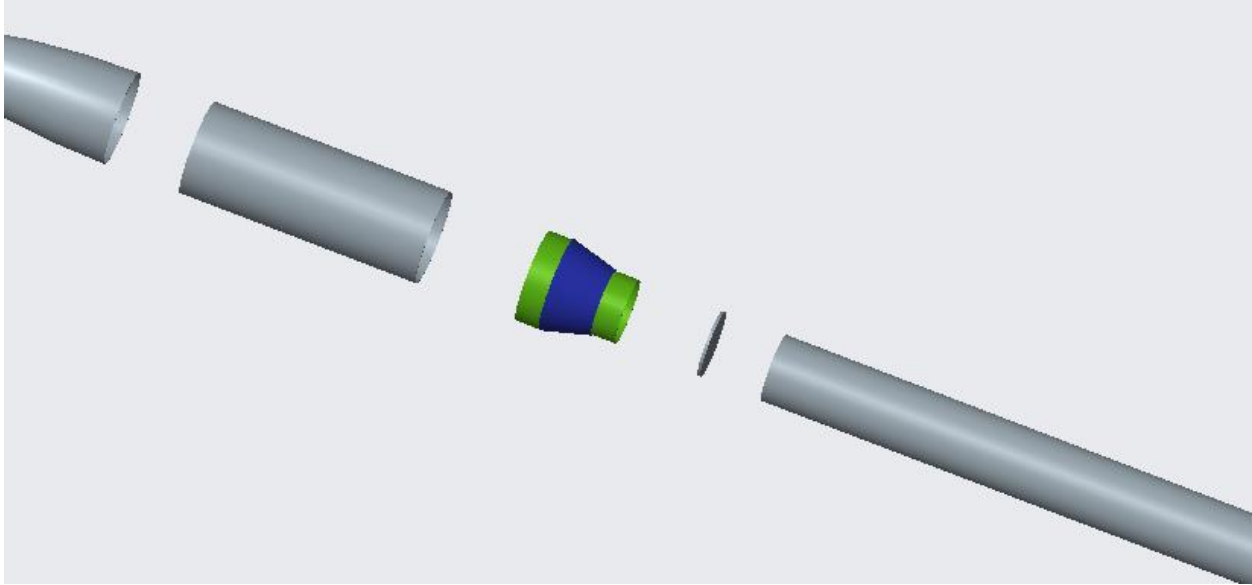
Figure 8. Transition Section (shown in blue) with Coupler (shown in green).
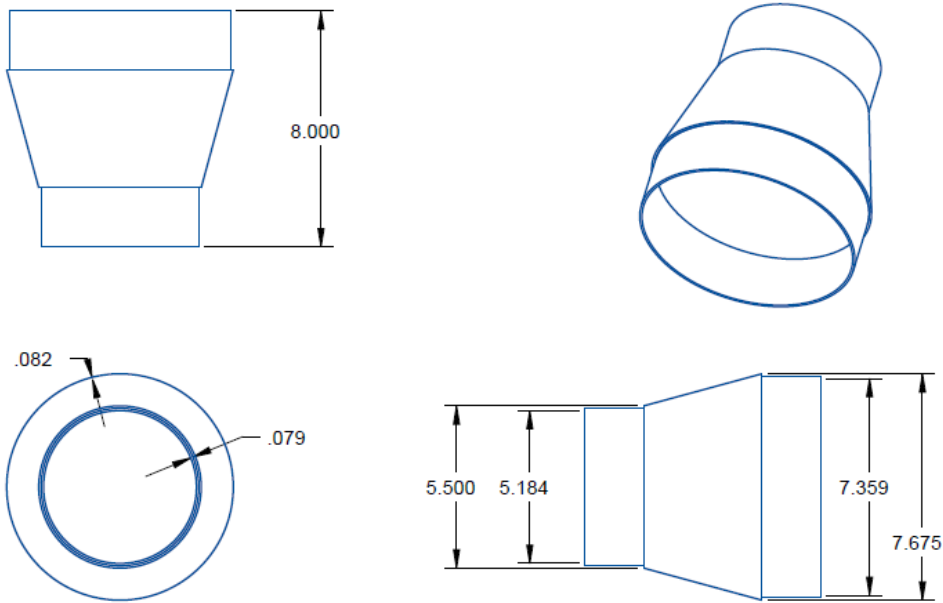
NDRT	Notre Dame Rocketry Team	Project: CDR	Drawn By: Joseph Gonzales	
	Year: 2017-2018	Title: Transition	Date: 12/12/17	Scale: 0.250

Figure 9. Transition Section and Coupler Dimensions. Dimensions in inches.
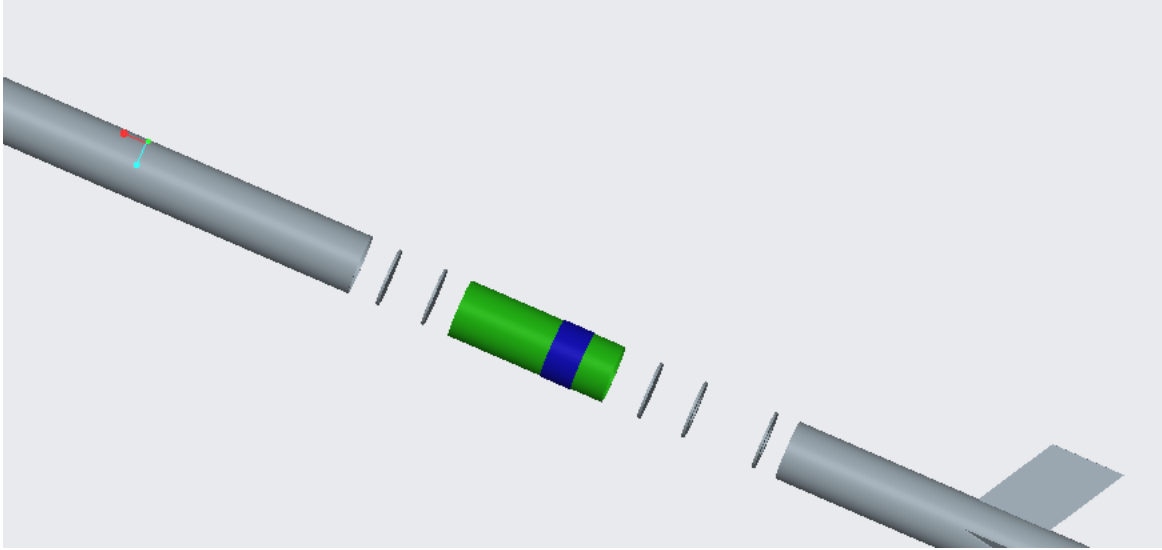
Figure 10. ABP (shown in blue) with Coupler (shown in green).

NDRT	Notre Dame Rocketry Team	Project: CDR	Drawn By: Joseph Gonzales	
	Year: 2017-2018	Title: ABP Coupler	Date: 12/12/17	Scale: 0.25
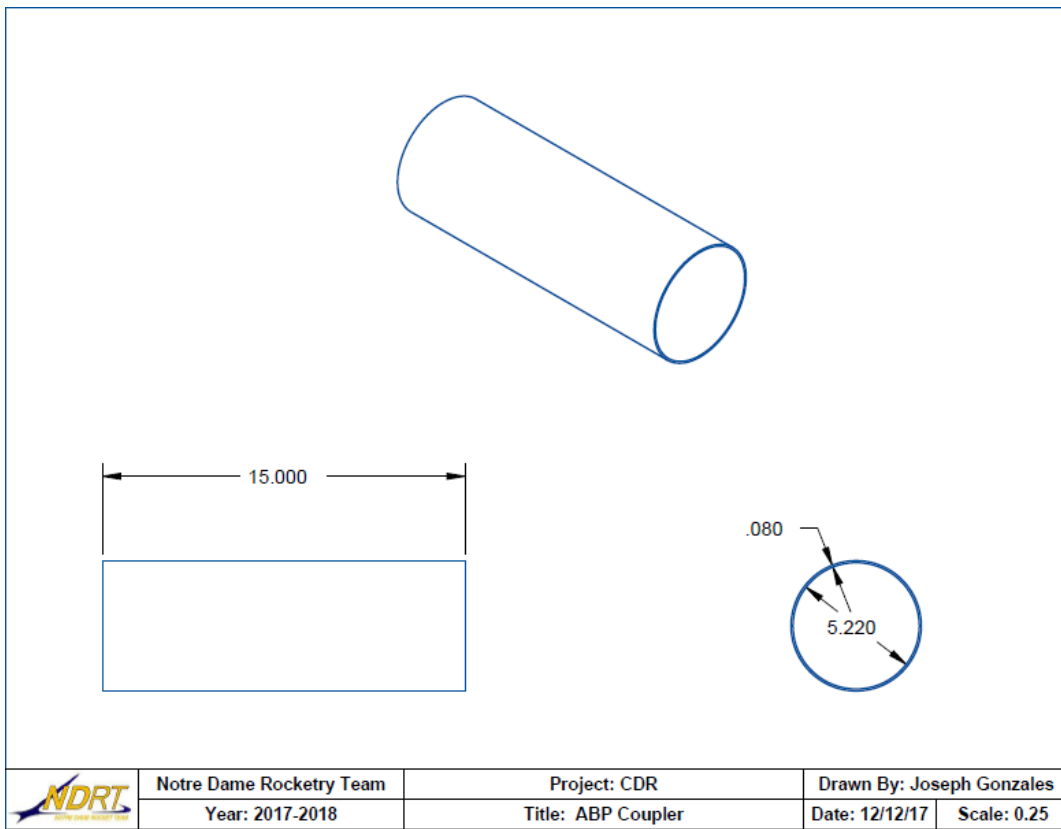
Figure 11. ABP Coupler Dimensions. Dimensions in inches.

3.1.6 Subsystem Design Review

3.1.6.1 Deployable Rover Payload Integration

The proper integration of the rover payload into the vehicle is essential for both the flight of the rocket, and the deployment of the rover. The rover must be able to fit inside of the vehicle's rover tube, which has an overall length of 20 inches and an internal diameter of 7.515 inches. The rover is not expected to be the exact length or width of the rover tube, and must be secured to prevent movement during flight. This prevention of motion is essential so as not to affect the flight pattern of the rocket, or to damage the rover itself. In order to do this, a pin and track system will be installed into the body tube of vehicle.

The main source of securing the rover will come from the dual-purpose servomotor that also drives the solar panel system. The brass racks upon which the solar panels rest must be retracted when the rover is within the rocket for the rover to fit inside. When the servomotor runs counterclockwise, these racks can be retracted slightly further to extend the non-panel-bearing ends of the racks into mounting blocks affixed to the interior wall of the fuselage. These two mounting blocks will be 3D-printed cube-like structures with slots for the ends of the racks to fit into. The blocks will be affixed to the interior wall of the fuselage with high-strength epoxy. These blocks will secure the rover in all directions.

The track system will provide a secondary source of securing the rover. The rover will rest on two of the four tracks during flight in order to allow the rover to drive out when the deployment sequence is initiated. The wells of the tracks add another level of securement. The tracks will be 3D printed in order to meet the custom requirements. The track system will also include a set of triangular supports, also 3D printed, which will function as the connection between the tracks and the body of the rocket. The tracks and supports will be adhered using RocketPoxy, as it provides a high-strength bond when joining fiberglass and carbon fiber. A diagram of this system is shown in Figures 12 and 13.

The nosecone will be held in place during flight with a series of shear pins. The exact number of pins will be determined with ground tests and shake tests once the launch vehicle is constructed.

During flight, the rover will be housed directly between the nose cone and the transition piece to the rest of the body. Once the rocket lands, the rover will exit through the nose cone. The nose cone will be removed using black powder charges. Importantly, the rover is designed and housed in such a way that it can exit the rocket no matter the orientation it lands. For this reason, the rover is designed with large wheels so that it can potentially drive in an inverted orientation. The rover will be able to drive out of the rover tube on two of the four tracks that are mounted inside. This feature, along with the oversized rover wheels, will ensure that the rover can exit the rocket.
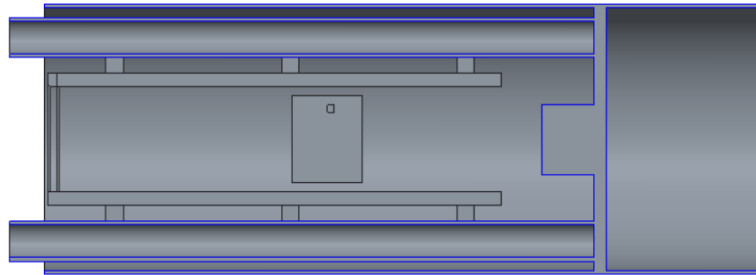
Figure 12. Cross section of the tracks and securing block inside the body of the rocket.
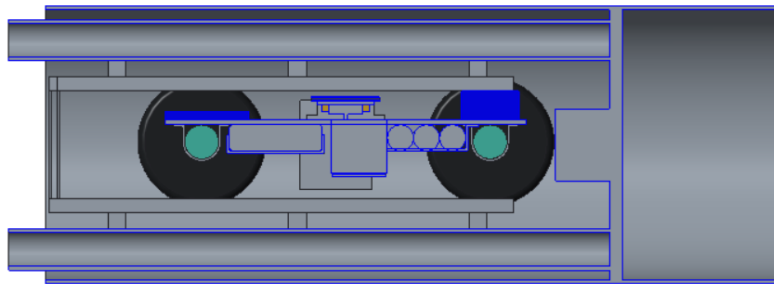
Figure 13. Cross section of the rover secured inside the body of the rocket.

3.1.6.2   Air Braking System Integration

The air braking system is placed inside the rocket in such a way that the ultra-high-molecular-weight polyethylene drag tabs will be located near the post-burnout location of the center of pressure. This ensures that moment arms created by aerodynamic forces will not cause stress or instability to the rocket. The system will be contained in a 15 inch long coupler located fore of the fin can section, and the drag tabs will protrude from the body tube, 3 inches above the aft end of the coupler. Four steel rods will protrude from the motor mount bulkhead and will cleave through the 15 inch long air braking system coupler. The two bulkheads of the coupler are made of fiberglass. The fore bulkhead is connected to the main parachute via an eyebolt and shock cord. Ends of the rods passing through the aft bulkhead will be epoxied to nuts to stop the coupler from sliding into the fin can. Ends of the rods passing through the fore bulkhead will be attached to lock nuts to secure the air braking system itself. This method of integration gives access to the air braking system while still maintaining the security of the payload during launch. The fore section of the coupler also is perforated with shear pin holes to keep the parachute body tube and fin can secured until main deployment.

3.1.6.3   Recovery Subsystem Integration

The vehicle's recovery subsystem is designed to secure a safe and controlled descent of the vehicle from apogee to landing. This system is vital in ensure reusability of the rocket and protection of the payload.

The recovery system is located in the center of middle section of the rocket as seen in Figure 14. The recovery section is attached to the nose and the tail sections by shear pins that detach when the charges are detonated in the CRAM to deploy the parachutes. The placement of the system is to avoid collision of the components during descent after the deployment of the drogue and main parachutes. The central location also allows for the ejection charges to be the same size, since the even spaces will require the same pressure on either side to release the shear pins. There is triple redundancy built into the CRAM to assure the parachutes are deployed so the vehicle can safely land.

The rocket's recovery system and avionics module will be located in the center section of the rocket and a diagram of the system can also be found in Figure 14 and the details of each labeled component can be found in Table 7.
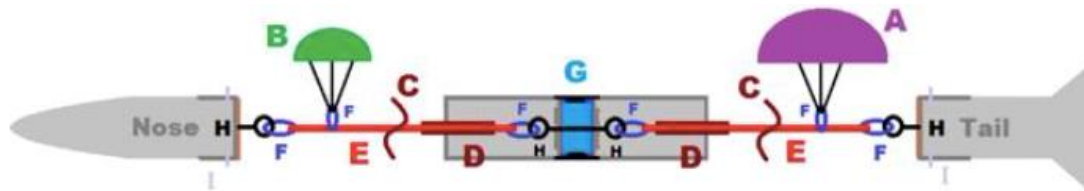
Figure 14. Recovery system diagram and layout in launch vehicle.

Table 7. Recovery component reference to information section in report.

Component	Location in Figure	Section
Main Parachute	A	3.1.6.3.1
Drogue Parachute	B	3.1.6.3.2
Nomex Cloth	C	3.1.6.3.2
Nomex Shock Cord Protectors	D	3.1.6.3.2
Shock Cords	E	3.1.6.3.2

Quick Links	F	3.1.6.3.4
CRAM	G	3.1.6.3.5
Eye-Bolts	H	3.1.6.3.4
Shear Pins	I	3.1.6.3.4
Bulkheads	N/A	3.1.6.3.3

3.1.6.3.1   Parachutes

Recovery will consist of a two-stage deployment system with the drogue parachute deploying at apogee and then a main parachute deploying at 600 feet above ground level. This system allows for quick descent, but also a descent with lower impact upon landing. Both parachutes are nylon. The 2 foot diameter drogue parachute will take approximately 10 cubic inches and the 12 foot diameter main parachute will take up approximately 150 cubic inches. They will be packed on opposite sides of the CRAM.

3.1.6.3.2   Harnesses

The rocket sections are attached to the parachutes by 1 inch tubular nylon shock cords allowing the sections to remain tethered after separation. These shock cords will also allow the large forces to be absorbed after the deployment of the charges. The shock cords are five times the length of the rocket to absorb the force and connect the sections adequately so that they do not impact each other during descent.

The portion of the shock cords closest to the separation charges will be wrapped in 12 inch long tubular pieces of Nomex cloth in order to protect against the cord from the explosion. In addition the end of the parachute facing the separation charges will be wrapped in 18 inch x 18 inch Nomex cloth to protect them from the explosion.

3.1.6.3.3   Bulkheads

The bulkheads are attached by carefully epoxying them to Section I and II of the launch vehicle. They will be made out of 0.25 inch acrylic due to its high compressive strength and resistance to wear. The bulkheads will keep the rocket attached even at the recovery events.

3.1.6.3.4   Attachment Hardware

The shock cords will connect each section of the rocket. The shock cords will be attached to each section by 6 inch quick links rated for 2000 lbs to ⅝ inch diameter eye bolts rated for 1500 lbs. The same quick links will be used to thread the shock cord through and attach the parachutes.

In order to attach the rocket during its ascent, shear pins will be used to connect the sections. At the respective parachute deployments, the detonated charges from the CRAM will provide a force great enough to shear the shear pins, thus separating the rocket and deploying the parachutes.

3.1.6.3.5   CRAM Mount

The Compactable Removable Avionics Module (CRAM) will be located in the center of the middle section of the rocket and will contain the altimeter and the charges. This year to ensure a successful recovery, the CRAM system contains triple redundancy with charges and altimeters. It will be screwed into a 3D-printed mount which is epoxied to the interior sides of the rocket vehicle. The mounts outer diameter will be the same at the inner diameter of the rocket to maintain a tight fit that will decrease any mobility of the system. To ensure even further that the CRAM remains immobile, it will be secured by a screw perpendicular to the rocket body. Small holes will be drilled into the rocket body in order to obtain accurate atmospheric pressure readings for the altimeter.

3.1.6.4   Propulsion

The propulsion system consists of the motor and its corresponding support systems, including a retention system and a centering/mounting system. After several OpenRocket simulations were completed with motors from reliable manufacturers Loki, Cesaroni, and AeroTech, the Cesaroni L1395-BS was chosen. This motor was selected because it gave the necessary impulse and apogee, but was smaller and lighter than similar motors, namely the Cesaroni L1685. The specifications and the commercially published thrust curve for the L1395-BS are shown below in Table 8 and Figure 15, respectively.

Table 8. Cesaroni L1395-BS motor specifications.

Property	Value
Diameter (in/mm)	2.95/75
Length (in)	24.45
Peak Thrust (lbf)	400.5

Average Thrust (lbf)	314.0
Total Impulse (lbf*s)	1101.5
Total Weight (oz)	151.31
Propellant Weight (oz)	82.77
Burn Time (s)	3.51
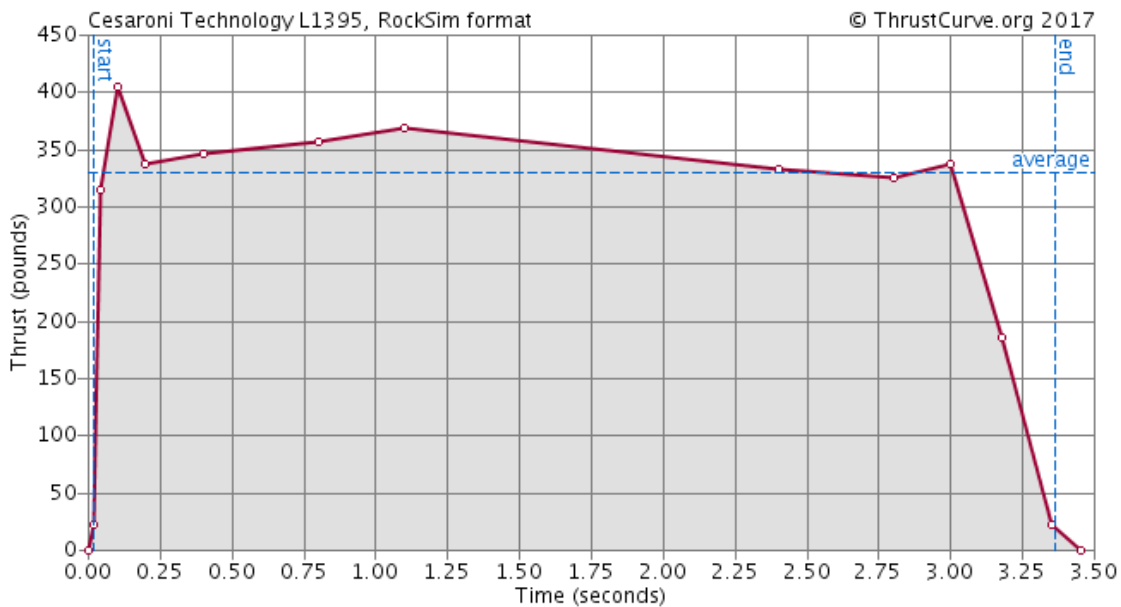
Figure 15. Thrust Curve for Cesaroni L1395-BS.

The main goal of the propulsion system is to safely bring the launch vehicle to 5,380±100 feet so that the Air Braking System may add the necessary amount of drag to bring the rocket to the exact 5,280 foot goal. The current launch vehicle with the motor totals to 773 oz. With this design, OpenRocket gives an expected apogee without drag tabs of 5,508 feet when in 10 mph winds at standard atmospheric conditions. For robustness, this simulation was repeated with varying wind speeds. The results can be seen below in Table 9. Most of these apogees are higher than the top end of the apogee range set for the Air Braking System to be effective (5,480 feet). This is to allow for any excess mass or drag that is added during the construction process. If the

mass stays the same, then ballast will be added to decrease the estimated apogees to between 5,380 and 5,480 feet.

Table 9. OpenRocket simulation apogee results.

Wind Speed (mph)	Predicted Apogee (ft)
0	5,561
5	5,547
10	5,508
15	5,464
20	5,416

If the mass is increased past 800 ounces with any future design changes, the predicted apogee drops to ~5,300 feet. This is too close to the 5,280 feet goal for the Air Braking System to have much effect. Therefore, in the event of a steep mass increase, the team would switch to either the Cesaroni L2375-WT-P or the Cesaroni L1115-0. Both motors are the same size as the current selection and thus would use the same motor casing and motor mount design. However, they offer a higher total impulse and would thus allow the heavier launch vehicle to still reach apogees around 5,400-5,500 feet. This change is not expected, but having back-up motors with known availability is a necessary precaution should any emergency design changes occur.

The motor support systems are discussed in detail in the following section.

3.1.6.5   Motor Mount and Retention

The motor will be located at the aft end of the launch vehicle, inside the fin can. It must be properly centered and secured in order for the launch vehicle to have a stable flight. The centering of the motor will be accomplished through a motor mounting system, while the security of the motor inside the rocket will be accomplished through a retention system.

It is critical that the motor and its casing are centered within the fin can as to not produce any torque that would lead to gimbaled thrust. As there is no thrust vectoring, the motor must be assembled in such a way that it is perfectly centered. In previous years, the team has used a series of three centering rings between the fin can body tube and the motor mount tube. These pieces were either laser cut or cut with a CNC machine to ensure that the dimensions are correct. Other options considered used similar logic to a centering ring, but used less material. These included

using a series of "legs" around the motor mount tube to ensure it remains centered. While this design would weigh less, it is much more difficult to assemble. Given that gimbaled thrust would cause a multitude of safety issues, the team decided to opt for the less efficient but more robust design and use centering rings, similar to previous years. A schematic of the design is shown below in Figure 16. The locations of the three centering rings were chosen to spread the load of the motor along the fin can without interfering with the fins themselves. They will have an inner diameter of 3.15 inches, an outer diameter of 5.38 inches, and will be positioned on the motor mounting tube 0.75, 13.5, and 20 inches forward of the rear end of the launch vehicle. These rings are going to be made from quarter inch thick fiberglass and will be cut to specification using a CNC router. The motor mount tube will be made of carbon fiber. It will have an inner diameter of 3 inches, an outer diameter of 3.125 inches, and a length of 24.45 inches, which is the length of the chosen motor. The carbon fiber can resist the high temperatures the mount will be exposed to during motor burn. The motor mount tube will be inserted into the fin can body tube, which is also made of carbon fiber. At the most fore point of the motor mount tube will be a quarter inch thick fiberglass bulkhead with a diameter of 5.38 inches. The purpose of this bulkhead is to ensure that the motor remains in the aft portion of the launch vehicle and does not move upward during burnout. The bulkhead will be epoxied to the fin can body tube. The centering rings will be attached to the fin can body tube in the same way. For this section of the launch vehicle, JB Weld will be used rather than conventional epoxy to account for the higher temperatures from the motor burn. The centering rings will be positioned in such a way that they ensure the motor casing remains perfectly centered throughout flight without compromising the motor retention system discussed earlier.
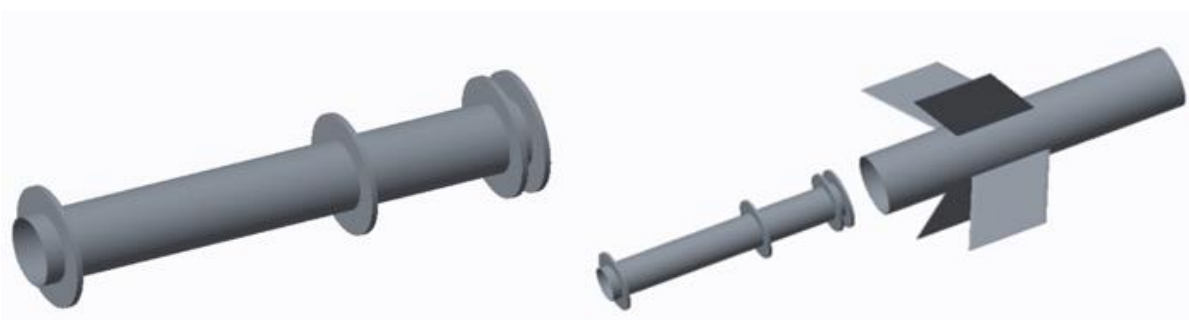
Figure 16. Schematic of motor mount design.

If the mass of the rocket is increased enough that a more powerful motor is needed, the two alternative motors already chosen are the same size and manufacturer as the current selection and thus will not require a change to this motor mount design.

The retention system consists of a 75 mm API Quick-Change motor retainer. This system from Aero Pack Incorporated consists of two pieces manufactured out of precision machined

6061-T6 aluminum. A threaded cylinder adaptor will be attached to the outside of the motor mount tube using JB Weld. Then, once the motor has been inserted into the motor mount, a retainer cap with matching threads to the adaptor is simply screwed-on to the adaptor to hold the motor and its casing in place. This system is compatible with Cesaroni Motors and allows for the motor to be removed without any screws. This system was selected for its simplicity and robustness. It will be purchased from the Aero Pack website for $50 and is currently in stock. An example of the system for a smaller Cesaroni Pro29 motor is shown below in Figure 17 for reference.

Figure 17. Cesaroni Pro29 motor assembly using 29 mm Aero Pack Quick-Change motor retainer system.

3.1.6.6   Fin Integration and Placement

The four fins have been placed at the rear of the rocket, 6.0 inches forward from the bottom of the fin can. They have been spaced at 90.0 degree intervals about the same axis of the body. The purpose of the fins is to move the center of pressure, which is where the lift and drag forces act, aft of the center of gravity. This provides stability whenever the rocket shakes during flight. The restoring force this provides will compensate for any wobble in the rocket due to wind gusts and it will realign the orientation of the rocket with the desired vertical flight path.

The fins will be constructed by using prefabricated carbon fiber plates. The plates will first be cut (using a diamond-edged saw) into the desired parallelogram shape seen in Figure 4.7, with a root and tip chord of 7 inches, a height of 7.2 inches, a sweep angle of 30 degrees, and a rectangular extension on the bottom of each fin of 1.1 inches. Each fin will be 0.125 inches thick. After the fins are cut into a proper shape, they will be sanded to create a symmetrical airfoil. The leading edge of the fins will be sanded at 90 degrees, and the trailing end will be sanded at 45 degrees to achieve the desired qualities. To attach the fins to the rocket, there will be four 0.125

inch slots in the rocket tube through which the fins can be inserted. These slots will be a part of the fin can when it is ordered, as seen in Figure 17. After the fins are inserted, Rocketpoxy will be used as an adhesive to completely attach the fins to the body of the rocket. The fins shall be inserted such that their rectangular bases face towards the body tube.

To ensure that the fins are aligned at exactly 90 degree intervals, a fin alignment mechanism has been developed. The fin alignment mechanism, previously described in Section 3.1.5.3, consists of two circular plywood plates that are laser cut so that fin holes are exactly 90 degrees from one another. These plates are then placed at each end of the fins for stabilization during the epoxying process. The same mechanism was used in last year's rocket design with satisfactory results.

3.1.6.7   Ballast Integration

If the stability of the rocket is not within its limits and needs to be changed, or if the apogee of the rocket needs to be decreased, it is not usually ideal to change the design of the rocket in order to fulfil this requirement. Therefore, ballast is used in order to change the center of gravity (CG) of the rocket, and therefore the stability and altitude. Ballast is usually placed near the nose of the rocket, moving the CG towards it. Since the center of pressure (CP) will not change (the mass is added inside the rocket and does not impact the aerodynamic properties), this increases the distance between the CG and CP, and therefore the stability of the rocket.

Ballast will be incorporated into the area between the bulkhead at the back of the Deployable Rover Payload and the coupler of the transition section. Here there will be a phenolic coupler with two plywood bulkheads attached, the one closest to the payload will be epoxied and immobile, while the one closest to the nose cone will be free to move. Ballast in the form of sand (96 lb/ft^3) will be measured to the correct weight and placed in durable plastic bags; these bags will be put in coupler between the two bulkheads. In order to keep the ballast and top bulkhead from moving during flight, three bolts will be evenly spaced and put through drilled holes in both bulkheads, and they will be tightened together using nuts, securing the ballast. To verify that the retention system will not fail during flight, a shake test will be performed once the ballast is in place. A model of the ballast retention coupler can be found in Figure 18.

NDRT	Notre Dame Rocketry Team	Project: CDR	Drawn By: George Porter	
	Year: 2017-2018	Title: Ballast Retention	Date: 1/6/2018	Scale: 1.00
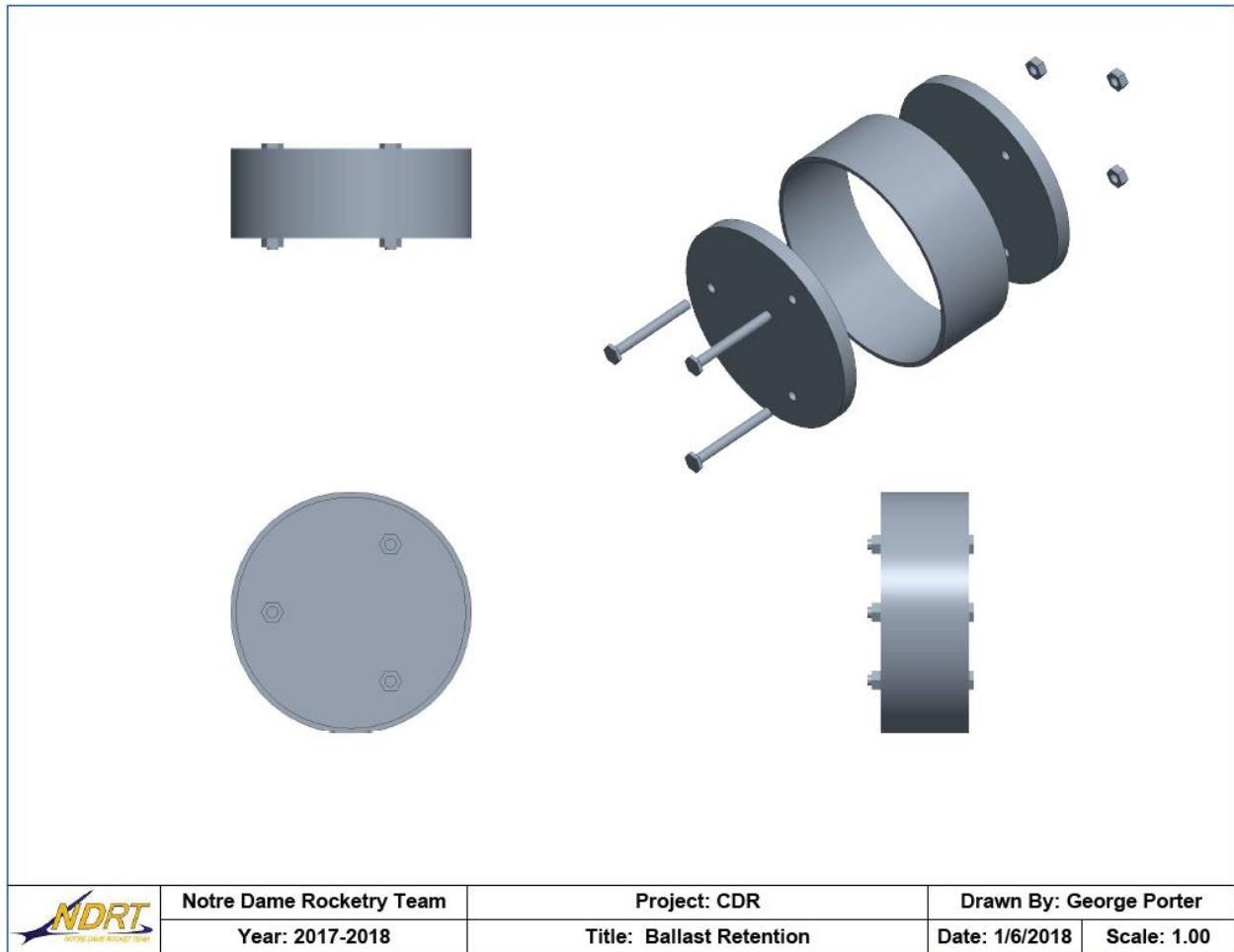
Figure 18. CAD representation of ballast integration.

3.1.7 Integrity of Design

3.1.7.1 Fin Shape and Style

The fin style chosen was described in Section 3.1.5.3 as excellent for maximizing stability and apogee, as well as minimizing flutter. This style was also chosen for the flexibility it offers the team. Following the full-scale test launch, the team will be able to make any necessary final adjustments to the fin configuration in order to perfect the launch vehicle. However, as a result of last year's success achieved by the same fin configuration, the team is confident in this design's ability to again produce satisfactory results.

Section 3.1.6.6 outlines the integration of the fins into the full-scale launch vehicle. This integration was also used on the subscale, although the materials used were plywood for the fins and phenolic for the body tubes. The fins performed well during the subscale launch, demonstrating a satisfactory stabilization of the flight of the rocket.

Another visual representation of the fin shape and style is shown in Figure 19. This CAD drawing includes the rectangular extrusion at the base of the fin, which extends below the fin can and onto the motor mount.
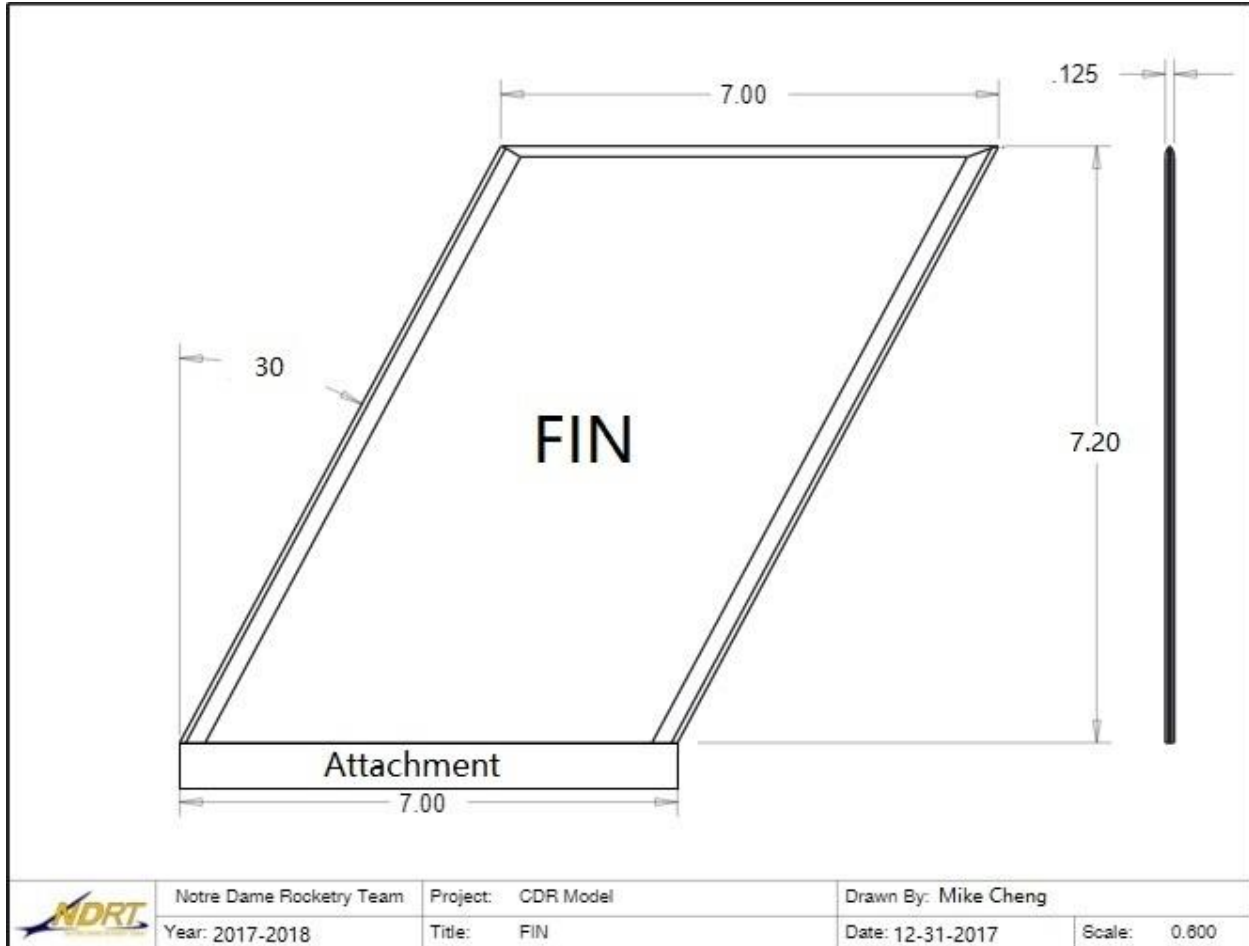
Figure 19. Final fin design. Dimensions shown in inches.

3.1.7.2   Materials

3.1.7.2.1   Full Scale

The materials used for the launch vehicle play a vital role in the overall design. The decision to use certain materials was based on a combination of material properties, cost, ease of construction, and availability to purchase from professional vendors. All materials being used for the launch vehicle itself i.e. not including the two scientific payloads, have been used by the team in previous years. The materials will be bought commercially. Some components of the launch vehicle will be purchased and cut to specification by the vendor, while others will be

purchased and cut to specification by facilities on Notre Dame's campus, such as the AME machine shop.

The nosecone for the full-scale vehicle is made of polypropylene. Polypropylene is a rugged thermoplastic polymer used in many hobby rockets. The nosecone will be purchased from Apogee Rockets, and will be modified during construction and assembly to integrate with the Rover Payload. Other options for the nosecone material were considered, namely fiberglass. Polypropylene is inferior to fiberglass in terms of material properties relevant to nosecone design. As the nosecone materials properties are not critical to the design, the benefits that fiberglass provides over polypropylene were not worth the increased cost. Material choices were further limited by the availability of nosecones that can be purchased commercially. The team considered fabricating a nosecone, but it was deemed that it offered little benefits over a commercially bought nosecone, but greatly increased the risk of manufacturing error.

Both carbon fiber and fiberglass are being used for the body tube sections of the launch vehicle. The team used these materials in the past, therefore is familiar with techniques to work with them. Other options were considered, namely phenolic and Blue Tube 2.0. Phenolic had been used many times in the past for a majority of the launch vehicle and had performed well. It provided adequate material properties at a low cost and was easy to work with using basic power tools. Carbon fiber and fiberglass offer better performance than phenolic, and given the increased budget the team has, these materials were chosen instead. Blue Tube 2.0 was also considered for the body tubes. It offers better performance overall than phenolic, but worse performance overall than carbon fiber or fiberglass. The cost was in between phenolic and carbon fiber/fiberglass. Given that Blue Tube 2.0 was less cost effective than phenolic but offered generally worse performance than carbon fiber and fiberglass, the team opted to use carbon fiber and fiberglass instead of Blue Tube 2.0.

Both fiberglass and carbon fiber have excellent performance and material properties for hobby rocketry, primarily because they are both lightweight and structurally strong. Both materials offer noticeable improvements over phenolic and Blue Tube 2.0. The main disadvantages are the high cost and difficulties associated with construction. To compensate for this difficulty, the vendors the body tubes are purchased from will cut the components to specifications.

Carbon fiber will be used for the main body tube that houses the recovery system and the fin can, that consists of the motor mount and the fins. The motor mount and air braking payloads are also made of carbon fiber. Carbon fiber is capable of handling the high temperatures the motor mount will be subjected to from the motor burn. All couplers will be made of carbon fiber. Fiber glass is used for the Rover Payload and the transition section. Fiberglass was chosen for the Rover payload as the ground station uses radio waves to communicate with the rover deployment system. These waves do not transmit through carbon fiber, but do through fiberglass. As the recovery system and air braking payload do not require this type of communication, carbon fiber is used instead as it offers lighter weight and adequate strength.

Bulkheads and centering rings will be made from fiberglass. Previously, the team had used plywood or 3-D printed material, but given the increased budget, materials with greater performance are now used. The increased performance of the bulkheads is crucial, as these bulkheads have been a point of failure for launch vehicles in the past. The team uses a CNC router to cut the fiberglass to the desired shape.

The fins will be made from carbon fiber, much like last year's design. The team will get these fins cut in Notre Dame's AME Machine Shop. The team will then sand down the fins' leading and trailing edge to ensure that flow remains attached. This will be accomplished using sanding blocks that the team constructed for use in previous years. Proper safety protocols will be followed during this sanding phase.

3.1.7.2.2   Subscale

While the full-scale launch vehicle focused on increased performance, the sub scale launch vehicle prioritized cost effectiveness and ease of construction. The materials used for the sub scale will consist of a polypropylene nosecone with phenolic body tubes/couplers, and plywood for fins and bulkheads/centering rings. The fins meant to represent the air braking payload will be 3-D printed, primarily because it allows the shape of the fins to be more precise when compared with laser cutters.

Material properties of all materials used in the launch vehicles are shown below in Tables 10 and 11.

Table 10. Material properties of materials considered for all part of launch vehicle besides nose cone.

Material	Component Use	Density (lb/in^3)	Tensile Strength (ksi)	Tensile Modulus (msi)	Shear Modulus (msi)	Com-pressive Strength (ksi)	Com-pressive Modulus (msi)	Specific Weight (lb/in^3)
Carbon Fiber	Body Tube, Fins	0.0578	300-350	15-30	0.6-.0725	82-120	18.5	0.065
Fiberglass	Body Tube, Bulkheads, Centering Rings	0.055	250-300	0.8-1.4	4.351	140-350		0.063

Phenolic Paper	Body Tube		12-15			32		0.049

Table 11. Material properties for polypropylene plastic.

Property	Value
Density (lb/in^3)	0.0342
Tensile Strength (psi)	5800
Compressive Strength (psi)	5800
Young's Modulus (msi)	217-290

3.1.7.3   Motor Mounting

The motor mounting system used on the launch vehicle has been used on both full scale and sub-scale launch vehicles for many years in the past. The design features two body tubes of different diameters, one bulkhead, three centering rings, and one motor retention system. One of the body tubes has an inner diameter equal to the outer diameter of the motor casing and is called the motor mount tube. The other body tube has an outer diameter equivalent to the main body tube. This body tube is referred to as the fin can. A bulkhead is placed at the most forward edge of the motor mount tube. Three rings are placed around the motor mount tube, and make contact with the inner diameter of the main body tube. These rings ensure that the motor casing, therefore the motor, remains centered throughout all stages of flight. This prevents any thrust gimbaling that would lead to catastrophic failure of the launch vehicle. For the entirety of the motor mounting system, components will be integrated using JB Weld, a heat resistant epoxy that is capable of handling the high temperatures the components experience during motor burn. To ensure the structural stability of this design with the current launch vehicle, multiple load analyses were completed. First, the maximum thrust of the motor, 400.1 lbf, was divided by the surface area of the cap bulkhead that will interact with the motor during its burn stage, 27.34 in^2 to give a maximum normal stress on the bulkhead of 14.63 psi. Fiberglass has a yield strength of ~30,000 psi, which makes it more than capable to hold the motor in place. Using the same maximum thrust of the motor and the surface area of contact between the bulkhead and the motor mount tube, the force felt by the JB Weld attaching the motor mount tube to the cap bulkhead will be only 166.3 psi, which is also well under the 3,960 psi yield strength of JB Weld. The only

force felt on the carbon fiber motor mount tube will be due to the shear stress between the motor and the carbon fiber itself. This was calculated by dividing once again the maximum thrust of the Cesaroni L1395 motor, 400.1 lbf, by the interior surface area of the motor mount tube, 230.44 inches, to give a stress of 1.74 psi. Carbon Fiber has a longitudinal tensile strength of 300,000 psi, which makes it more than capable of handling the load of this design.

The motor is retained using the AeroPack motor retention system described in Section 3.1.6.5, which was used last year to great success. It was chosen again for its ease of installation and use and its reliability in flight. The AeroPack website claims that the retention system is capable of securing Cesaroni motors and reviews from other hobby rocketry websites suggest similar results. To further validate the system, another load analysis was conducted on the adaptor piece of the retainer to ensure that the JB Weld epoxy would hold throughout the flight. The retainer requires there to be at least 0.75 inches of motor mount tubing protruding from the aft centering ring. This meant that the minimum surface area for the epoxy to be applied is 7.363 in^2. The stress on the cured epoxy would be the weight of the motor, 9.457 lbs, assembly divided by the surface area covered by epoxy, yielding 1.284 psi, which again is much less than the yield strength of JB Weld epoxy, 3,960 psi.

These analyses show that the dimensions the team has chosen for the motor mount tube are sufficient to withstand the stresses exerted by the most powerful motor under consideration, and that the location where the motor retention system is connected to the launch vehicle is capable of withstanding the maximum loads that can be applied to it. Proper construction protocol will ensure that all components are assembled properly. As the materials being used are purchased and customized commercially and the materials have been used successfully in the past, the team is confident that this proven design will ensure proper motor mounting and retention in the full-scale launch vehicle.

3.1.7.4 Mass of Launch Vehicle

Mass is one of the primary driving factors of apogee and performance, and is therefore important to track in the design of the launch vehicle. For this reason, Table 12 shows the weight of each component of the vehicle.

Table 12. Weight of major rocket structural components.

Component	Mass (oz)
Nose Cone	30.7
Rover Payload Bay	
Rover Tube	40.8
Transition Tube and Coupler	17.3

Payload Equipment	88
Bulkhead	6.45
Parachute Bay	
Parachute Bay Body Tube	67.8
Main Parachute	53.7
Drogue Parachute	18
CRAM	44.3
Air Braking Payload Bay	
Bulkheads (2X)	5.66
Payload Equipment	113.4
Fin Can	
Fin Can Body Tube	43.1
Motor Mount Tube	14.7
Bulkhead	6.08
Centering Rings (3X)	3.99
Motor	153
Fins (4X)	29.6
Motor Retainer	5.6
Tie Rods (4X)	3.36
Miscellaneous Mass	3.96
Total	773

The above estimates are based on past experience with certain materials, as well as with manufacturers' specifications. The OpenRocket simulation of the rocket has the center of gravity

at 79.83 inches aft of the tip of the nose cone. Based on rockets from previous years, the launch vehicle is not expected to increase in mass by more than approximately 5% over the remainder of the project. Any remaining change in mass will most likely be due to errors in manufacturer's posted properties as well as some added weight from miscellaneous sources, such as epoxy. An increase in mass more than this will require another motor to be selected. Additionally, if the mass of the vehicle continues to decrease, ballast can be use in order to control the apogee of the rocket. A ballast retention system has been designed for this purpose, the details of which can be found in Section 3.1.6.7.

3.1.8 Construction and Assembly

Construction of the full-scale launch vehicle will begin at the beginning of the 2018 spring semester. A general construction and assembly plan is laid out for the full-scale vehicle. This plan will be followed as a general guide, but will be modified as necessary during construction to ensure a robust design. Proper safety precautions will be followed at all points during construction and assembly. All materials used in this design have been used previously, so safety techniques for working with these materials are already known. Given that carbon fiber and fiberglass are difficult to work with, the team will be ordering these components from professional vendors. Certain sections will be cut to specifications by the vendors themselves. These include the body tube and transition sections, as well as couplers. Other parts of the vehicle will be cut to proper specifications on Notre Dame's campus by the AME Machine Shop in Cushing Hall, run by Leon Hochtla, once the proper material is ordered. The construction and assembly plan will be laid out in three main sections. These are the same sections discussed earlier that correspond to the separate tethered sections during recovery. The first is the Rover Payload Section, which consists of the nosecone, the rover payload, and the transition section. The second section, the Air Braking Payload Section, consists of the main body tube, the recovery components/parachute, and the air braking payload. The third section, the Fin Can, consists of the Motor mount and fins. Each section will be further divided into their specific components. For certain components, no construction is required as the component is purchased in its entirety. Therefore, only assembly will be covered for these components.

Many aspects of the launch vehicle can be assembled and constructed concurrently. The Air Braking Payload, CRAM, and Rover Payload are constructed separately from the rest of the launch vehicle.

When epoxying, time must be taken to ensure that the epoxy has time to properly set. This is especially important during construction of the fin can. The fins must be applied separately to ensure that the epoxy does not shift during the waiting period. Each fin will be done separately to eliminate this problem.

3.1.8.1 Full Scale

Section 1 – Rover Payload Section
The Rover Payload Section consists of the nosecone, the rover payload, and the transition section.

1.   The nosecone will be purchased from Apogee Rockets in its entirety. Therefore no construction is required. More information on the nosecone specifications can be found in Section 3.1.5.1. Prior to assembly, the nosecone will likely be sanded with a very fine sand paper to reduce drag. The nosecone will also be painted, though it is currently unknown if this will be before or after the test launches. As discussed in Section 5.1, the nosecone must be capable of separating from the rover body tube. A bulkhead will be placed in the nosecone at roughly half of its length. Another bulkhead, which will be used to integrate the nosecone with the rover payload, will be placed in the shoulder of the nosecone. These bulkheads will be paced in the nosecone using epoxy. When the charges in the Rover Payload are deployed, the nosecone will be ejected.

2.   The details of the Rover Payloads construction can be found in Section 5.1. As discussed earlier, a bulkhead will connect the nosecone to the Rover Payload.

3.   The transition section will be bought from Carolina Rocketry in its final configuration. The team does not have the proper tools or expertise to properly machine a piece of this complexity. The transition section features a shoulder/coupler section on both ends that allow it to integrate with the Rover Payload at the wider section, and the main body tube at the smaller section. The top of the transition section will be integrated to the rover body tube using four bolts placed 90° from one another. The holes for these bolts will be drilled with a drill press located on Notre Dame's campus. A fiberglass bulkhead will be placed at the top of the coupler that attaches the transition section to the main body tube. The bulkhead will be epoxied to the coupler. This bulkhead will be cut by the AME Machine Shop on Notre Dame's campus as discussed earlier. It will also feature a hole to allow the mounting of an eyebolt for recovery purposes. As this entire section must separate during recovery, shear pins will be used to for integration purposes between the main body tube and the bottom of the transition section. Holes will be drilled into the transition section and the body tube using a drill press located on Notre Dame's campus. Four shear pin holes will be drilled at 90° apart to ensure that the sections do not separate prior to the black powder charges being activated.

Section 2 – Air Braking Payload Section
The Air Braking Payload Section consists of the main body tube and the air braking payload.

1.	The main body tube will be purchased from Carolina Rocketry, already cut to specifications. This body tube will house both the drogue and main parachutes, the CRAM (recovery module), and the air braking payload. Construction of the CRAM is covered in Section Section 3.3. Construction of the air braking payload is covered in Section 5.2. There is no further construction that must be done on the main body tube. In order to integrate the main body tube with the transition section coupler, shear pins will be used as discussed earlier. This allows the vehicle sections to be properly integrated during launch but remain capable of separating during the recovery stage. Similarly, the main body tube and air braking payload coupler will be integrated using shear pins to facilitate separation during recovery. The fore bulkhead, located at the top of the air braking payload coupler, will feature a 1,500 lb rated eyebolt as discussed in Section 3.3. The shock cords will be attached to this eyebolt with a 2,000 lb rated quicklink, as discussed in the section mentioned above. The bulkheads are attached to their respective components using epoxy. All bulkheads are made of fiberglass, and are cut in the AME machine shop on Notre Dame's campus.

2.	The air braking payload construction is covered in Section 5.2. The air braking payload coupler and the fin can will be attached using threaded rods and two bulkheads, one at the top of the motor mount and another at the bottom of the air braking payload coupler (Aft bulkhead). four rods, each 0.25 inches in diameter, will extend through the air braking system through both bulkheads. Locknuts will be used to secure the rods to the bulkheads. These bulkheads are also made of fiberglass and cut to specification in the AME machine shop.

Section 3 – Fin Can
The Fin Can consists of the motor mount and the fins.

1.	The motor mount system is composed of two body tubes, one bulkhead, one motor retention device, and three centering rings. The fiberglass bulkhead discussed in the Air Braking Payload (ABP) section that is attached to the motor mount serves to integrate the ABP section with the fin can. The centering rings ensure that the body tube the motor casing will be placed in is properly centered. The two body tube sections are purchased from professional vendors and cut to specifications. The fiberglass bulkheads and centering rings are cut in the AME machine shop to the proper size. Epoxy will be used to integrate the centering rings and bulkhead to the fin can tube at the proper locations. To form the entire motor mount, motor mount tube will be inserted into the series of three centering rings that are now epoxied to the fin can body tube. The motor retention system is described in Section 3.1.6.5. To attach the centering rings, epoxy will be applied to the inside of the fin can body tube slightly before proper location. The ring will be inserted into the tube, which will push the epoxy slightly forward into the proper location, along with the ring. More epoxy will be applied at contact points between the tube and the ring. The bulkhead will be attached in a similar manner.

2.   The fins are made of carbon fiber. The fins will be cut in Notre Dame's AME Machine Shop. Once the fins are cut to size, the edges must be sanded down. Using a set of sanding blocks that the team has used in the past, the leading and trailing edges of the airfoil will be sanded down to different profiles. The thicker radius at the leading edge helps keep flow attached over the fins. The leading edge has a thinner radius than the trailing edge. The tip chord of the fins will also be sanded to reduce drag. To integrate the fins into the fin can, the fins will be inserted into the slots that are cut in the fin can. At this point, they will be inserted until the root chord is level with the motor mount. The fins will then be epoxied and filleted to ensure that the fins remain attached during flight without a dramatic increase in drag. Epoxy will be applied on the underside of the root chord of the fin prior to inserting it into the fin can. More epoxy will be applied at the intersection between the fin can and the fins themselves. A fin alignment guide will be made using either a laser cutter or via 3-D printing to ensure that the fins remain perpendicular to the fin can.

3.   When assembling the fin can, it is crucial that the centering rings are epoxied in such a way that rail buttons can be properly placed. To ensure the rail button remains attached properly, a small block of wood will be placed on the inside of the fin can. A hole will be drilled through the fin can into the block of wood. The rail button will then be inserted. If the centering rings are applied improperly, it can lead to the rail button locations being inaccessible, which means that the wooden block cannot be used to support the rail button. This will lead to safety problems during launch, as the rail button is more likely to fail.

4.   Since the rocket is variable diameter, a standoff is needed for the rail buttons. These will be printed on Notre Dame's campus and allow for the buttons to be mounted clear of the larger 7.5 inch diameter. These standoffs will be epoxied radially in the same location, and axially one will be placed one inch from the aft of the fin can and the other one inch from the fore of the fin can. They will be aligned using a straightedge and verified with a piece of 1.5 inch rail to ensure that they do not interfere with the main fins. Inside the body tube at these locations, a nut, washer, and wooden blocks will be epoxied so that bolts can secure them. The buttons will be secured with 2.5 inch bolts that attach to these interior nuts.

3.1.8.2 Subscale

The parts necessary for the subscale construction were all acquired during the 2017 fall semester. Guidelines and instructions key to the assembly of the subscale were prepared in advance to the actual construction of the model in order to ensure maximum success in the assembly process. Section I is comprised of the Nose Cone and Upper Body Section, and Section II is comprised of the Fin Can, and Motor Mount. Assembly was decomposed into these two sections resulting in the acceleration of the integration of all parts. Furthermore each process was altered

as necessary once construction had begun in order to mitigate any pertinent issues found during assembly. The subscale model was launched twice. Once with a smooth fuselage and a second time with a 3D printed approximation of the extended Air Braking Payload (ABP). In order to accomplish this, the parachute had to be able to be removed from the rocket so that 3D printed piece could be inserted without hassle. A quick-link was used to create a two-piece shock cord such that a permanent shock cord loop was placed in the upper stage and the rest of the cord and parachute could be attached and detached as necessary. The workshop was utilized when available for all members to participate in the construction of the subscale model, and each section will be described in detail in the following outline.

Section I

The Upper Body Section was comprised of three main components: the larger diameter body tube, the transition, and part of the smaller diameter body tube.

Larger Diameter Body Tube

1. The larger diameter body tube measured 8 inches in length and 3.14 inches in diameter and is made of phenolic. Obtain these dimensions through the use of power tools in the workshop.

Transition

2. To create an aerodynamic transition from the larger diameter body tube to the smaller diameter body tube, construct a transition piece out of cardboard with a fore diameter of 3.14 inches and an aft diameter of 2.27 inches. In order for the shape to be designed in two dimensions and assembled in three, use a template from *ApogeeRockets.com* to create the desired shape.

Upper Smaller Diameter Body Tube

3. The upper part of the smaller body tube measured 9 inches in length and 2.27 inches in diameter and was made of phenolic. Obtain these dimensions through the use of power tools in the workshop.

Shock Cord/Bulkhead

4. Inside of the tube, place a bulkhead made of birch plywood 5 inches from the opening to ensure the stages would separate properly. Attach a small loop of shock cord using generous amounts of epoxy at the end of the tube in order to attach the main parachute shock cord and allow for the interchange the ABP as explained above.

Nose Cone

5.   The Nose Cone is 11.25 inches in length and 3.14 inches in diameter made of polypropylene. Attached it to the main body tube by methods of bolting in order retain structural integrity for the duration of the flight. As a result, it remained in place for the entire flight.

Section II

Fin Can

6.   The Fin Can measured 12.2 inches in length and 2.27 inches in diameter made of phenolic. Obtain these dimensions through the use of power tools in the workshop.

3D Printed Air Braking Payload

7.   Attach the 3D printed ABP model to a coupler with epoxy such that it can be interchanged with a plain coupler in order to simulate the effect of the air braking tabs during flight.

Centering Rings

8.   The three centering rings were 2.15 inches in diameter, with a 1.28 inch inner diameter, and .25 inches in length made of birch plywood. Three of these were used to center the motor mount. Secure them inside the fin can with epoxy at the following distances from the aft side of the fin can: 0.25, 2.00, and 5.50 inches.

Parachute and Shock Cord

9.   Attach the parachute to the shock cord and use the quick-link to attach and detach the main part of the parachute to the small loop in Section I as described above.

Motor Mount

10.   The motor mount measured 6.5 inches in length and 1.28 inches in diameter made of phenolic. Obtain these dimensions through the use of power tools in the workshop. Secure the motor mount inside the centering rings with epoxy.

Fins

11.   The fins were trapezoidal, with the root chord and tip chord both 2.8 inches in length, with a 31.6 degree sweep angle. All four fins were made of birch plywood. Cutting four equally spaced slots in the base of the fin can, insert the fins and secure them with epoxy such that the root of the fin is touching the motor mount. It is crucial that the fins are placed at ninety degrees to the fin can as it will otherwise result in unstable flight.

3.1.9 Verification of Vehicle Design

Requirement	Requirement will be verified by:	Method of verification and status
Airframe Strength and Structural Stability	- Vehicle will be designed using materials strong enough to withstand forces of flight and landing. -Conduct finite element analysis - Inspect airframe after full-scale test to identify any damage	-The launch vehicle has been chosen to be made from carbon fiber and fiberglass, both strong enough to survive flight. - FEM Analysis in ANSYS through Notre Dame's Center for Research Computing (CRC) - Inspection after full-scale test launch in Feb. 2018
Accuracy of Center of Mass Calculations	-Estimations of individual masses and center of mass location using software -Measurement of individual masses and center of mass	-Center of Mass calculated using Openrocket and RockSim program models -Weigh each component with scale before assembly and balance assembled full scale rocket at center of mass
Effectiveness of Air Braking Payload	-Drag estimation using computational fluid dynamics -Subscale wind tunnel testing measurements -Subscale flight test measurements	-Analysis in ANSYS Fluent through Notre Dame's Center for Research Computing -Force measurements at different wind speeds using a force balance -Subscale flights completed on Dec. 2nd, altitude data confirms significant change in altitude with Air Braking Tabs Deployed.

	-Full scale testing measurements	-Comparison of between altitude data with payload deactivated and activated during Full Scale launches in Feb. 2018.
Aerodynamic effect of variable diameter rocket geometry	-Computational fluid dynamics simulation to ensure no boundary layer separation or shock over the length of the rocket -Subscale wind tunnel testing to verify computer simulations	-Initial Analysis in ANSYS reveals no boundary layer separation or shock. -Additional analysis in ANSYS Fluent through Notre Dame's Center for Research Computing -Force measurements at different wind speeds to ensure no significant increases in drag due to these effects
Fin Strength and Alignment	-Design Fins using materials strong enough to withstand forces of flight and landing -Creating finite element models and analyzing potential loads -Analyzing fins prior and after each launch for damage -Ensuring proper alignment during construction with laser cut fin alignment mechanism	-Fins designed to be made from carbon fiber, strong enough to withstand these forces. -FEM Analysis in ADINA -Post Full Scale Launch Test Inspections -Visual inspection and angle verification with protractor
Air Braking System Integration	-Ensuring the payload tabs do not endanger the structural integrity of the launch vehicle	-Full Scale Tests in Feb. 2018.
Deployable Payload Integration	-Ensuring rail system for rover is secured to body tube, and that the rover is secured to the rail system	-Visual inspection during construction in Jan. 2018, overseen by construction expert. -Shake Tests in Feb. 2018.

Recovery Integration	-Shear pins shear as predicted -Ensuring that the bulkheads and eye-bolts supporting the system are robust	-Black powder charge tests before launch -Shake testing before launch -Inspection of system after full scale flight in Feb. 2018.
Motor Integration and Retention	-Verifying the sizes of purchased material prior to construction -Performing load analysis on chosen system using simulations -Launching full scale rocket with the chosen motor	-Inspection and measurements using calipers and rulers upon reception of material in Jan. 2018. -FEM Analysis in ADINA -Inspection of motor retention after full scale test flight
Motor Performance	-Simulations to predict apogee of rocket with chosen motor -Subscale flight to compare prediction software to actual results -Full scale flight to measure apogee of rocket with chosen motor	-Simulations run in RockSim and OpenRocket verify that apogee is acceptable. -Successful subscale flight on Dec. 2nd used to compare simulation data to achieved apogee -Gather and analyze altimeter data of full scale test flight in Feb. 2018.
Ballast will not move throughout flight.	-Proper retention of ballast within ballast container, and proper retention container in the body tube -Full scale flight to ensure that ballast and ballast container does not puncture or move during flight	-Shake tests of ballast container with ballast loaded and body tube with container loaded -Inspection after full scale test flight in Feb. 2018.

KEY: Not started; In Progress; Finished

3.1.10 Risks and Mitigations

The team understands engineering projects often run into problems such as scarcity of time, budget, resources, etc. The team uses the following mitigation techniques in Table 13 to ensure that the project is not derailed.

Table 13. Risks and mitigations.

Risk	Likelihood/Impact	Mitigation Technique
Budget	Low likelihood/Low Impact	The Vehicles Sub-team has developed a budget within whose bounds it always tried to stay. There is material left over from previous years. This material is used to perform tests or to test out ideas, particularly in form of payload integration. The budget for the Vehicles Sub-team is shown in Appendix K. The team estimates that the budget can only go down because it shot high to start choosing expensive material (such as Carbon Fiber and Fiberglass) that may not end up being needed. This covers the oversights. The only foreseeable budget problems lie in integration material, such as screws and nuts, but these items are not overly costly and the University workshops keep them.
Time	High Likelihood/Medium Impact	The Vehicles Sub-team is organized in such a way as to help members stay on top of their work while not being affected by those who may be behind. Members own certain sections and work on these throughout the design and construction process. All members are aware of launch dates and deadlines and work with an internal deadline of one week before the NASA SL or launch deadline. In cases of testing, scheduling is done in the month of November for December test dates, results of which are included in the CDR.
Resources	Low Likelihood/High Impact	It is unlikely that the team runs out of physical resources, as plans will be made for any needed resources and they will be ordered before they are required, but using up all available resources and not planning will slow the project. Material for

		construction of full scale is ordered in December for January launches so that any missed material can be ordered in time. In terms of human resources, the Vehicles Sub-team has a member who "owns" a sub-system, but there is usually a secondary person who is somewhat familiar with the sub-system and who can take over should the primary owner not be available.
Functionality	Medium Likelihood/High Impact	Functionality of the rocket is a top priority for the team. Testing, computer models, and subscale models will help the team determine what steps need to be taken to ensure the final product meets project goals. The Sub-team emphasizes the need for robust verification methods to ensure that what has been designed meets the requirements. Functionality goes hand in hand with time, because whatever doesn't work as intended must go through a redesign process. Resources also play a role because resources must be moved around so that certain functionalities can be perfected. Functionalities that directly affect flight are prioritized.
Safety	Low Likelihood/High Impact	Dangerous materials (rocket motors and carbon fiber) and tools will be used to construct the rocket. Ensuring safety through proper protective equipment and communication with the team's safety officer will mitigate risk to team members. The mentor handles the motors; therefore, this is not a concern. The Carbon fiber may be a bit tricky since the team has not used it before to this scale, but workshops exist on campus with construction experts that are willing to help the team with ventilation.

3.2 Subscale Rocket

In order to verify that the full-scale rocket will be stable as well as test the altimeters being used for the full scale, a subscale rocket was build and launched. The main goal of this rocket was to not only verify stability and the altimeters, but to compare altimeter data to that of

OpenRocket and Rocksim. Doing this allows the team to gage how much it can rely on the simulation software for the prediction of flight data for the full-scale rocket.

3.2.1 Rocket Scaling and Materials

The subscale rocket was built to a 40% scale of the final design by axial length and body tube diameters. This scaling was due to the existing supply of body tubes available to the team, and because of this certain components were not scaled to exactly 40%.

The subscale's aerodynamic structure is very similar to that of full scale, with the exception of the nose cone. The axial length and diameter of both the forward, aft, and transition sections of the rocket all scale correctly to 40%, however, the nose cone was commercially bought, and does not scale to exactly 40%. This complication was taken into account in the simulations and was determined not to be a critical issue for the rocket.

The subscale's internal structure, however, was much different than the full scale. This was mainly due to the fact that the Deployable Rover Payload was not simulated in the vehicle. Therefore, to compensate for the lost weight of the payload, the avionics were placed in the forward section of the rocket where the Deployable Rover Payload would be. Additionally, the CRAM recovery system was not needed, since the motor used in the launch had an ejection charge built in. Finally, the Air Braking System was simulated by an interchangeable coupler, one with a length of phenolic body tube and another with a 3-D printed section with air braking tabs scaled to 40%. There was no internal structure to the Air Braking System for two reasons. It was not needed to control the extension of the tabs, and it would interfere with the deployment of the parachutes upon ejection charge ignition.

Another major difference between the subscale and the full scale was the choice of materials. For the subscale, due to limited time, funds, and workshop access, phenolic was used for the main body tube structure and couplers. Birch plywood was used for the bulkheads, centering rings, and fins. And finally, Bristol paper was used to craft the outer structure of the transition section. A summary of the material properties can be found in Section 3.1.7.2.

3.2.2 Subscale Characteristics

A summary of the subscale rocket's dimensions can be found in Table 14. As stated above, some of these dimensions are not exactly 40% of the full-scale size due to constraints such as material availability and mission requirements.

Table 14. Subscale rocket dimensions.

Property	Value
Length of Rocket (in)	52.25
Fore Outer Diameter of Rocket (in)	3.14
Aft Outer Diameter of Rocket (in)	2.27
Transition Length (in)	1.6
Number of Fins	4
Fin Root Chord (in)	2.8
Fin Tip Chord (in)	2.8
Fin Sweep Angle (°)	31.6
Fin Height (in)	1.77
CG Position from Nose Cone (with motor) (in)	32.48
Weight without Motor (lbs)	2.23
Weight with Motor (lbs)	2.51
Estimated Stability Margin without Motor	3.44
Estimated Stability Margin with Motor	2.74

The motor used for the subscale rocket was chosen due to the fact that it has a relatively similar thrust curve to the full scale's motor, the L1395. The Aerotech G78-7G was chosen as the propulsion for the subscale rocket, and its thrust curve can be found in Figure 20. This motor has a 7 second delay deployment charge built in, which eliminates the need for the CRAM recovery system. The characteristics of this motor can be found in Table 15.

Table 15. Characteristics of the G78-7G.

Motor Classification	AeroTech G78-7G
Diameter (in)	1.14
Length (in)	4.88
Average Thrust (lbf)	17.96
Maximum Thrust (lbf)	22.91
Total Impulse (lbf*s)	24.70
Burn Time (s)	1.4
Total Weight (lb)	0.28
Propellant Weight (lb)	0.13
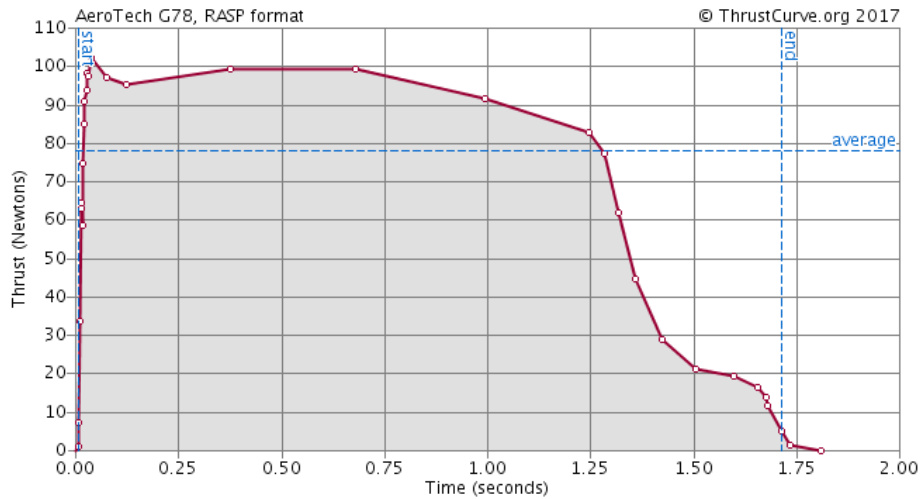
Figure 20. Thrust Curve of the Aerotech G78-7G.

Finally, an image of the fully assembled rocket can be found in Figure 21.

Figure 21. Subscale rocket fully assembled.

3.2.3 Subscale Results

The subscale launch took place on Saturday, December 2nd, 2017 in Three Oaks, Michigan. Two flights were carried out, one with the control body tube coupler and another with the simulated drag tabs. The launch conditions for this day can be found in Table 16.

Table 16. Launch Day Conditions in Three Oaks, MI (12/02/17).

Condition	Value
Temperature (°F)	42
Wind Speed (mph)	10
Pressure (inHg)	30.13

Latitude (°N)	41.799
Longitude (°W)	86.611
Altitude (ft)	692

Using these conditions, the subscale rocket was modeled in OpenRocket and Rocksim. The model was made for only the control flight, since neither of these software packages are able to physically model the drag tabs. Additionally, they are also able to accurately model the rail buttons made for the rocket, and therefore these were not included either. These results for the simulated flights, as well as the actual subscale launch, can be found in Table 17.

Table 17. Subscale predictions and results.

Source	OpenRocket	Rocksim	Subscale Control	Subscale With Tabs
Apogee (ft)	976	989	919	858
Off-rail Velocity (ft/s)	63	58	60	--
Flight Time (s)	211	218	54	--
Time to Apogee (s)	7.74	8.01	8.71	--

As seen in the table above, the predictive software overestimated the apogee by approximately 60 feet in OpenRocket, and 70 feet in Rocksim. This overestimation suggests that the software packages do not correctly estimate the drag on the rocket, which can be attributed to the absence of rail buttons on both models. The off-rail velocity and time to apogee were estimated fairly accurately, and the flight time is irrelevant for these purposes.

The subscale launch was a success from the standpoint that the team knows that the rocket design is aerodynamically stable. This verifies the previous CFD analysis on the variable diameter design, and allows the team to move forward with this for the full-scale vehicle. Additionally, the test flight with tabs deployed verifies that the Air Braking System does indeed

have a significant impact on the aerodynamic drag of the rocket. The altimeter data from the launch will be analyzed further in order to create an accurate altitude control model for the full-scale system.

However, the subscale launch also reveals to the team that the predictions in OpenRocket and Rocksim are not to be taken as exact. The overestimation by both programs is taken into account for the full-scale models, and as of now both programs will continue to be used as sources of simulation data. These models will be assessed once again after the completion and acquisition of full-scale test launches scheduled for February 2018.

3.3 Recovery Subsystem

3.3.1 Component Selection

Altimeter - Based on the specifications of the altimeters, the *Raven 3* is the final choice for the recovery systems altimeter. The *Raven 3* is smaller and lighter, which will allow it to fit comfortably into the final CRAM design.

Battery Connector - Based on the needs of the recovery system and desire for greater reliability, the battery box is the final choice for battery connector. This method has the added benefit of containing a convenient arming switch for the independent avionics systems.

Eyebolts and Connector Nut - Since reliability and robustness is the most important aspect for the recovery system components, the stainless steel eyebolt and coupling nut are the finals choices for the harness hardware.

Bulkhead - With the possible need for repeated manufacture and also for resistance to wear under use, acrylic is the final material for the recovery bulkheads.

Harness Connector - Since accessibility and rapid-securing is of importance to this part of the recovery design, the choice between clip and screw carabineer is not immediately obvious. However, the added reliability of the screw connector Quick links makes them the final design choice.

3.3.2 Parachute and Harnesses

Parachutes - Two parachutes will be employed in the recovery system. A drogue parachute will deploy at apogee and a larger main parachute will deploy at 650 feet above ground level using the primary charge. The drogue parachute selected is the *FruityChutes Iris Ultra 24" Compact Chute.* The parachute is made of Nylon with Kevlar bridles. The main parachute selected is the *FruityChutes Iris 144" Compact Chute.* Also made of Nylon with Kevlar bundles, this larger

chute will ensure a gentle and energetically-appropriate landing with the increased mass of the rocket (compared to previous years).

Harnesses - The harnesses of the recovery system are *FruityChutes* Nylon shock cords. Measuring 9/16 inches in width and rated for 2400 lbs, this selection exceeds expected forces by approximately five times, ensuring successful tethering. The shock cords will be tied at each junction with the parachutes or recovery hardware wherever necessary using highly secure knots. The length of shock cord between each body tube section will be approximately 40 feet upon descent. The parachutes will be secured at one-third the total length to ensure the body tube sections do not interfere during descent. To protect the shock cords and parachutes form black powder charges, Nomex cloth will be implemented in the harnesses. Two 24 inch octagonal Nomex blanket from *FruityChutes* will provide coverage for the drogue and main parachutes. Two 30" tubular Nomex pieces from *Apogee Rockets* will be positioned on the combustion end of each shock cord to prevent damage from the explosive hot gas.

Bulkheads - There are two bulkheads within the recovery system which shield the CRAM and its associated electronics from the black powder charges and forces experienced during flight. Quarter-inch, high strength, clear Acrylic from *McMaster Carr* has been selected for this purpose. It will be machined to to fit the shape of the top and bottom surfaces of the CRAM and secured with aerospace grade epoxy.

Attachment Hardware - The most important attachment hardware in the recovery system are the eyebolts and Quicklinks because they will bear the entirety of the force experienced during flight and from parachute deployment. The Quicklinks selected are ⅜ inch zinc-plated steel components from *McMaster Carr,* rated for 2,200 lbs. The eyebolts selected are ⅜ inch forged steel components from *McMaster Carr,* rated for 1,400 lbs. One connector bolt will be implemented inside the CRAM to secure each of the protruding eyebolts. The components selected is an extreme-strength steel coupling nut from *McMaster Carr* with a Grade 2H fastener strength rating. At each interface where eyebolts are screw and unscrewed, split lock washers will be implemented to ensure the motion of the rocket in flight does not cause the connections to loosen.

3.3.3 Electrical Components

The electrical components of the recovery system have been streamlined and improved from previous iterations. A commercial altimeter - the *Featherweight Raven 3* - controls the system, a Duracell 9V battery (housed within a battery switch box) powers it, electronic matches provide the pyrotechnics, and solid-core electrical wiring connects everything together. In previous years, screw terminals were used to join the electronic matches to the other wiring components of the recovery system. However, due to the difficulty and uncertainty of making a robust connection in this manner, they will be replaced with Twist-On No-Crimp Butt Splices

from *McMaster Carr.* These components are the ideal choice for this application because they are quick, require no outside tools, and form highly robust interfaces.

Redundancy is always a major priority for the recovery system, but this aspect is receiving an even more prominent role in this year's design. Instead of the usual double redundant system, the team is employing a *triple* redundant recovery system. More specifically, every aspect of the recovery system will replicated such that there are three independent subsystems which could individually recover the rocket if anything were to fail. Three independent batteries will power three independent commercially-available altimeters, which will ignite three independent charges for the drogue parachute and three independent charges for the main. The axial symmetry of all three redundant systems ensures that preference is not shown to any one in particular and eliminates the variables which would accompany a non-symmetrical layout.

3.3.4   System Design Overview and Update

The following images, Figures 22 and 23, feature the final CAD models of the recovery system. They have not changed since PDR, but are shown here for conceptual clarity moving forward.
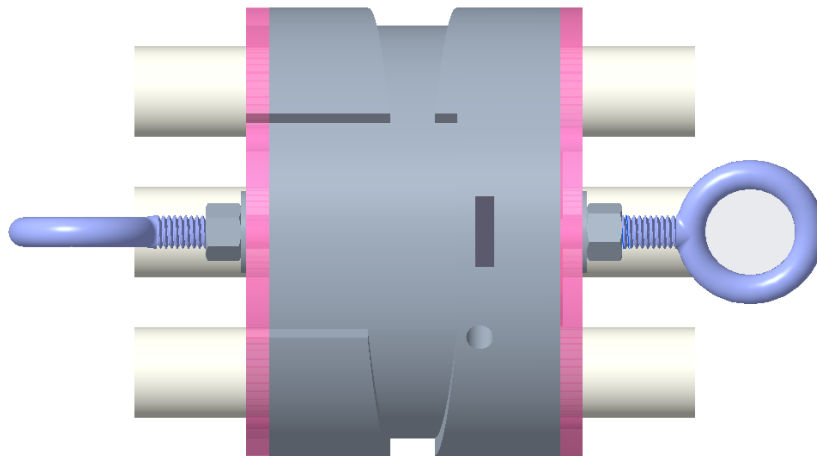
Figure 22. Side view of fully assembled CRAM v4.
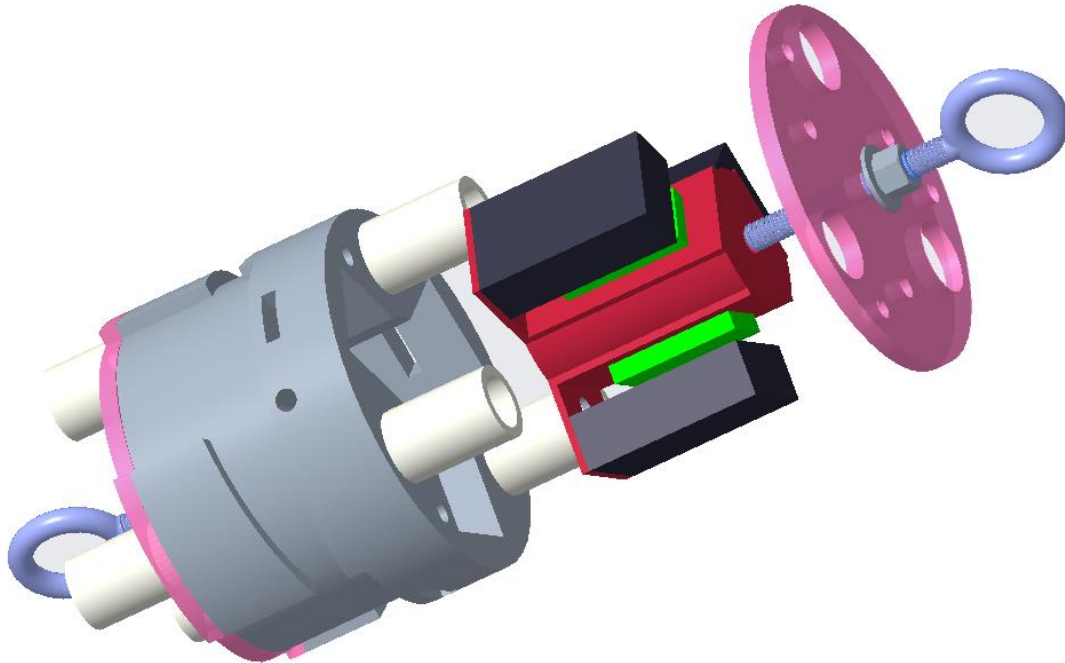
Figure 23. Exploded view of CRAM v4.

Construction of the recovery system has commenced and will ramp up considerably following CDR. The two central components - the CRAM body and the core - have been 3D printed in their final state and are shown in the following picture sequence. Figure 24 shows a top view of the CRAM body and an isometric view. Figure 25 shows an isometric view of the core and the two pieces together to provide a sense of scale.
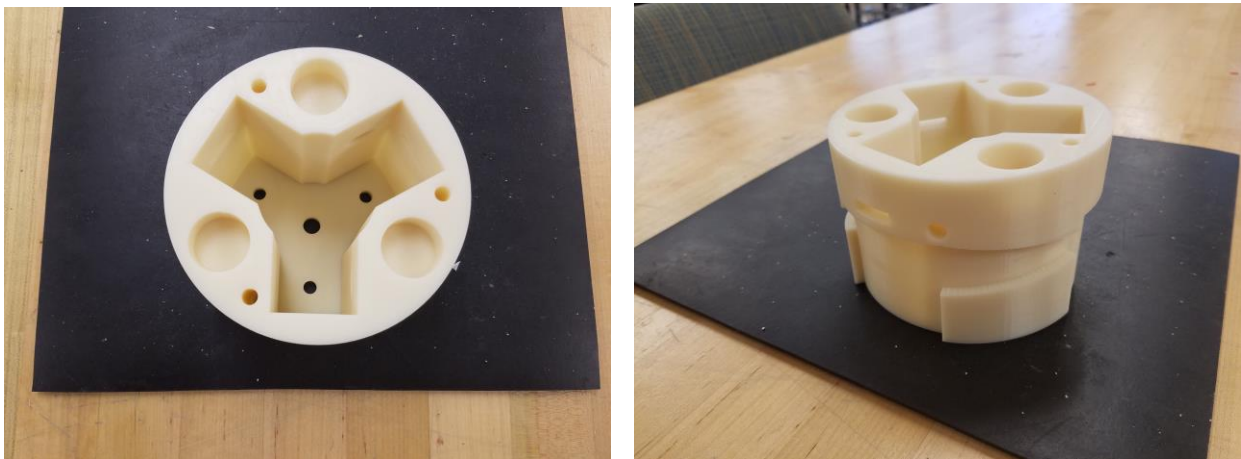
Figure 24. Left - CRAM top view. Right - CRAM isometric view.
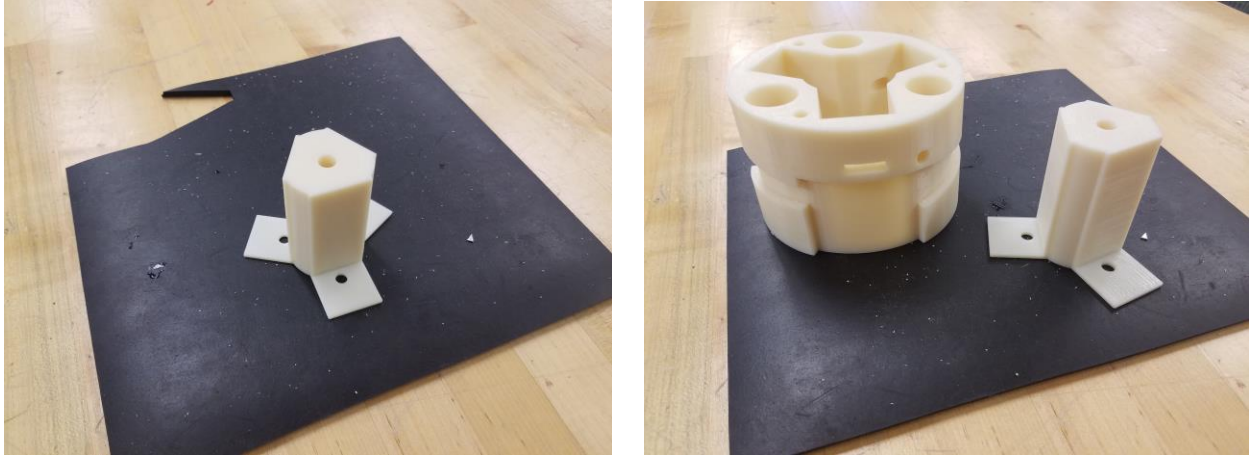
Figure 25. Left - CRAM core isometric view. Right - Whole CRAM system.

3.3.5 Electronics programming and wiring

The subsequent figures serve to explain the logic of the electronics within the recovery system. As part of its triple redundancy, all three altimeters are programmed slightly differently in order to complement each other's timing in the case of a perfectly operational launch, but not so differently that the individual functionality is compromised. This is achieved through slight but sufficient delays between the ejection charges. The logic for all three altimeters is shown in Figure 26 below.
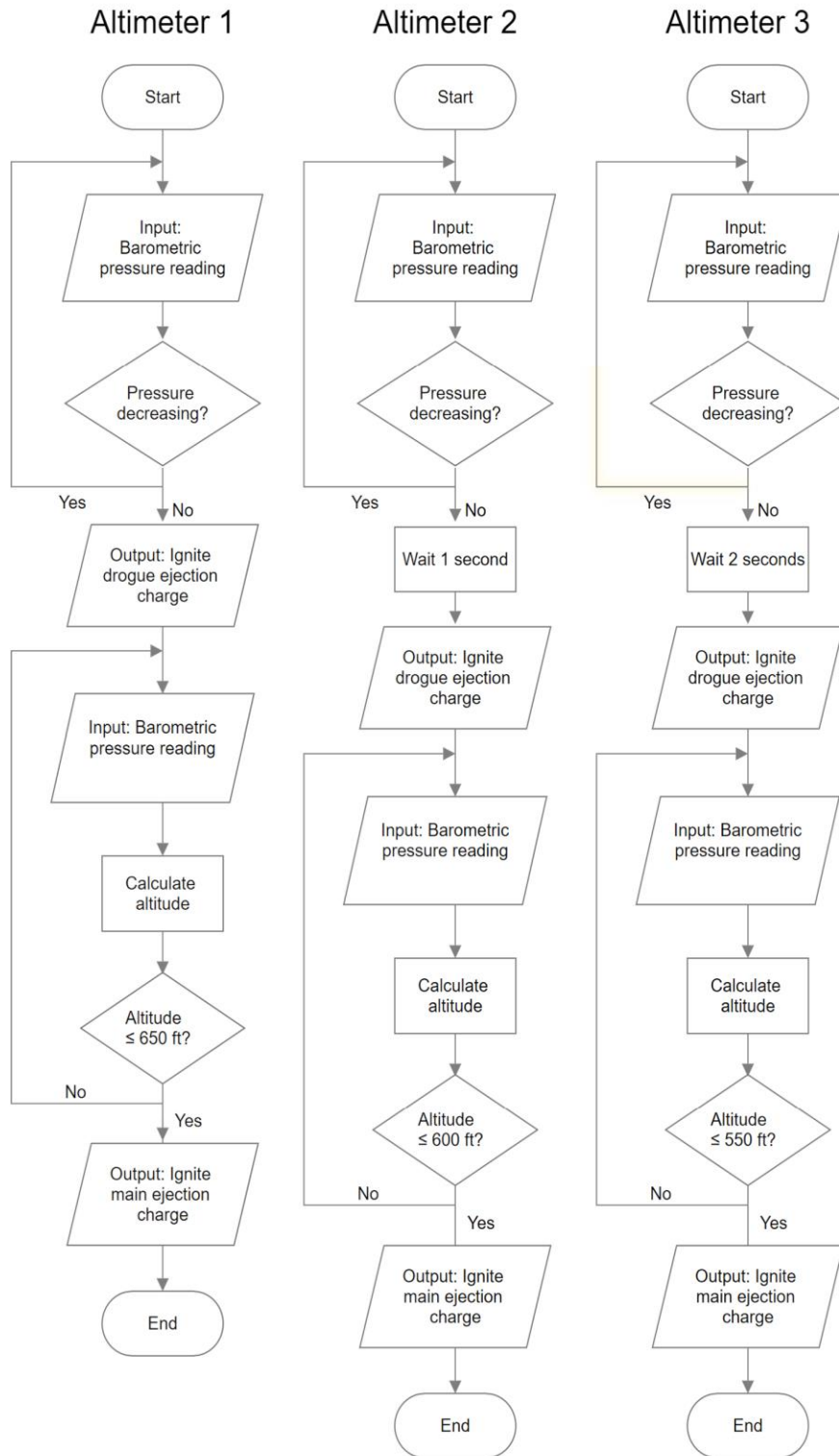
Figure 26. Logic flowchart for the altimeters.

Along a similar vein, the physical logic of the recovery has also been developed. A battery box will power the altimeters which will ignite e-matches situated on the drogue and main sides of the CRAM. The basics of the wiring for these connections are shown below in Figure 27. The same schematic is applicable to all three redundant subsystems.
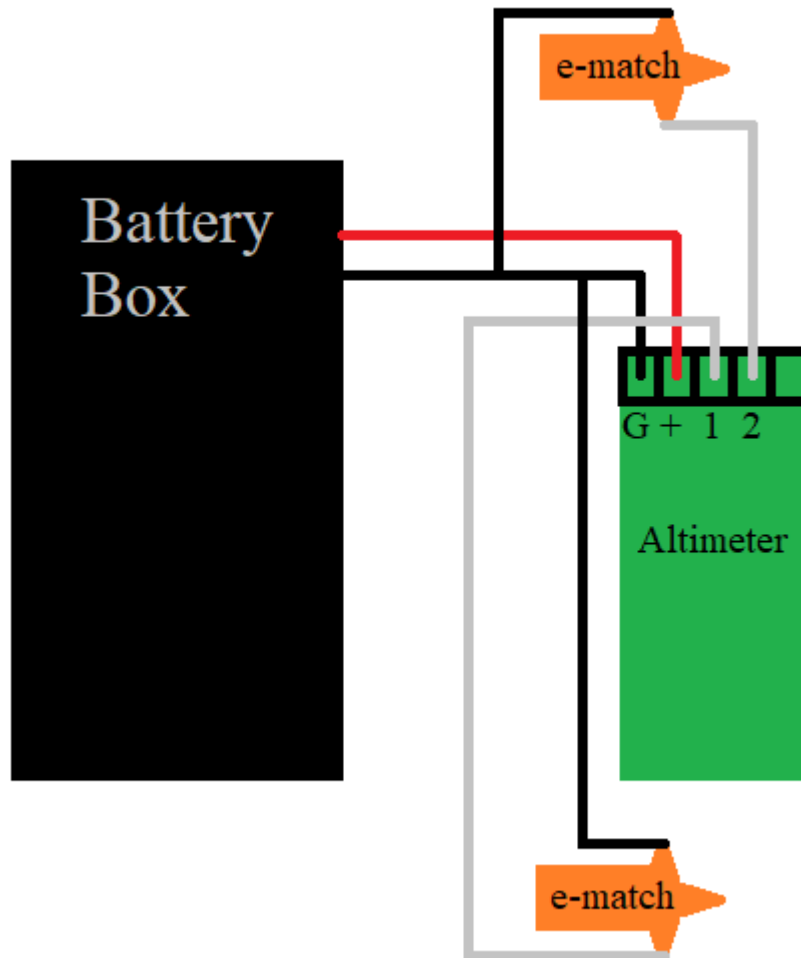
Figure 27. Electrical schematic of battery/altimeter/e-matches.

3.3.6 Mission Performance

Kinetic Energy

The kinetic energy at landing for each rocket section is a function of the descent velocity and the mass of the section in question. Specifically, the kinetic energy equation is shown below in Equation 1.

$$KE = \frac{1}{2}mv^2, \qquad \text{Eq. 1}$$

where *KE* is the kinetic energy, *m* is the mass, and *v* is the velocity. For ease of calculation, quantities are often converted to SI units for use in this equation. Table 18 below shows some various relationships which were used to find the desired values.

Table 18. Useful unit conversions for KE calculation.

SI Unit	Imperial Equivalent
1 Joule (J)	0.7376 ft-lbf
1 kilogram (kg)	35.274 oz
1 meter per second (m/s)	3.28 ft/s

The parachute sizing calculations recommended a 12 foot diameter main parachute to produce a final descent velocity of 12.57 ft/s. The speed can be used in conjunction with the estimated masses of the rocket section to find their kinetic energies. Table 19 below shows the predicted final KE of each section of the rocket upon landing.

Table 19. KE at landing for rocket sections.

Rocket Section	Mass (oz)	Kinetic Energy (ft-lbf)
Nose cone	183.4	28.08
Recovery tube	184	28.17
Fin can	253	38.73

Clearly all the final kinetic energies are within the 75 ft-lbf limit of the competition. In general, the mass of the predicted mass of the rocket has been fine-tuned and thereby reduced since PDR. There remains significant leeway in case a section of the rocket, such as the fin can, ends up considerably heavier than expected.

Wind Drift

To calculate the wind drift, the primary method the team employs is a legacy Matlab code which utilizes the 4th Order Runge-Kutta method to simulate the descent of the rocket for various environmental conditions. The relevant inputs are the rocket weight and the size of the main and drogue parachutes. The code can calculate the velocity descent path, the horizontal descent path, accelerations experienced throughout the flight, and even the kinetic energies of the segments at various times. For the purposes of this section however, only the horizontal path is shown, as seen in Figure 28 below.
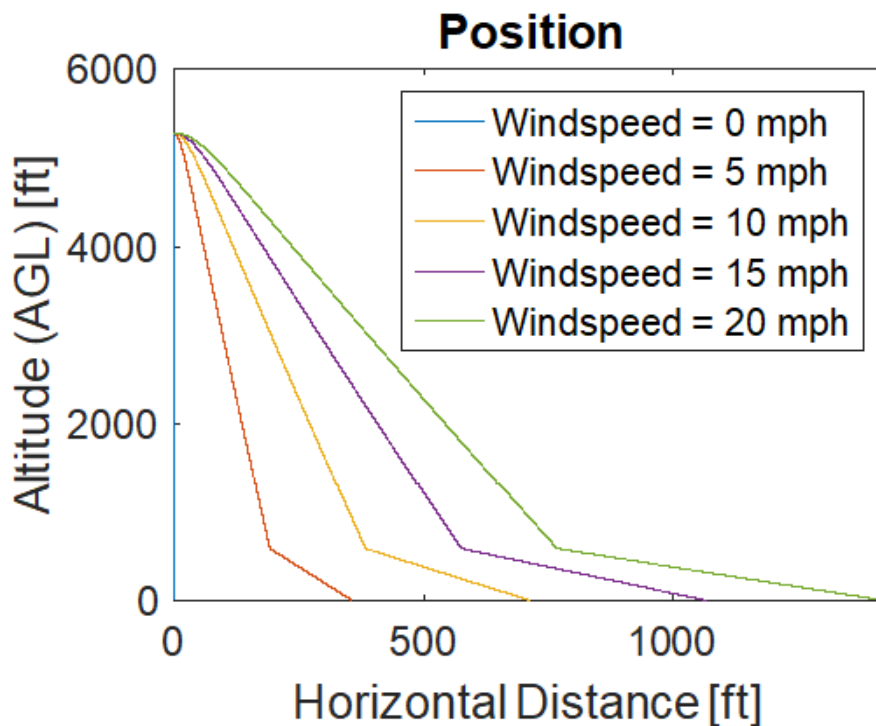
Figure 28. Horizontal flight profile under various wind conditions.

Because the predicted final mass of the rocket has been reduced since PDR, the wind drift has increased for each wind velocity across the board by approximately 200 ft. However, even

under the worst of conditions, the maximum wind drift remains under 1500 ft. This is corroborated by the secondary verification method.

The second method used to calculate drift is through OpenRocket simulation. All the launch vehicle specifications are entered into the program, and it produces data for a wide variety of desired outputs. Figure 29 below graphically displays the simulation data under various wind conditions.
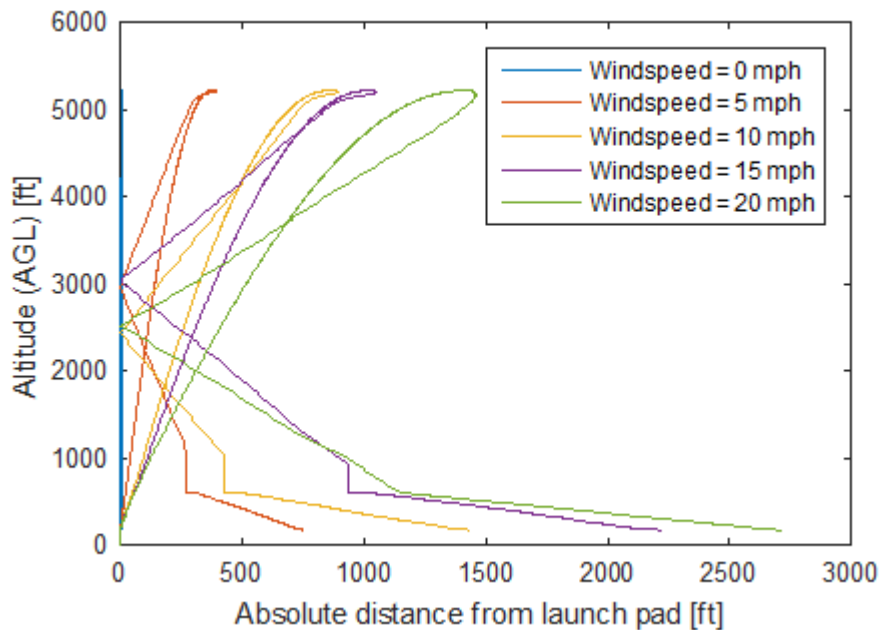
Figure 29. Predicted wind drift from OpenRocket simulation.

Some key differences are apparent between the Matlab program and the OpenRocket simulation. Perhaps most notably, OpenRocket takes into account more launch conditions such as the launch rail angle, wind direction relative to it, and the lateral distance data is taken as an absolute value. This accounts for the looped and backtracking shape of the OpenRocket graphs because the rocket first travels away from the launch pad into the wind, but then passes directly back over the pad during flight due to the wind's influence on the parachutes. Another notable difference is the predicted range of the drift. OpenRocket predicts a much further lateral distance than Matlab. The team has not used OpenRocket for drift simulation in the past and the Matlab program has always been satisfactorily accurate. This means the OpenRocket simulation is most likely in need of further work because its predictions are almost certainly overestimates according to past experience. However, going forward the two methods will be refined and averaged to produce the most accurate possible prediction.

3.3.7 Project plan and verifications

In addition to construction, the other important remaining task for the recovery team is to perform tests and verifications. In the hopes of improved reliability, the team has devised numerous additional tests to be performed on the hardware and software of the system. These are identified and described below.

E-match ignition

The objective of this test is to determine the reliability of the e-matches by passing a current through the bridge wire of the match from a safe distance and without black powder. The test is necessary because there have been issues in previous years of failed e-match products. The test is successful if the pyrogen burns, which is required to ignite black powder. If the pyrogen fails to burn, the set of matches from the same package will be examined for defects and replaced if necessary. Thus, there is no need to make changes to the vehicle or payload.

Altimeter simulation

The objective of this test is determine if the altimeters and their associated voltage ports are operational. The test is necessary because there is no other way besides the included simulations to verify the altimeters are in working order other than a full rocket launch due to the programming of the altimeters. *Featherweight Raven3* altimeters come with simulation software preinstalled. All that is needed is to program them with the desired flight parameters and build a prototype board with indicator lights. When the simulation runs, it will send power from the drogue voltage port to one LED at "apogee" and from the main voltage port at a desired altitude (650, 600, or 550 feet). The test will be deemed successful if the LEDs are illuminated at the appropriate times, as indicated by the simulated altimeter readouts on a computer screen. If the simulation fails, no change will be made to the rocket design but new altimeters will need to be purchased.

Black powder/shear pin

The objective of the black powder test is to ensure that the amount of black powder in the rocket is sufficient to separate the parachute bay from the forward and rear sections (by breaking the securing shear pins) as well as eject the main and drogue parachutes. The test is necessary because too few shear pins with too much black powder may cause the sections to split prematurely, and too many shear pins with too little black powder may cause the sections not to split at all. The test begins by setting up a charge of black powder with an e-match, which is inserted into the parachute bay with parachutes. Next, the sections of the rocket are assembled and secured with shear pins. Then the rocket is placed with its longitudinal axis parallel to the

ground, and the charge is detonated remotely from a safe distance. The test is successful if both the forward and rear sections separate from the parachute bay. Furthermore, the amount of black powder is increased if the test proves unsuccessful, so no changes to the vehicle is necessary. The previous year's black powder test showed that about five grams of powder is sufficient. If the test fails to separate the sections, additional black powder will be implemented in the recovery system.

Connection shake test

The objective of this test is to determine if the new screw-to-lock butt connectors are sufficiently robust for application in the recovery system. The test is necessary because significant forces will be exerted on all recovery system components and it is critical that these forces do not compromise the ejection charge connections. To perform this test, two stray wires will be secured together with the screw-to-lock butt connectors. Then, the connectivity will be tested using a voltmeter. Following the test, the components will be shaken violently by hand to simulate a flight and the forces experienced during a parachute deployment. After one minute of shaking and two drop tests, the connection will be re-tested for connectivity. The test will be deemed successful if the electrical connection between the two ends of the wire is maintained. This test may also be combined with the e-match test to further ensure the reliability of the integrated systems. If the test fails, the recovery system design will call for a different kind of wire connectors.

Altimeter activation

The objective of this test is to validate a system by which the state of the altimeters can accurately be determined on the launch pad. A common issue with the altimeters used by the team is that it is difficult to distinguish if they are all active on the launch pad. While they do emit audible and visible indication, sometimes these indicators overlap, making it difficult to determine if one, two, or three altimeters are active. To overcome this obstacle, a series of tests will be performed to formalize a launch procedure which will reliably determine the state of all three altimeters. First, they will all be installed in the CRAM and the CRAM installed in the body tube, just as they would be before a launch. Then, the battery boxes controlling the power state of the altimeters will be switched on while a nearby stopwatch counts up. The team will turn on the altimeters at different intervals, starting with 5 seconds in between for the first iteration, then 6 seconds in between, etc. The test will be deemed successful when an interval is discovered that makes it clearly apparent, both visually and audibly, that all three altimeters are armed and ready for launch. If the test fails, the recovery system design will call for a specialized audio/light enhancing tool to block out interfering indicators and focus in on the desired altimeter signals.

3.3.8 Recovery System Requirements and Verification Plan

Requirement	Verification Plan
The launch vehicle will stage the deployment of its recovery devices, where a drogue parachute is deployed at apogee and a main parachute is deployed at a lower altitude. Tumble or streamer recovery from apogee to main parachute deployment is also permissible, provided that kinetic energy during drogue-stage descent is reasonable, as deemed by the RSO.	Demonstrate this requirement with a successful launch wherein a drogue is deployed at apogee and a main is deployed a lower altitude.
Each team must perform a successful ground ejection test for both the drogue and main parachutes. This must be done prior to the initial subscale and full-scale launches.	Test this requirement by fine-tuning the proper black powder/sheer pin ratio in a series of tests prior to first full scale launch.
At landing, each independent sections of the launch vehicle will have a maximum kinetic energy of 75 ft-lbf.	Analyze for this requirement by performing simulations and performing calculations which accurately predict vehicle parameters and select design variables which satisfy these parameters.
The recovery system electrical circuits will be completely independent of any payload electrical circuits.	Inspect for this requirement by ensuring no wires from other vehicle sections pass through or enter into the recovery section.
All recovery electronics will be powered by commercially available batteries.	Demonstrate this requirement by indicating the commercial brand name on the batteries power the recovery system and showing no other possible sources of power in the system.

The recovery system will contain redundant, commercially available altimeters. The term "altimeters" includes both simple altimeters and more sophisticated flight computers.	Demonstrate this requirement by pointing out the three axially symmetrical subsystems which independently carry out the task of recovery.
Motor ejection is not a permissible form of primary or secondary deployment.	Demonstrate this requirement by showing separate ejection charges within the recovery system for parachute deployment and indicate no possible way for motor ejection to separate the necessary section.
Removable shear pins will be used for both the main parachute compartment and the drogue parachute compartment.	Inspect for this requirement by ensuring the correct number of shear pins are present at all separation point prior to launch.
Recovery area will be limited to a 2500 foot radius from the launch pads.	Analyze and demonstrate this requirement by running simulations to predict drift radius and observing the actual distance relative to these predictions after full scale launches.
An electronic tracking device will be installed in the launch vehicle and will transmit the position of the tethered vehicle or any independent section to a ground receiver.	Inspect for this requirement in the air-braking payload section of the launch vehicle which will house this instrument in place of the recovery section.
Any rocket section, or payload component, which lands untethered to the launch vehicle, will also carry an active electronic tracking device.	Demonstrate this requirement by noting that only one connected series of rocket sections will descend together and that a tracking device is situated in the air-braking payload.

The electronic tracking device will be fully functional during the official flight on launch day.	Test and inspect for this requirement by determining the capabilities and limitations of the device in test launches, and maintaining appropriate operating conditions (weather, interference from other transmitters) on launch day.
The recovery system electronics will not be adversely affected by any other on-board electronic devices during flight (from launch until landing).	Test and inspect for this requirement by attempting to interfere with the recovery system remotely in a lab setting and ensuring the copper coating is pieced together properly before each launch.
The recovery system altimeters will be physically located in a separate compartment within the vehicle from any other radio frequency transmitting device and/or magnetic wave producing device.	Demonstrate this requirement by locating the altimeters and the radio transmitters and noting they are housed in distinct sections.
The recovery system electronics will be shielded from all onboard transmitting devices, to avoid inadvertent excitation of the recovery system electronics.	Inspect for this requirement by checking for holes or tears in the protective copper tape.
The recovery system electronics will be shielded from all onboard devices which may generate magnetic waves (such as generators, solenoid valves, and Tesla coils) to avoid inadvertent excitation of the recovery system.	Demonstrate that no such devices are utilized in the launch vehicle and refer to previous verifications regarding EM radiation.
The recovery system electronics will be shielded from any other onboard devices which may adversely affect the proper operation of the recovery system electronics.	Test and demonstrate that the transmitters/receivers aboard the rocket do not interfere with the shielded recovery system.

Additional Requirement 1. The recovery system will utilize heat-resistant materials on all surfaces exposed to black powder charges.	Demonstrate that high quality, heat-resistant epoxies, acrylics, PVCs, and electronic components are used on the exterior of the CRAM.
Additional Requirement 2. The recovery system will use <u>new,</u> *Duracell* brand batteries because of their exceptionally robust fused composition.	Demonstrate that only the proper brand of batteries is purchased and installed - <u>new</u> - before each flight.

3.4 Mission Performance Predictions

3.4.1 Validity of Analysis

3.4.1.1 Performance Prediction Program

The Notre Dame Rocketry has created a performance prediction program in Python to calculate both the apogee and the stability of the rocket. The apogee is calculated using the rocket mass, the engine mass, the propellant mass, the air density, the drag coefficient during the thrusting phase, the drag coefficient during the air braking phase, the drag coefficient during the coasting phase, the cross-sectional area, the thrust from the engine, the acceleration due to gravity, and the motor burnout motor time.

The coefficients of drag are especially important in this calculation. This is because there are three distinct different drag coefficients throughout our rocket's flight due to its changing speed and air brakes: the thrusting drag coefficient, the air braking drag coefficient, and the coasting drag coefficient which happens after the air brakes retract. The drag coefficients were calculated using OpenRocket, subscale testing, and wind tunnel testing. Because each of these phases took an amount of time that could be understood as a fraction of the time of flight, the apogees from these phases were summed in a way that took into account each of their respective durations. In other words, to calculate the apogee, the apogee was calculating for each phase, dependent on the previous phase, and then finally summed. The apogee was calculated to be 5330 feet. This is only a rough estimation because the duration of the air braking phase was estimated using subscale flights.

The center of pressure and subsequently, the stability, were also calculated in Python. This was done using the length of nose, the diameter at base of nose, the diameter at front of transition, the diameter at rear of transition, the length of transition, the length from the tip of nose to front of transition, the fin root chord, the fin tip chord length, the fin semi-span, the length of fin mid-chord line, the radius of body at aft end, the distance between fin root leading edge and fin tip, the leading edge parallel to body, the length of rocket minus length of fins and

the number of fins. The stability calculated in this Python program matched previous stability calculations.

3.4.1.2   Wind Tunnel Tests

On November 9th, 2017, both the Vehicle and Air Braking System sub-teams were able to perform wind tunnel testing in the Hessert Laboratory for Aerospace Research. By this time, construction of the subscale rocket was completed, and its design was intended not only for launch, but for testing in the wind tunnel. The characteristics of the subscale rocket can be found in Section 3.2.

The purpose of wind tunnel testing was to verify the drag predictions from OpenRocket and Rocksim. Additionally, the team wished to measure the impact of fully extended Air Braking Tabs on the drag coefficient of the rocket.

To perform the test, a force balance was set up in a wind tunnel big enough to fit the rocket. Data was able to be collected with a drag transducer. The setup for the test can be seen in Figure 30.

Figure 30. Wind tunnel test setup.

Once testing was completed, the data from the transducers was inputted into Matlab in order to yield useful information. However, upon analysis of the data using code created by the

team, it was revealed that the pressure transducer to gage wind speed in the tunnel had been faulty, and all of the data for this tool was corrupted.

However, using the calibration found in Figure 31, force data for the model was able to be found. The results of the wind tunnel testing can be found in Figures 32 and 33.
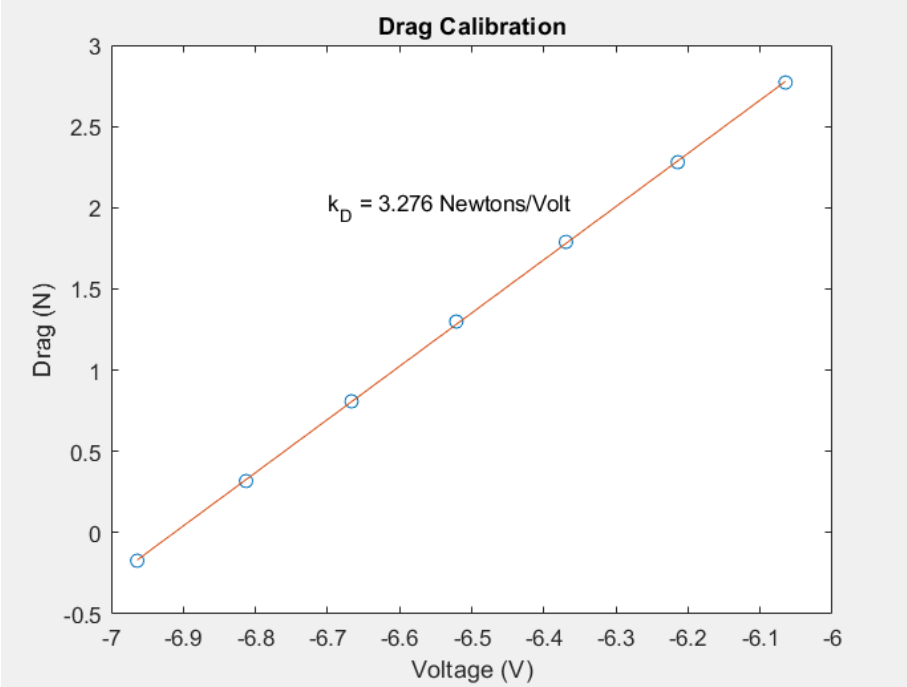
Figure 31. Drag calibration for the force balance.
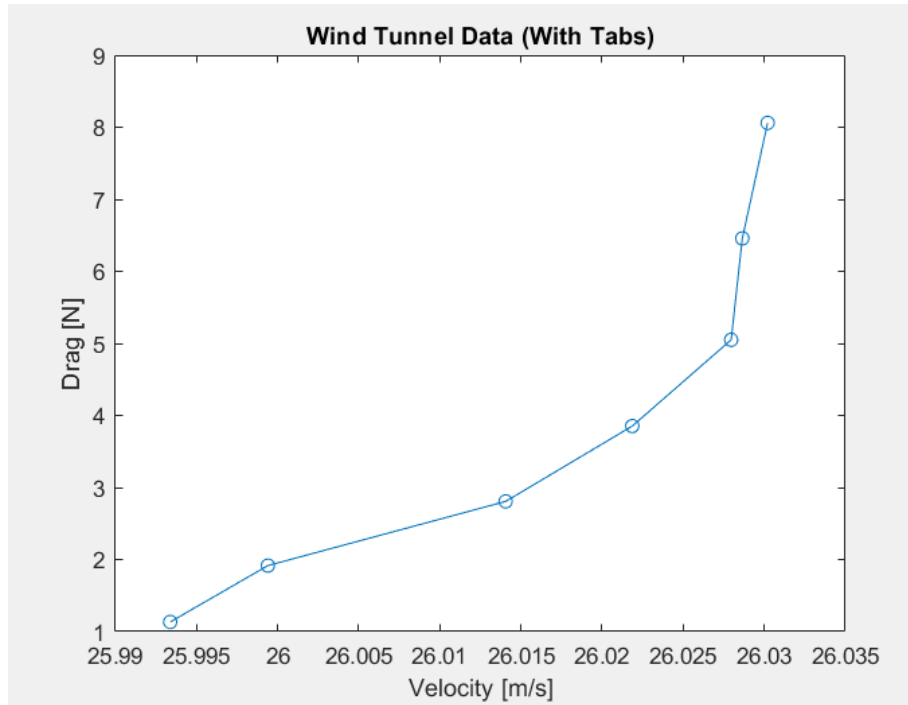
Figure 32. Drag forces on rocket with tabs deployed.
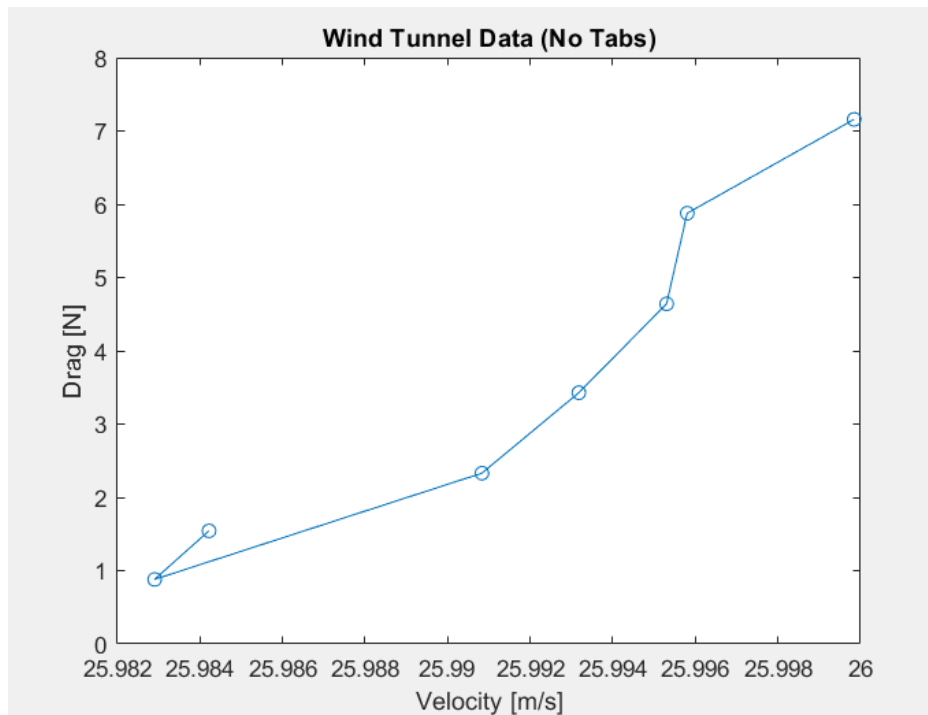
Figure 33. Drag forces on rocket with no tabs.

While the curves found do not indicate a true relationship between drag and fluid velocity, it does indicate the forces that the subscale rocket would experience during flight, as the tunnel velocity was incremented from 0 m/s to approximately 50 m/s. Assuming the largest drag value can be attributed to the largest wind speed, it can be seen in the Figures above that the rocket experiences no more than 9 Newtons of drag at the maximum fluid velocity. However, without velocity data, it is unreasonable to assume anything about the aerodynamics of the rocket based on these wind tunnel tests.

3.4.2 Apogee Approximations

In order to predict the apogee of the launch vehicle, two software packages have been used to construct a complete model of the rocket and run flight simulations. OpenRocket and RockSim were chosen as the simulation software in order to ascertain a more accurate estimation of the actual flight path and ensure that the launch meets the mission success criteria of reaching a predictable apogee. The information gathered from the simulations influenced design decisions such as motor choice, ballast mass, and fin design.

Since the launch vehicle utilizes an Air Braking System to reduce the rocket's apogee, the flight requirement was determined to reach an apogee of 5480 ± 100 feet without the deployment of the air braking tabs, rather than reach an apogee of 5280 feet exactly. This allows for the application of the Air Braking System to operate and reach the competition target rather than relying solely on the motor thrust and launch conditions. Both simulation software packages allow for the input of different launch conditions such as wind speed, temperature, and pressure at the launch site. For each simulation, temperature and pressure were held constant at conditions likely to be seen at competition, and wind speed was determined to be the dominant variable in flight performance. Wind speeds of 0, 5, 10, 15, and 20 miles per hour were simulated to provide a range of flight prediction data that could be seen at a launch. A summary of the predictions for the OpenRocket and RockSim simulations for a Cesaroni L1395 motor can be found in Tables 20 and 21, respectively.

Table 20. OpenRocket Predictions with Cesaroni L1395 Motor.

Wind Speed	0 mph	5 mph	10 mph	15 mph	20 mph
Apogee (ft)	5561	5547	5508	5464	5416
Off Rail Velocity (ft/s)	58.8	58.8	58.8	58.8	58.8
Maximum Velocity (ft/s)	632	632	631	631	629
Maximum Liftoff Acceleration (ft/s^2)	236	236	236	236	236

Time to Apogee (s)	19.1	19.1	19.1	19.0	18.9
Flight Time (s)	195	197	194	196	193
CG Location from Nose (in)	79.8	79.8	79.8	79.8	79.8
CP Location from Nose (in)	101	101	101	101	101
Stability Margin with Motor	2.71	2.71	2.71	2.71	2.71

Table 21. RockSim Predictions with Cesaroni L1395 Motor.

Wind Speed	0 mph	5 mph	10 mph	15 mph	20 mph
Apogee (ft)	5649	5633	5582	5496	5377
Off Rail Velocity (ft/s)	58.3	58.3	58.3	58.3	58.3
Maximum Velocity (ft/s)	634	634	633	633	633
Maximum Liftoff Acceleration (ft/s^2)	266	266	266	266	266
Time to Apogee (s)	19.3	19.3	19.2	19	18.8
Flight Time (s)	200	200	182	198	226
CG Location from Nose (in)	78.8	78.8	78.8	78.8	78.8
CP Location from Nose (in)	100.4	100.4	100.4	100.4	100.4
Stability Margin with Motor	2.82	2.82	2.82	2.82	2.82

The launch rail used for simulation and at competition will be 12 foot 1515 rail. The fore rail button will be located 8.5 feet from the tip of the nose cone and will separate from the rail when the rocket reaches an altitude of 8.5 feet. The velocity at rail exit is predicted be 58.3 ft/s and 58.8 ft/s by OpenRocket and RockSim respectively and climes to approximately 72 ft/s

when the final rail button clears the rail. This meets the mission requirement of at least 52 ft/s at rail exit providing for a safe takeoff velocity.

As stated in Section 3.1.6.4, the Cesaroni L1395 motor was chosen due to a lower weight and similar impulse with motors considered in PDR. It also allows for lower liftoff accelerations than other L-class motors and reduces the risk of damaging the experimental payloads. Both OpenRocket and RockSim provide a predicted flight profile of the altitude, velocity, and acceleration of the launch vehicle vs. time. Figure 34 shows the OpenRocket simulation of the L1395 at 10 mph wind speed.
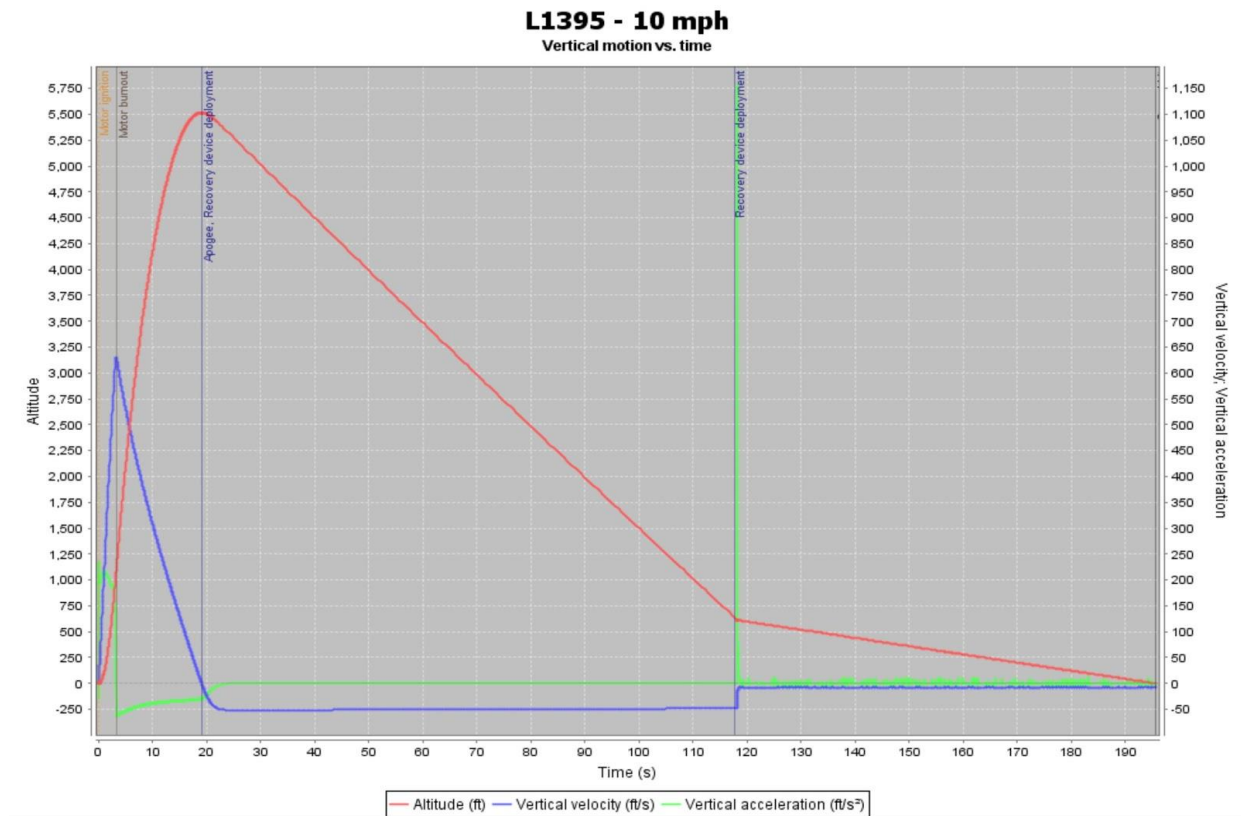
Figure 34. OpenRocket Flight Profile for 10 mph wind speed.

In order to verify the accuracy of these simulations, flight data was compared to simulation models and is discussed in Section 3.2. As seen in Tables 20 and 21, most predicted apogees at low wind speeds are above the 5480 target. This is not a concern because the Air Braking System is capable of reducing apogee by up to 400 ft if necessary. However, what is a concern is the RockSim predictions for low wind speed, which exceed the launch ceiling of 5600 ft. Both OpenRocket and RockSim simulations are greatly affected by the material finish of the launch vehicle. Each program has different finishes and roughness levels that can be applied to components in the flow field and therefore, have different calculations for the drag coefficient,

C_d, of the rocket. By comparing the calculations for drag coefficient in OpenRocket and RockSim in Figure 35, it can be seen that RockSim's calculation has a lower resolution and underpredicts the C_d when compared to OpenRocket. Therefore, it can be assumed that RockSim is an over approximation of apogee. OpenRocket has also been proven to be reliable in the past and is used as the primary simulation software.
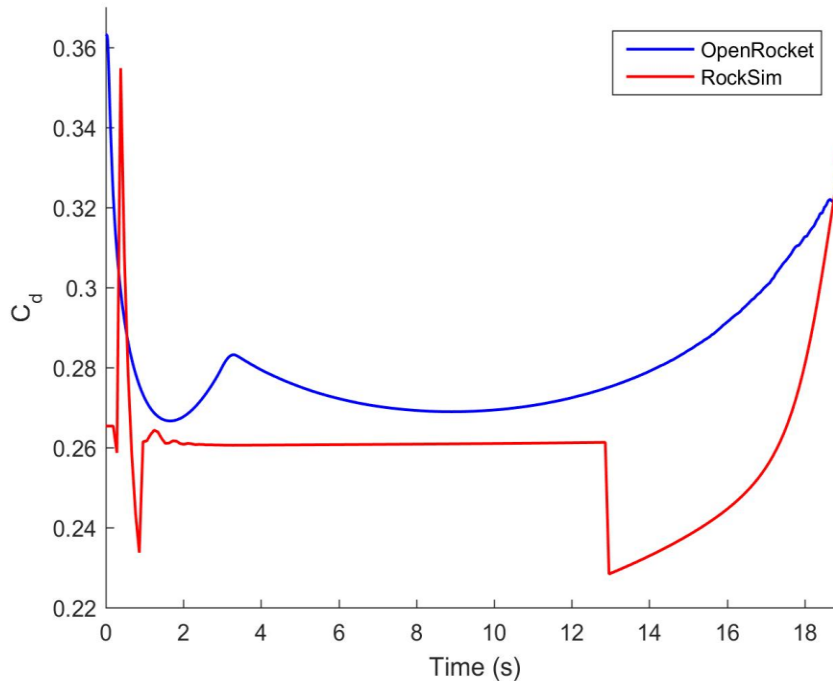
Figure 35. Plot of Cd vs. Time in OpenRocket and RockSim from ignition to apogee.

Additional simulations have been run as component masses have been finalized and it was determined that at the current total mass of 48.3 lbs or 773 ounces, the rocket is capable of overshooting the mission apogee of 5,280 feet by a margin correctable by the Air Braking System. Through the use of ballast mass in simulation, if the total mass exceeds 800 oz, the predicted apogee is much closer or even below 5,280 feet. This would not allow for the use of the Air Braking System or even result in not reaching the apogee goal. It would then be necessary to use either a Cesaroni L2375 or Cesaroni L1115 motor, both of which provide a higher apogee and similar accelerations, but utilize the same motor casing as the L1395, alleviating the need for changes in the overall vehicle design.

3.4.3 Stability

In order to ensure a safe flight, the launch vehicle must achieve a minimum stability margin of 2 calipers at rail exit or an altitude of 8.5 ft. This stability should remain throughout

burnout and only decrease as the rocket nears apogee. According to OpenRocket calculations, the center of gravity (CG) of the launch vehicle will be located 78.8 in from the nose cone and the center of pressure (CP) will be located 101 in from the nose. With a maximum body tube diameter of 7.675 in, this gives the rocket a static stability margin of 2.7 calipers with the motor. The locations of both the CG and CP however, vary during flight as velocity and mass change during burnout. An OpenRocket prediction of their locations from the nose cone is given in Figure 36 and the calculated stability margin is shown in Figure 37.
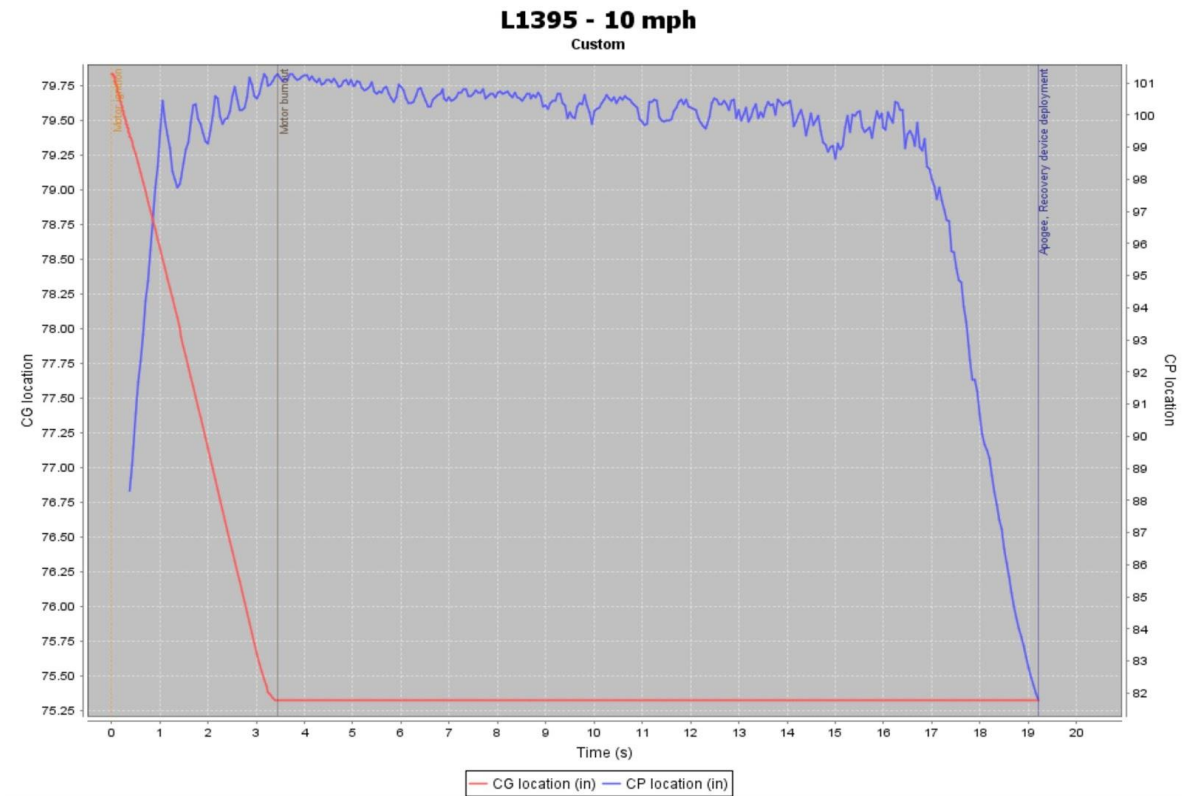
Figure 36. OpenRocket Simulation of CG and CP locations vs. Time at 10 mph wind speed.
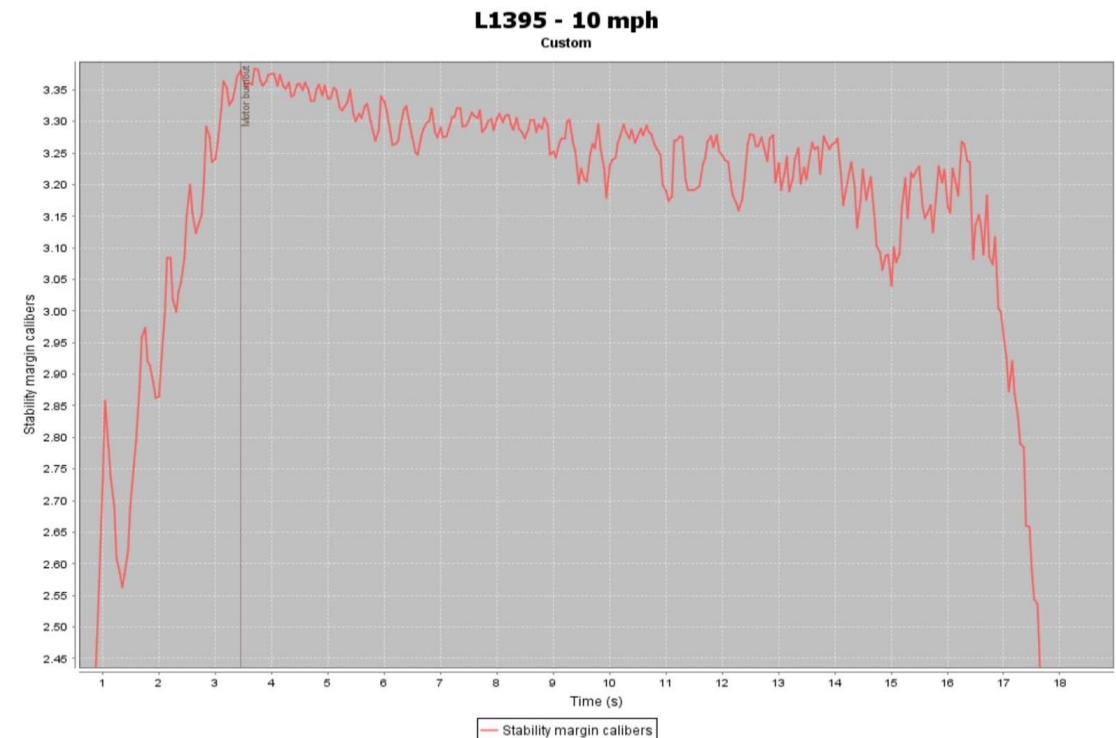
Figure 37. OpenRocket Simulation of Stabilty Margin vs. Time at 10 mph wind speed.

Based on this information, it is shown that the launch vehicle will remain stable throughout the duration of the flight. As mass decreases, the stability margin rises to approximately 3.35 at burnout. This could lead to slight weather cocking in high wind conditions but will not significantly affect the flight path or apogee.

Additional care must also be taken in construction of the rocket in order to accurately document its weight. Miscellaneous weights such as epoxy are not accurately modeled in OpenRocket and due to the amount necessary for construction of the fin can have the potential to lead to lower stability. If this became an issue, ballast can be added in the transition section to move the CG location and increase stability.

3.5 Launch Procedures

The team has developed procedures to follow for every launch, including the test launches and the launch in Huntsville. The launch procedures are going to be followed in order to ensure a flawless flight and to help meet the mission success criteria.

Each sub-team has its launch procedures to follow for assembling its payload/sub-systems. Designated members of the sub-team sign off on the launch procedures followed by the leaders of the sub-team to ensure that the procedures were followed correctly.

These procedures are listed in Appendix A.

3.6 Vehicles Test Plan

In order to verify that the design of the launch vehicle is sound, testing must be done. These test will be run on the materials being used for the full scale rocket, as well as on the full scale rocket itself.

3.6.1 Subscale testing

Since it is unreasonable to do all testing on the full scale rocket, a subscale rocket was to be built and tested. Testing only the full scale is unreasonable due to factors such as time, budget, and testing apparatus constraints, and for this reason, a smaller rocket made of cheaper materials was made. Details of its design can be found in Section 3.2.

3.6.1.1 Subscale Flight

As discussed in Section 3.2.3, the rocket underwent two flights on December 2nd, 2017 in Three Oaks, Michigan with the Michiana Rocketry Club. The objective of this test was to gather altimeter data to compare with simulation packages as well as test the effectiveness of the Air Braking Tabs when fully deployed. The results of this test are discussed in Section 3.2.3, where it is mentioned that the simulation packages overestimated the apogee by approximately 60 feet, and the Air Braking Tabs did indeed have a significant impact on the flight.

3.6.1.2 Wind Tunnel Testing

The subscale rocket was also subjected to wind tunnel testing in the Hessert Laboratory on Notre Dame's campus on November 9th, 2017. The purpose of these tests were to derive drag coefficients for the subscale rocket with and without drag tabs deployed, as well as verify initial CFD findings that there is no separation of the boundary layer aft of the transition section. The results of the testing can be found in Section 3.4.1.2, where it was revealed that an instrumentation error caused no velocity data to be gathered, and as such no coefficients of drag could be found. It was, however, verified that there was no separation due to the magnitude of the drag forces on the aerodynamic structure of the rocket.

3.6.2 Software

Another way of testing the rocket while being cost and time effective is to use software packages to predict the performance of the rocket. An abundance of these programs are used to predict the flight, aerodynamics, and structural integrity of the design.

3.6.2.1 Flight Simulations

The rockets initial design occurs in flight simulation software. The Notre Dame Rocketry Team primarily uses the packages OpenRocket and Rocksim to predict the flight of the rocket, and the rocket is entirely modeled in these. The objectives of the tests run in these packages are to predict the apogee, velocities, accelerations, and flight times of the final rocket, as well as gain

data on the physical nature, such as center of gravity and center of pressure. The program results are compared to one another to verify that the team is getting reliable results.

Testing in these packages has been ongoing since September 2017, and new simulations are run with each change in the rocket. Once materials are acquired and construction begins, each component in the model will be updated so that accurate final flight predictions can be made. These predictions will then be compared to full scale flight data. Construction is to begin in January 2018 and the full scale flights are scheduled for February 2018.

3.6.2.2 Computational Fluid Dynamics

Initial CFD analysis began in September 2017, when it was decided that a variable diameter rocket was going to be used for the full scale vehicle. ANSYS AIM Student was used to simulate the environment around the rocket during a 200 m/s flight. This test was run with forward diameters ranging from 5.5 inches to 8.5 inches, and the boundary layer of each rocket was observed. None of these tests revealed any separation of the boundary layer or any excessive turbulence, and therefore the design was able to move forward.

Further CFD with the Notre Dame Center for Research Computing was begun in November 2017 to further investigate the validity of these findings, and are currently underway. However, as discussed in Section 2.1, this additional testing will only be carried out if time allows for it.

3.6.2.3 FEM Analysis

Analysis of the structure of the rocket is paramount to a successful flight. In order to do this, the Finite Element Method software ADINA is currently being used in order to verify that the structure of the rocket will hold up to the forces experienced during flight. Additionally, the connections between sections during separation and descent are being looked at to make sure that they are able to handle the stresses of the controlled black powder explosions, as well as the stresses from the parachute and shock cords upon parachute deployment.

These tests should yield results by the test flights in February 2018. It should be noted as well that this is only a precautionary measure, as the materials being used for the structure of the rocket as well as the adhesives used for connections have been chosen due to their excessive strength and used before with success.

3.6.3 Physical Testing

Once the materials for the full scale are in the team's hands, physical testing can begin on them. This is to ensure that manufacturer data is accurate, as well as ensure that the designed rocket is able to withstand some of the events that may happen during flight.

3.6.3.1 Stress Testing

In order to verify that the carbon fiber and fiberglass body tubes being used for the rocket are up to manufacturer specifications, stress testing will be done in Notre Dame's Fitzpatrick Hall. Here the body tubes will undergo extreme compressive and tensile stresses to ensure that the stress moduli are accurate, and that the software models, mentioned earlier, have correct values. This testing will be done once the materials in hand, most likely in February 2018.

3.6.3.2 Shake Testing

Once the vehicle's components are built, their integration into the rocket must be verified. This will be done with shake tests. These tests will be done for the following components:

- Motor Mount
- Fins
- Air Braking System
- Recovery System
- Deployable Rover Payload
- Transition Section Connection
- Ballast Integration

To test these, each section will be placed and secured in its correct position in the rocket. Then, the rocket will be shaken vigorously in the horizontal and vertical directions. This is to simulate any turbulence that the rocket might experience during flight, as well as the violent vibrations felt during descent and separation. The components being tested will be visually examined and deconstructed (if possible) after the test to ensure that they were not damage and did not shift a significant amount during testing.

These tests will be carried out once materials have been acquired, and once each section has been built. This will most likely begin in late January 2018.

4 Safety

As with every design review, safety will constantly and heavily be enforced throughout the academic year. This is to provide awareness and alertness to the hazards and precautionary measures of sensitive materials, whether it is physical or theoretical. The team will be enforcing the overall safety of the project by creating a team which derives all levels of safety requirements. This will identify serious and crucial criteria necessary for the team to maintain an acceptable level of safety.

The team will be creating safety requirements that will ensure all aspects of safety are met for NASA's final rocket launch. There will be two categories addressing the necessary safety

requirements for the team. Those two categories consist of Human Safety and Environmental Safety.

- The Human Safety criteria includes any and all material, physical or psychological, that will injure the individual or the team. This category is broken up into five separate sections; Vehicle, Payload, Recovery, Air Braking System, and Launch Day.
- The Environmental Safety criteria includes any and all material that affects the relationship between humans and nature. This category consists of two separate sections; Team Effecting the Environment and Environmental Concerns

4.1 Risks and Concerns During Pre-Launch

Knowledge regarding to the launch of the rocket is essential in order to facilitate the team and the overall general public of its safety procedure. For example, based on the FMEA chart, cause and failure mode are both utilized by the team to help reduce all possible hazards that might hinder before and during the launch of the rocket. The team also used both the launch procedures and assembly of the rocket in order to address any and all possible types of hazards before the rover safely deploy.

Most of the information prior to launch stems directly to technical blueprints of each component of the rocket which includes the assembly of the rover vehicle. By exploring each component within the rover, the team addressed a Failure Mode Effect Analysis (FMEA) table to identify the cause and failure mode criteria. Each individual section is outlined to best represent the safety hazards that are probable or not.

4.1.1 Rover Vehicle

The rover vehicle incorporates the deployment aspect of the cause and failure mode analysis. In this case, most of the hazards begin to occur as soon as the rover safety ascends and descends upon launch and as the rover deploys itself from the rocket at ground level. A greater breakdown of what hazards are incorporated into this section are located in the Rover Vehicle FMEA table.

4.1.2 Payload System

The payload system incorporates hazards during assembly, especially as the solar panels and the sub-component electronics are being assembled within the body of the rover. With the complexity of the payload system, hazards associated with launching were broken up into individual FMEA sections within the same table.

4.2 Safety Officer

The Notre Dame Rocketry Team has chosen Robert Stiller as the Safety Officer for the 2017-2018 year. This is Robert's second year on the team, and he has rocketry construction experience. He is a senior physics major at Notre Dame. Robert will oversee ensuring the team

carries out the proper safety procedures and will perform risk and mitigation analysis along with contingency planning for all safety aspects of the project.

The safety officer will ensure that MSDS and other safety documents are up to date and readily available to all team members. MSDS will be heavily emphasized during the 2017-2018 year. The safety officer will be present throughout the construction process and whenever a potential hazard exists for any personnel if the safety officer cannot be present, then he will appoint a capable representative to take his place. All members of the Notre Dame Rocketry Team have signed a safety agreement to ensure safe practices throughout the year and this agreement can be seen in Appendix B.

4.3 Checklist of Final Assembly and Launch Procedures

A detailed pre-launch checklist will guide the final assembly process for the rocket with step-by-step instructions. A repeatable launch procedure will also be developed to mitigate risk of failure at the launch site, and a post-launch procedure will ensure the all personnel retrieve the rocket in a manner that is safe for both the personnel and the rocket. These steps must be followed precisely to ensure successful execution of the project. These procedures can be found in Appendix A.

4.4 Preliminary Personnel Hazard Analysis

The Notre Dame Rocketry Team understands that the construction, testing, and launch of the rocket pose several potential hazards to team members. The table below explores the personnel hazards that may occur during different phases of constructing or testing the launch vehicle and its subsystems. Similar to the FMEA table, a severity, likelihood, and overall risk level was assigned to each hazard to better understand what mitigations are necessary. The risks and likelihoods were assessed assuming that all team members have been properly trained, are following the correct procedures, and are wearing the proper personal protective equipment (PPE). By recognizing these hazards now, the team can be better prepared to mitigate them and to take the proper actions in the event that an accident occurs. This table can be found in Appendix C.

4.5 Preliminary Failure Modes and Effects Analysis (FMEA)

A Failure Modes and Effects Analysis (FMEA) table was developed to identify the potential technical failures of the vehicle. For each failure, the effects and causes were identified, as well as their likelihood of happening, and the severity of their occurrence. The last two parameters were used to assess the risk of each failure through the Risk Assessment Codes (RACs) suggested in the handbook for the competition. These charts can be seen below in Tables 22 and 23.

Table 22. Severity definitions.

Description	Personnel Safety and Health	Facility/Equipment	Environmental
Catastrophic	Loss of life or a permanent-disabling injury	Loss of facility, systems or associated hardware.	Irreversible severe environmental damage that violates law and regulation.
Critical	Severe injury or occupational-related illness.	Major damage to facility, systems or associated hardware.	Reversible environmental damage causing a violation of law or regulation.
Marginal	Minor injury or occupational-related illness.	Minor damage to facility, systems or associated hardware.	Mitigatable environmental damage without violation of law or regulation where restoration activities can be accomplished.
Negligible	First aid injury or occupational-related illness.	Minimal damage to facility, systems or associated hardware.	Minimal environmental damage not violating law or regulation.

Table 23. Probability definitions.

Description	Qualitative Definition	Quantitative Definition
Frequent	High likelihood to occur immediately or expected to be continuously experienced.	Probability is > 0.1
Probable	Likely to occur or expected to occur frequently within time.	$0.1 \geq$ Probability > 0.01
Occasional	Expected to occur several times or occasionally within time.	$0.01 \geq$ Probability > 0.001
Remote	Unlikely to occur, but can be reasonably expected to occur at some point within time.	$0.001 \geq$ Probability > 0.000001
Improbable	Very unlikely to occur, and an occurrence is not expected to be experienced within time.	$0.000001 \geq$ Probability

The risk matrix used, based on the one shown in the handbook's appendix, is shown in Figure 38.

Probability	Severity			
	Catastrophic	Critical	Marginal	Negligible
Frequent	High	High	High	Low
Probable	High	High	Moderate	Low
Occasional	High	Moderate	Moderate	Minimal
Remote	Moderate	Moderate	Low	Minimal
Improbable	Low	Low	Low	Minimal

Figure 38. Risk assessment chart.

After classifying the risk of each failure mode, mitigations and controls to prevent said failures were developed. It is important to note the importance of first determining the level of risk of each failure as to implement appropriate mitigation levels. Figure 39 depicts how the failure modes were divided into six categories: Structural, Recovers, Propulsion, Stability, and relating to the specific payloads. The FMEA table for all possible failure modes the launch vehicle and its subsystems may experience can be found in Appendix D.
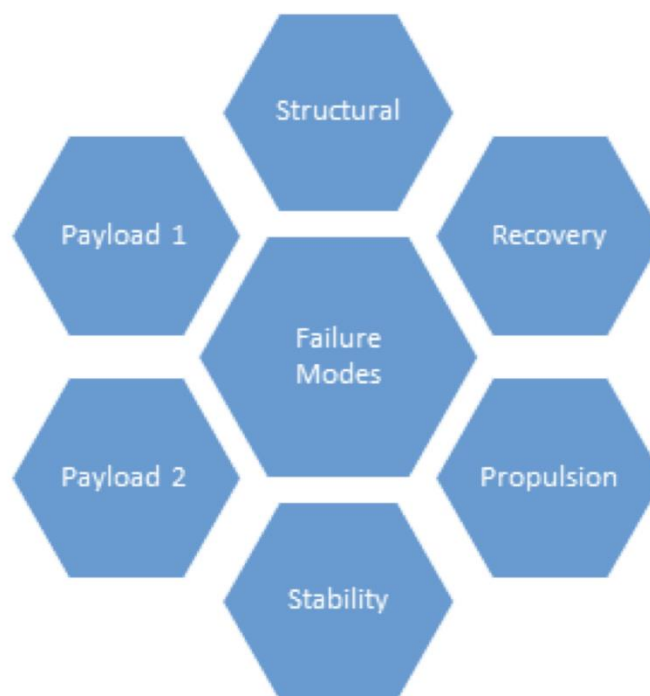
Figure 39. Failure Mode Classification.

4.6 Environmental Concerns

The environment in which the rocket will be operated also poses a certain amount of risk. Specific problems related to inclement weather at the launch and landing sites have been identified and solutions have been devised to decrease the negative effects of the environment on

the rocket. Additionally, many of the materials used in the construction of the rocket pose a significant hazard to the environment if they are improperly handled. By considering these things, one can ensure that the rocket is able to adequately perform and not be negatively affected by the environment. Failure modes tables have been constructed for both the environmental effects on the rocket and the rocket's effect on the environment. These tables can be found in Appendix E and F, respectively.

4.7 Project Risks

There is the possibility of encountering a number of roadblocks throughout the rocket design and launch process. Each of these risks has been identified and categorized in terms of their potential impact on the project and the likelihood of that specific problem occurring. Risk is minimized with specific mitigation plans for each scenario. Failure to mitigate these risks will result in significant time delays for the project, which in turn lowers the chance of success on launch day. A table has been constructed outlining potential risks associated with the project, their likelihood, their impact on the project, and how they will be mitigated. This table can be found in Appendix G.

5 Payload Criteria

5.1 Deployable Rover Payload

5.1.1 Objectives

The Deployable Rover Payload is required to deploy a rover contained within the rocket for the duration of the flight. Upon deploying the rover, it will autonomously move five feet away from the rocket and unfold two sets of solar panels.

Radio frequency will be used to activate the rover after blowing off the nose cone. Ejection charges of black powder will remove the nose cone after landing to allow the rover to exit the rocket cleanly. Tracks have been placed on both top and bottom of the rover to allow it to drive out whether the rocket lands "upside-down", or "right side up". A LiDAR (Light Detection and Ranging) sensor will be used for object avoidance so the rover can safely move 5 feet away from the rocket in order to deploy the solar cells. The solar cells will be attached to a fireproof cloth and a metal frame to allow for ease of deployment. The rover will be cut from HDPE to allow for customization. The final design of the deployable rover can be seen in Figures 40, 41 and 42 below.
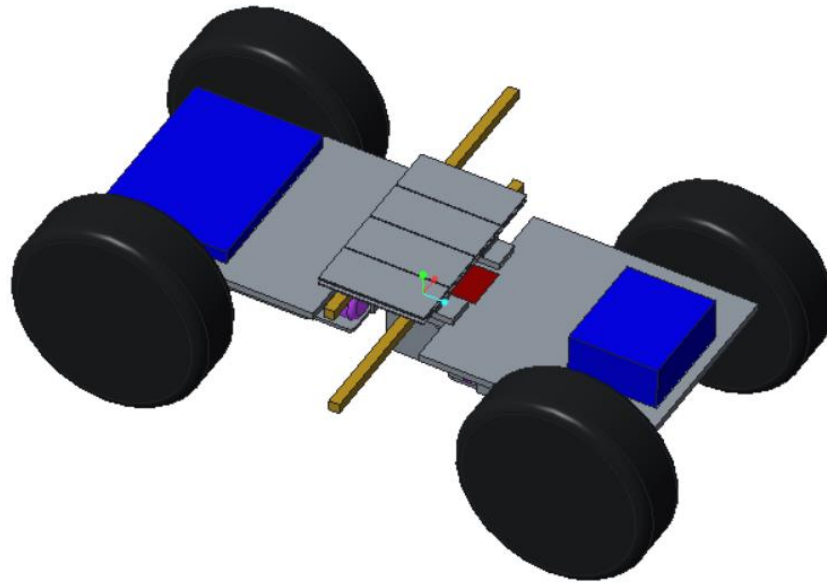
Figure 40. Full CAD model of the deployable rover, seen from the top. The blue rectangles are the coverings for the sensors and electronics.
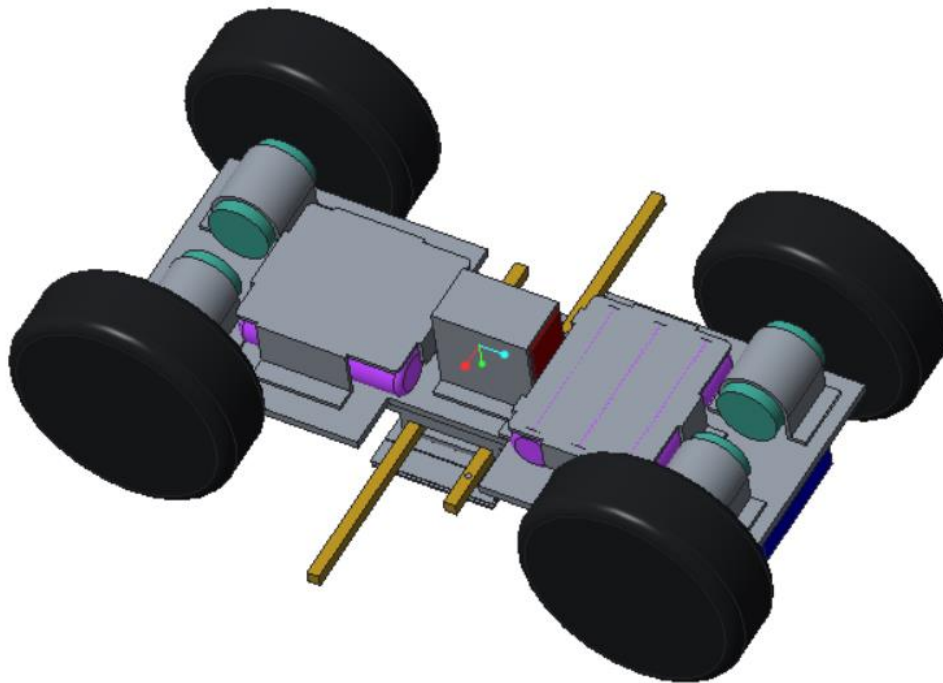
Figure 41. Full CAD model of the deployable rover, seen from the bottom. The teal canisters are the motors and the purple canisters are the batteries.
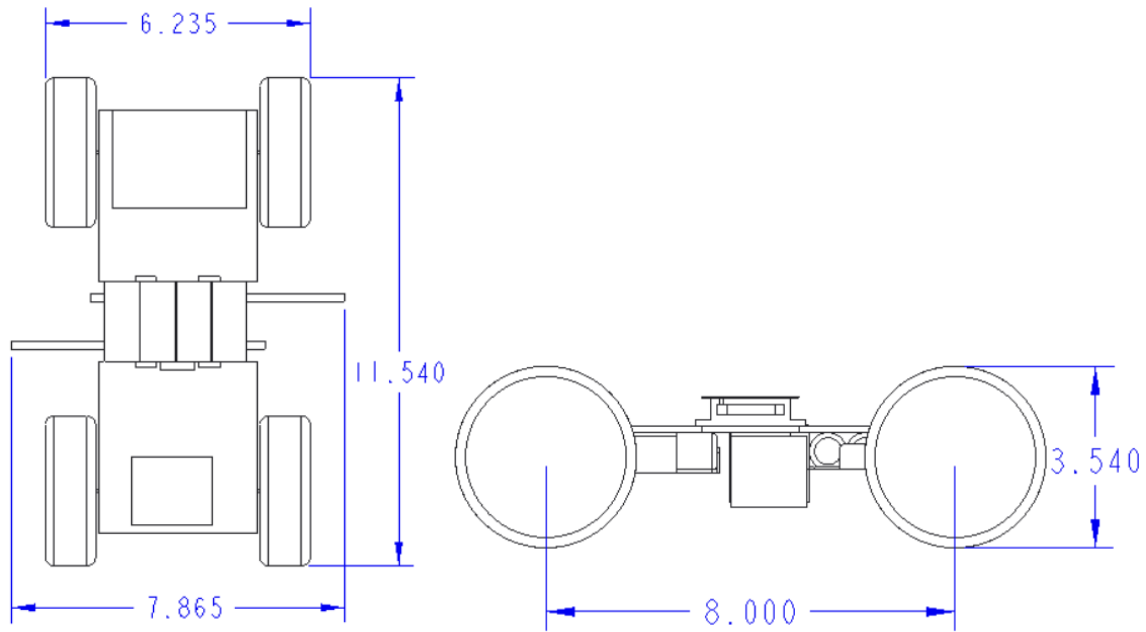
Figure 42. Overall dimensions of the rover with the solar panels folded. Dimensions in inches.

5.1.2 Success Criteria

The payload will be considered successful if all of the following criteria are met:

1. The rover autonomously drives five feet away from the rocket
2. The solar panels unfold and provide power to the rover
3. The rover will be ready to be used again on the same day

5.1.3 System Level Design Review

5.1.3.1 Rover (Body)

The body of the rover will be made out of High-Density Polyethylene (HDPE). This is different than what was initially determined in our Preliminary Report. Initially design was to machine the body out of a block of aluminum; however, with further research, it was determined that HDPE was a more effective and cost efficient material to use. The body will be cut out of a quarter inch thick block of HDPE using the techno router in Stinson Remick 214. This follows the original plan for the aluminum block that allowed for a fully customized body. Although Aluminum is stronger than HDPE, HDPE is a lighter and more flexible substitute that will lower the overall weight of the payload and make it more resistant to potential damage during launch and traversing the launch site upon deployment.

5.1.3.2 Rover (wheels & motors)

The mobility of the rover will be accomplished with four Goolsky FY-CL01 wheels and corresponding Turnigy XK2435-4900KV Brushless Inrunner motors. They can be seen in Figures 43 and 44. The wheels will be oversized measuring 3.54 inches across the diameter, 1.18 inches wide and weighing 65.5 grams each. This allows the rover to drive in two orientations depending on how the rocket lands. The large size of the wheels will also help the rover roll over any obstacles that it may encounter. For simplicity each wheel will be independently powered using a motor without any gearing. Gearing would be traditionally necessary to achieve the maximum power transfer, and protect the motors from burning out at low rpms. In this instance however, having four 328 W motors, a light load, and a short target distance make the inefficiency acceptable. The sensor-less, brushless DC motors are .944 inches in dia. and 1.38 inches in length, and are relatively light at 55 grams each. They will be mounted to the HDPE chassis using a custom 3D printed bracket. As the chosen motors do not include encoders, an encoder kit from DAGU will be used. This can be seen in Figure 45.
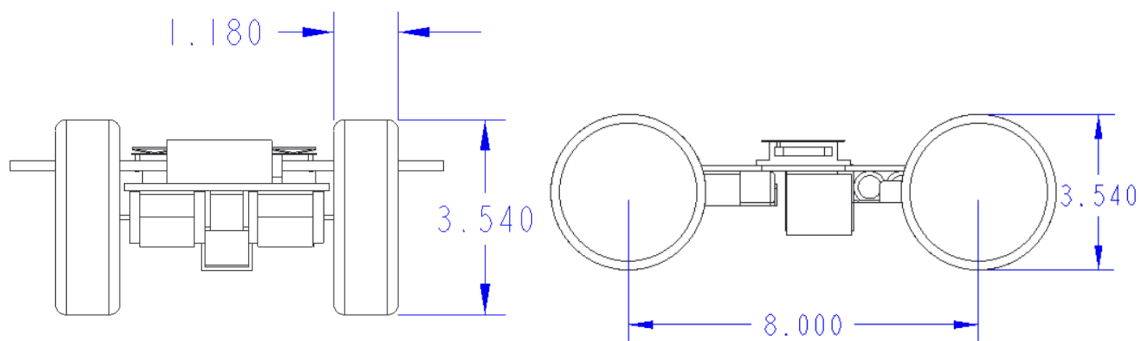
Figure 43. CAD model of the rover including the dimensions of the wheels. Dimensions shown in inches.

Figure 44. Four Goolsky FY-CL01 wheels and four Turnigy XK2435-4900KV Brushless Inrunner motors will be used to drive the rover upon deployment.

Figure 45. Wheel Encoder Kits from DAGU will be used with the Turnigy motors.

5.1.3.3   Servomotor and Solar Panels

In addition to the onboard batteries, the rover will collect solar energy via a folded solar array. The solar cells will be mounted on an array made from a foldable fire-retardant fabric that will deploy once the rover has exited the body tube. Physical prototypes were used to ensure the folding extension mechanism would work as expected. The rover will use monocrystalline solar

cells sheets, which can be cut to the exact size needed for each panel of the folded array. There will be solar cells on both the top and reverse sides of the array to allow them to function if the rover is inverted, and the base plate will have cutouts to allow maximum light in this case. Both the collapsed and fully extended states of the array are shown in Figures 46 and 47.

The whole array will then be attached to and driven by a rack-and-pinion system. This will use a Hitec HS-7245MH Servomotor with a brass pinion gear to allow exact control of the rack extension. The rack-and-pinion system will have teeth with a 20° pressure angle which increases the strength of the system and allows it to handle higher loads. The system has a pitch of 32. The racks themselves will be made from a sturdy brass to ensure there is no stripping and have a face width and height of 3/16 inches.
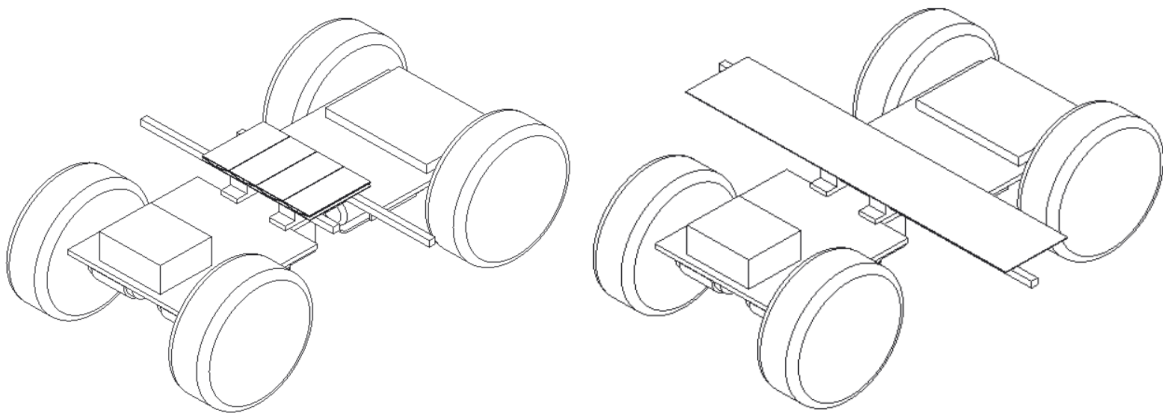
Figure 46. CAD model of the rover in both the folded and extended solar panel states.
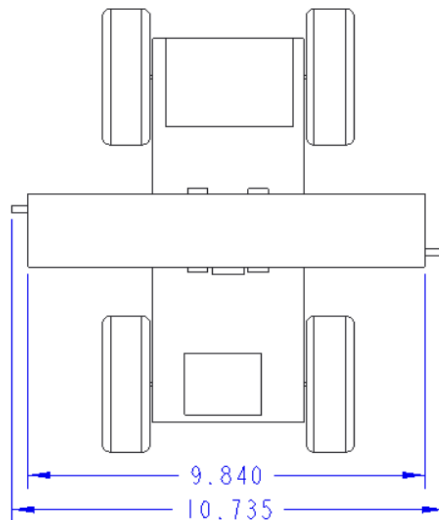
Figure 47. Dimensions of the solar panel array once fully extended. Dimensions shown in inches.

5.1.3.4   Securing System

During the rocket's flight, the rover must be secured within the body of the rocket to prevent damage to either system. This will be achieved by using the solar panel deployment system. The brass racks upon which the solar panels rest must be retracted when the rover is within the rocket for the rover to fit inside. When the servomotor runs counterclockwise, these racks can be retracted slightly further to extend the non-panel-bearing ends of the racks into mounting blocks affixed to the interior wall of the fuselage. These two mounting blocks will be 3D-printed cube-like structures with slots for the ends of the racks to fit into. The blocks will be affixed to the interior wall of the fuselage with high-strength epoxy.

This method was chosen over other methods of securing the rover because it utilizes one mechanism to serve multiple purposes. The other methods considered—such as a sliding rail system that locks the rover's wheels in place—would require additional mechanisms to operate, which would add to both the complexity and the weight of system. In the method chosen, the only additional weight is from the two 0.25-inch cube-like mounting blocks. The tracks upon which the rover rests will secure the rover in the y-direction, as well as preventing rotation about the z-axis. The insertion of the racks' ends into the blocks' slots will then fully secure the rover, allowing zero degrees of freedom. The racks are made of brass and will be strong enough to hold the rover in place. The securing system can be seen in Figures 48 and 49.

To ensure the integrity of the securing system, several tests will be performed. One will be to test the structural strength of the brass racks to ensure that they will not deflect under the strain of the rover with one end pinned inside the mounting block. Another test will be to attempt to rotate the rover while it is secured in the mounting blocks to ensure that the racks' ends do not strip the 3D-printed slots. Another will be a shake test of the fully assembled payload, detached from the rest of the rocket. This will reveal any uncontained translational and rotational motion while also assessing the severity of the system's vibrations.
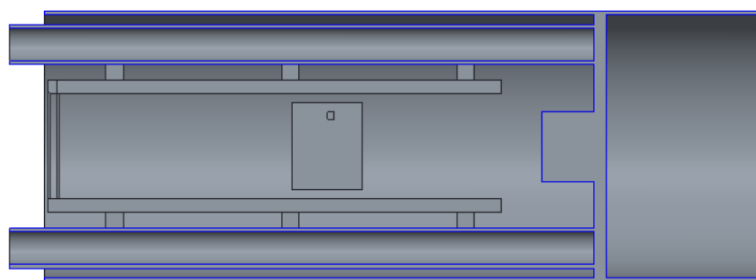
Figure 48. Cross section of the tracks and securing block inside the body of the rocket.
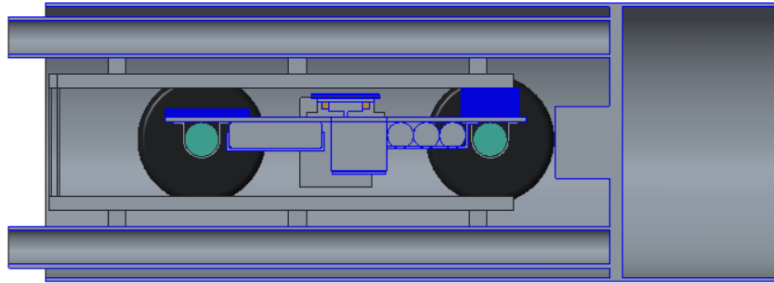
Figure 49. Cross section of the rover secured inside the body of the rocket.

5.1.3.5   Deployment System

Upon safe landing, the ground station will signal the ejection of the nose cone allowing the rover to exit from the top of the body tube. The ground station will be discussed in detail further in the report. Deployment will be facilitated by a charge of 6 grams of black power to separate the nose cone from the payload bay. Charges will be housed in two long PVC tubes that run above and below the rover and are mounted on a bulkhead at the back of the payload. The second tube serves as a redundant system for the first containing another 6 grams of black powder. The tubes will run through slots in one bulkhead at the base of the nose cone and end before reaching a second bulkhead closer to the top of the nose cone. This configuration can be seen in Figures 50 and 51. The use of these two bulkheads protects the payload bay from the black powder charges so that the only space exposed to the heat and forces of ignition is the void between bulkheads. The charges will be lit via electronic matches that run along the PVC pipes to ignite at the front (top) of the black powder section when they receive a signal from the ground station. The electronics receiving this signal to ignite the matches will also be mounted on the bulkhead at the base of the payload bay. Once the nose cone is removed, the rover will drive out of the payload bay. In the payload bay, the rover will be positioned between the four rails that run parallel to the roll axis and include wells to keep the wheels on track. Originally the fronts of the rails were going to slide through the bulkhead at the base of the nose cone, but this was changed due to the addition of spring loaded ramps. Spring loaded ramps, positioned perpendicular to each set of rails (to account for either landing orientation), will unfold as the nose cone is removed. These ramps were not originally part of the design, but were added to ensure that the rover does not bottom out as it exits the body tube. The ramps can be seen in Figure 52 in both the folded and released configurations.
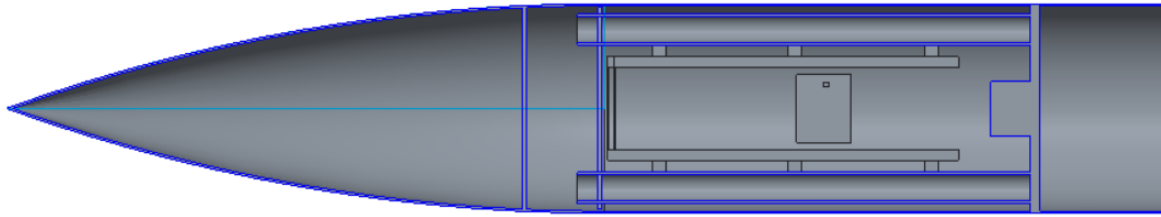
Figure 50. Cross sectional view of the deployment system of the rover.
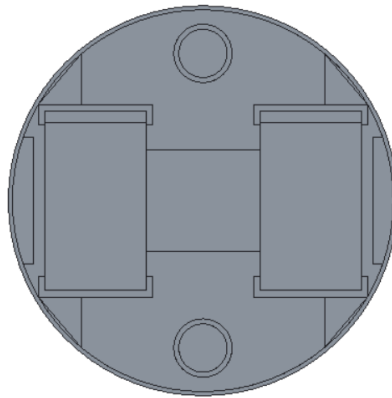
Figure 51. Cross sectional view of the deployment system view from the top of the payload.
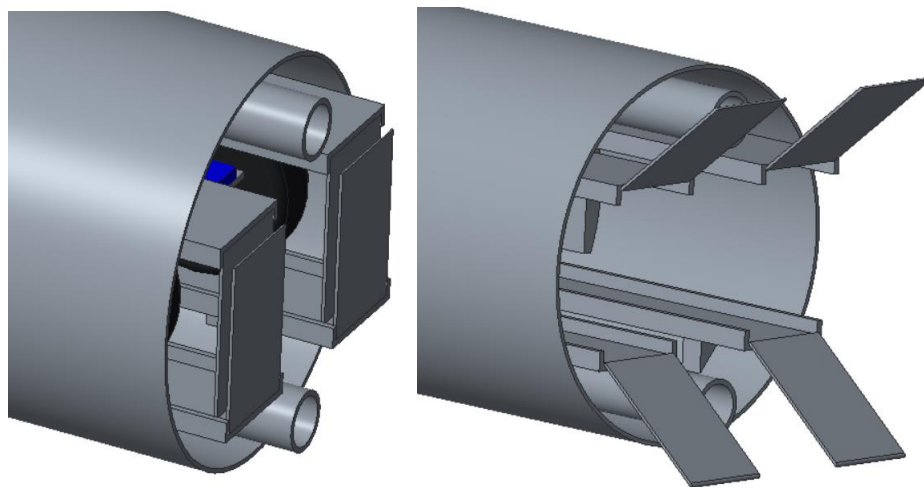
Figure 52. The spring loaded ramps will be folded during the flight of the rocket and will release when the nose cone is removed.

5.1.3.6   Electronic Control System

The following Figures 53 through 57 show the different components of the overall electronic control system present on the rover payload as well as the various subsystems under the overall system. The schematics of the individual subsystems can be found in Appendix H.
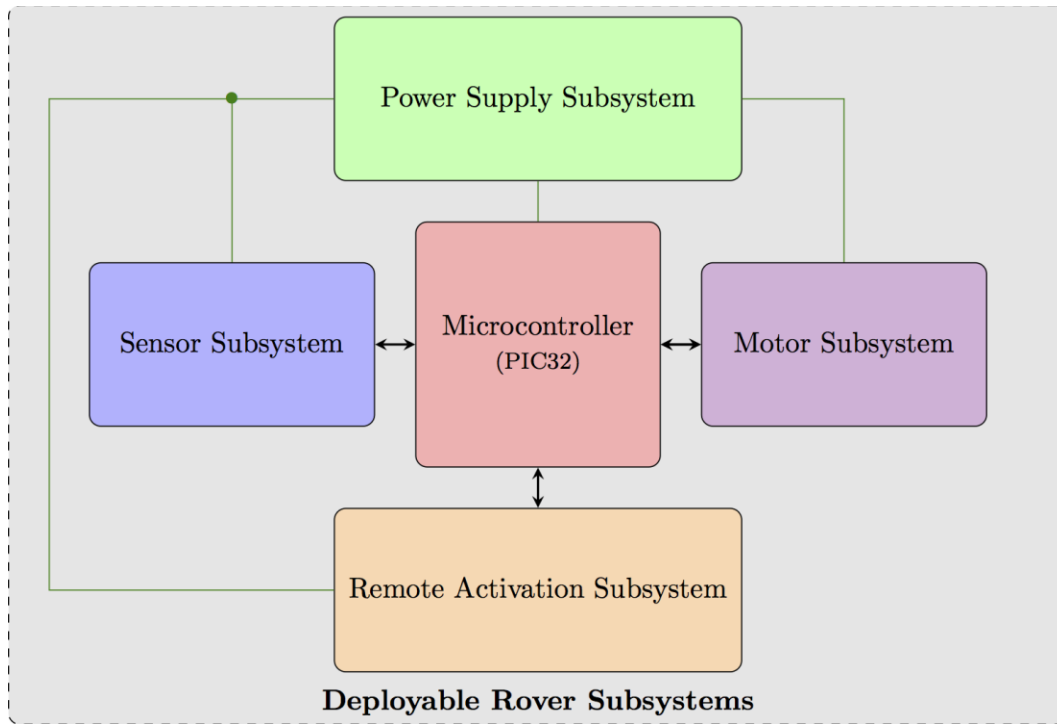
Figure 53. Overall Rover Electronic Control System.
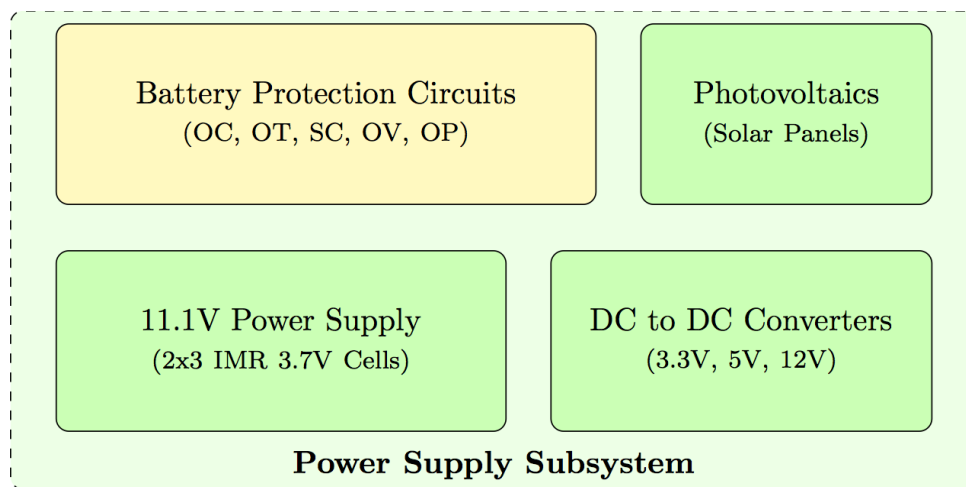
Figure 54. Power Supply Subsystem Components.
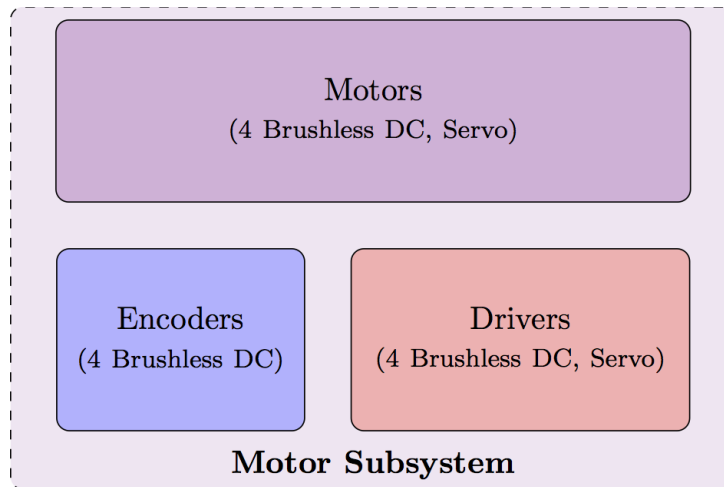
Figure 55. Motor Subsystem Components.
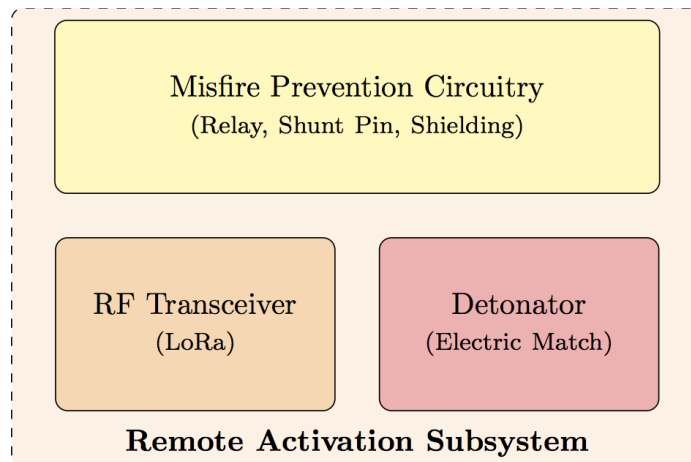
Figure 56. Remote Activation Subsystem Components.
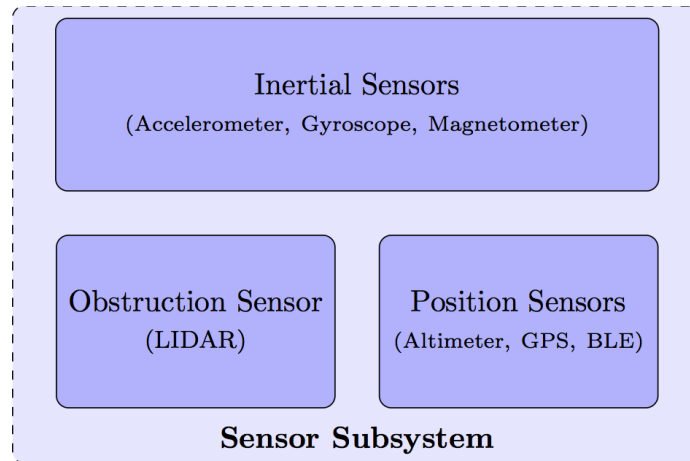
Figure 57. Sensor Subsystem Components.

5.1.3.6.1 Microcontroller

For the processor, a PIC32MX795 microcontroller will be used as the control unit for the rover and rocket as a whole. The PIC will be used to complete the major goals of the rover: object avoidance, autonomous movement from the rocket, and communication of important parameters to the ground station. The PIC was chosen due to the convenience of the IDE, as well as its comparatively low cost and larger number of re-mappable pins and greater options for customizations. The PIC32MX795 was chosen over other types of PIC's for its large data memory (128 KB) and program memory (512 KB). A PIC24 was considered; however, some of the sensors require 8 byte data streams, so the PIC32 was necessary. The PIC24 also does not have the required number of re-mappable pins. In the final design, all but 7 of the pins are used. This chosen solution has the added benefit of reducing the footprint that the electronics will consume. Using a predesigned breakout board from Sparkfun or Arduino would prevent the placement of altimeter, gyroscope, GPS module, Bluetooth module, and communications devices all on the same board.

5.1.3.6.2 LoRa

A LoRa (Long-Range Low-Power) device was chosen for the wireless communications portion of the rover deployment and data communication. LoRa has a number of significant advantages over traditional radio communications that led to choosing it over other communications protocols. The first major advantage of LoRa is that is uses a 900 MHz band, which is an unlicensed band, allowing communications without FCC approval. A similar solution such as cellular or radio, would require specific licensing for each user, which would add an extra step and would be frustrating for each member of our group. Secondly, LoRa has significantly larger range (theoretically 13.6 miles) than other IoT solutions. A different solution such as Bluetooth or WiFi, have a range on the order of meters, and since the data from the

rocket will be transmitted in real time, WiFi or Bluetooth would not have anywhere near the range necessary to do this. Additionally, in the past, Notre Dame has encountered problems with interference from other teams' radio communications. These issues will be alleviated by the use of a LoRa module. The unique CSS (Chirp Spread Spectrum) protocol provides excellent resilience to interference, and resistance to the doppler effect and other issues that may arise from frequency modulation. Nevertheless, there will be several tradeoffs that come about as a result of using LoRa. First, there is a significant decrease in speed from traditional radio communications. LoRa sends very small packets infrequently, and are only available to downlink for a moment after uplinking. This provides significant power advantages, but greatly reduces the speed. For our purposes, this lower speed should not be a significant hindrance. The RN2903 has a maximum output power of +18.5 dBm (70.8 mw), alleviating concerns regarding the black powder charges used in separating the nose cone from the rocket.

5.1.3.6.3   LIDAR

A LiDAR sensor was chosen as the primary means of object avoidance. The LiDAR sensor will be a Garmin LiDAR Lite v3, SEN-14032 and can be seen in Figure 58. This specific sensor was chosen due to its easy Inter-Integrated Circuit (I^2C) interface, as well as its reliability. The sensor measures distance by transmitting Near-Infrared laser signals and calculating the time delay between transmission and reception of reflected signals. After initialization the sensor is capable of up to 400 kHz data transfer. In addition to simple distance measurement, this sensor can measure velocity peak distance and provide a history of recorded data. A LiDAR sensor was chosen in spite of its greater cost due to its greater reliability in a greater number of conditions. Other possible solutions considered were an ultrasonic sensor, which would have been significantly less expensive; but excessive ambient noise, adverse weather conditions, or other unavoidable conditions can cause interference that reduces the ability of the sensor to give accurate measurements. LiDAR does not have these same issues, so the additional expense is necessary.

Figure 58. A Garmin LiDAR Lite v3, SEN-14032 will be used for object avoidance.

5.1.3.6.4   GPS/Bluetooth

A secondary system for navigation will include a Global Positioning System (GPS) module as well as a Bluetooth beacon system. The GPS will be used to transmit the current position to the ground station. A GlobalTop FGPMMOPA6H standalone GPS module will be used. It has the capability of sending an updated position 10 times per second. Additionally, this module was chosen for its low power consumption, easy 3.3 V operation, and a theoretical limit of 40 km operation. Additionally the GPS utilizes a universal asynchronous receiver-transmitter (UART) interface, which allows for quick retrieval of position data, and its low footprint is perfect for the designed sensor board. In addition to GPS, Bluetooth (specifically Bluetooth Low Energy, or BLE) will be used to ensure that the competition requirement of the minimum 5 feet distance from the rocket is met. One to two Bluetooth beacons will be placed in each section of the rocket, in addition to 3 Bluetooth modules on the rover, for a total of at least 10 Bluetooth transceivers. Details of the rover's use of these Bluetooth modules are given in Section 5.1.3.7. The Bluetooth modules presently designed into the rover prototype printed circuit board (PCB) are JDY-08 BLE UART Transceiver Modules. This model was chosen due to its programmability and its low cost of about $4 each. As there will be 10+ of these transceivers, higher costs per chip could become prohibitive. This is especially the case if higher accuracy position calculations are required, which would most effectively be obtained via a greater number of beacons. An alternative still potentially in consideration is the MDBT42–512K, which is attractive due in part to being newer, but mostly due to its approximately 50% smaller footprint (0.54 inches by 0.35 inches compared to the JDY-08's footprint of 0.77 inches by 0.59 inches), however its cost nearly makes it prohibitive at just over $10 each. The nominal connection distance for these modules is 100 feet, a range long enough to ensure the rover has moved far enough. The maximum output power of the JDY-08 module is +6 dBm (4 mW), and -148dBm (<1mW) for the FGPMMOPA6H.

5.1.3.6.5   Gyroscope/Accelerometer/Magnetometer

An LSM9DS1 three-in-one gyroscope/accelerometer/magnetometer module was chosen for determining the orientation of the rover and allowing for the correct processing of LiDAR and GPS data. This particular model was chosen for its ability to handle the rocket's acceleration profile based off of previous years' flight data. Again, its low cost was particularly important.

5.1.3.6.6   Altimeter

The rover will utilize an MPL3115A2 altimeter to measure altitude data during the rocket's flight as well as determine when the rocket has touched down. This particular altimeter was chosen because of its simple Inter-Integrated Circuit (I^2C) interface, its wide pressure sensing range (50-110 kPa), and its adjustable acquisition rate, which can provide data up to once per second. In addition, this particular altimeter comes with a built-in altitude calculation, so it requires no calibration reading or calculating.

5.1.3.7   Algorithms

Using the MPLabX IDE, the PIC32 microcontroller will be programmed to communicate with the base station, triangulate current position with respect to each section of the rocket, and handle object avoidance. The PIC32 will also control the four brushless DC (BLDC) motor drivers, as well as the servo driver. For position and orientation relative to the rocket sections, the rover will periodically receive a signal from each Bluetooth beacon within range. From the in-range beacon signals, the rover will utilize the value of the received signal strength indicator (RSSI) on each of its three Bluetooth modules. This information will enable the rover to determine its orientation, as well an estimate of its distance, relative to any section of the rocket within range. With these values, the rover can calculate which direction most efficiently leads away from the sections of the rocket within range. Any section of the rocket outside the range of the rover's Bluetooth modules will be a sufficient distance away from the rover to meet the competition requirement of 5 feet from any part of the rocket.

5.1.3.8   Power Control System

The rover will use 6 IMREN 18650 3000 mAh High Drain Batteries. These 3.7 V rechargeable IMR cells can provide a current of up to 20 A continuous and 40 A pulse. The cells will be configured such that they provide a 3-cell voltage (3 cells will be in series) and a 2-cell current (each series cell will be paired with an additional cell parallel to it). This configuration will provide a nominal voltage of 11.1 V that produces a current of up to 40 A continuous and 80 A pulse. The Power Supply Subsystem consists of these 6 IMR cells supplying 11.1 V to the DC to DC converters, which convert the 11.1 V to 12 V, 5 V, and 3.3 V to fully power the rest of the deployable rover. The photovoltaics supply a variable voltage to the DC to DC converters, which store this energy back in the IMR cells. There are a number of circuits to ensure the IMR cells

are in healthy condition and that they do not damage the other components of the rover. These circuits provide overcurrent (OC) protection, over temperature (OT) protection, short circuit (SC) protection, overvoltage protection, and overpower (OP) prevention.

This new battery was chosen over the initially selected battery, the Tracer 12V 8Ah Lithium Polymer Battery Pack, in order to reduce the weight of the rover and therefore the entire payload. The new batteries are also smaller and in turn fit on the rover in a more practical manner. The layout of the new batteries can be seen in Figure 42.

5.1.3.9 Ground Station

Like the rover, the ground station will consist of a PIC32 and RN2903 LoRa module, which will communicate with the RN2903 LoRa module on the rover. The ground station will consist of the same PIC and LoRa module models as those used on the deployable rover, thus simplifying the code writing process. The ground station PIC32 will be interfaced with a laptop via serial USB. The ground station will serve as an easy way to display the rover's current status and provide a place from which to remotely deploy the rover from the rocket, thus beginning its autonomous movement. This particular setup was chosen mainly for convenience because it only involves connecting a serial device to a team member's laptop in order to communicate with the rover.

5.1.3.10   Payload Interface

The rover payload will be integrated into the vehicle using a track system comprised of four 3D printed tracks and triangular supports as discussed in Section 5.1.3.4. This track system is intended to provide a platform for the rover wheels, restricting any radial and tangential motion relative to the rocket body. It is crucial that the track system is integrated into the rocket body effectively to prevent any undesired displacement of the rover payload during flight. A diagram of this concept can be found in Figure 49. The system includes a set of tracks for each wheel and triangular supports. The tracks will extend 10 inches, along the length of the rover tube. The triangular supports will serve as the mating connector between the tracks and the rocket body. To adhere the triangular supports to the tracks and the rocket body, RocketPoxy will be used. The epoxy provides high strength bonds for joining the fiberglass and carbon fiber materials of the rocket body to that of the triangular supports, resulting in a robust integration between the rover payload and the rocket body. In addition to the tracks two 3D printed mounting cubes will be attached to the inside of the body tube in a similar fashion as the tracks. These cubes allow for further securement of the rover.

The deployable rover payload will implement three bulkheads: one at the rear of the payload that will be epoxied in place and will be mounted with the deployment system, one epoxied at the opening of the nose cone with circles cut out for the PVC pipes of the deployment system, and one epoxied part way down the nosecone to cap off the space used for the ejection charges. These payloads help to protect the payload from the ejection charges as well as contain the payload. These bulkheads will be custom sized in-house.

5.1.4 Testing of Payload Equipment

The deployable rover will have various stages of testing to ensure a safe, robust, and reusable system. The initial tests will be ground tests to ensure each component of the payload performs as expected. These ground tests will ensure the reliability of the electronic control system and all physical mechanisms. Each step of the system will be tested until the process is successful for at least five consecutive runs. The ground tests will help determine if any changes are needed to the design. Determining any necessary adjustments prior to a full-scale launch will help mitigate any potential failures at a larger scale. This will not only help save the team money in the long run but also lead to a safer and more robust payload. The deployment and securing system will be further tested with a drop test. The payload will be dropped from a various heights to simulate the body tube landing after a successful flight. During these tests the payload will be tested with both the drogue parachute deployed and without the drogue parachute. This second condition will test the payload if a hard landing is achieved. The securing system will be analyzed after the drop to confirm the rover was secure during the impact. The deployment system will then be tested again to ensure it functions in a reliable manner. Once the ground and drop tests have achieved the desired results the payload will be tested with a full-scale test flight. The team is scheduled for a full-scale test flight on February 10. A summary of the testing that will be performed on each system of the payload can be found in Table 24.

Table 24. A summary of the verification method for each system of the rover payload.

Subsystem	Requirements	Verification Method
Rover	Avoid objects and drive 5ft	Ground testing, full-scale test flight
Solar Panel System	Deploy solar panels	Ground testing, full-scale test flight
Deployment System	Deploy rover upon landing	Ground testing, drop test, full-scale test flight
Internal Locking System	Lock rover during flight	Ground testing, drop test, full-scale test flight
Electronic System & Sensors	Interface between components, record and store data	Ground testing, full-scale test flight

Rover Algorithm	Track location, provide object avoidance	Ground testing, full-scale test flight

5.2 Air Braking System

5.2.1 System Overview

5.2.1.1 General System Design

As stated in Section1, the system is comprised of three major components, the aerodynamic system, the mechanical system, and the electronic system. The aerodynamic system is the part that will directly alter the flight of the rocket. It does this by inducing drag through the use of drag tabs, which are four flat plates evenly spaced around the rocket body that are variably extended into the airflow. The variable extension of the tabs allows for the control of the magnitude of the drag force on the rocket as needed. The mechanical system is the physical component that controls the extension of the drag tabs. It is a crank-slider mechanism with links connecting a central shaft to the tabs. By rotating the shaft in a particular direction, the tabs extend or retract linearly. The final component, the electronic component, is what controls the actions of the mechanical system. It does this by using a combination of accelerometer and barometer data to determine the velocity of the rocket and predict a flight path and final apogee. Then using a microcontroller and control algorithm, it compares this to an ideal flight path and determines the drag force required to match the real flight to the ideal. From there it determines the tab extension required to achieve this force and relates this to an amount of rotation in the central shaft of the mechanism. After obtaining the rotation required, the microcontroller sends this to the servomotors and they turn the shaft. This process begins after the sensors register that the motor has burned out and is carried out and repeated continuously until the sensors register that apogee has been reached. During motor burn and during descent, the tabs will remain fully retracted into the rocket body. The assembly and layout of the entire system is shown in Figure 59.
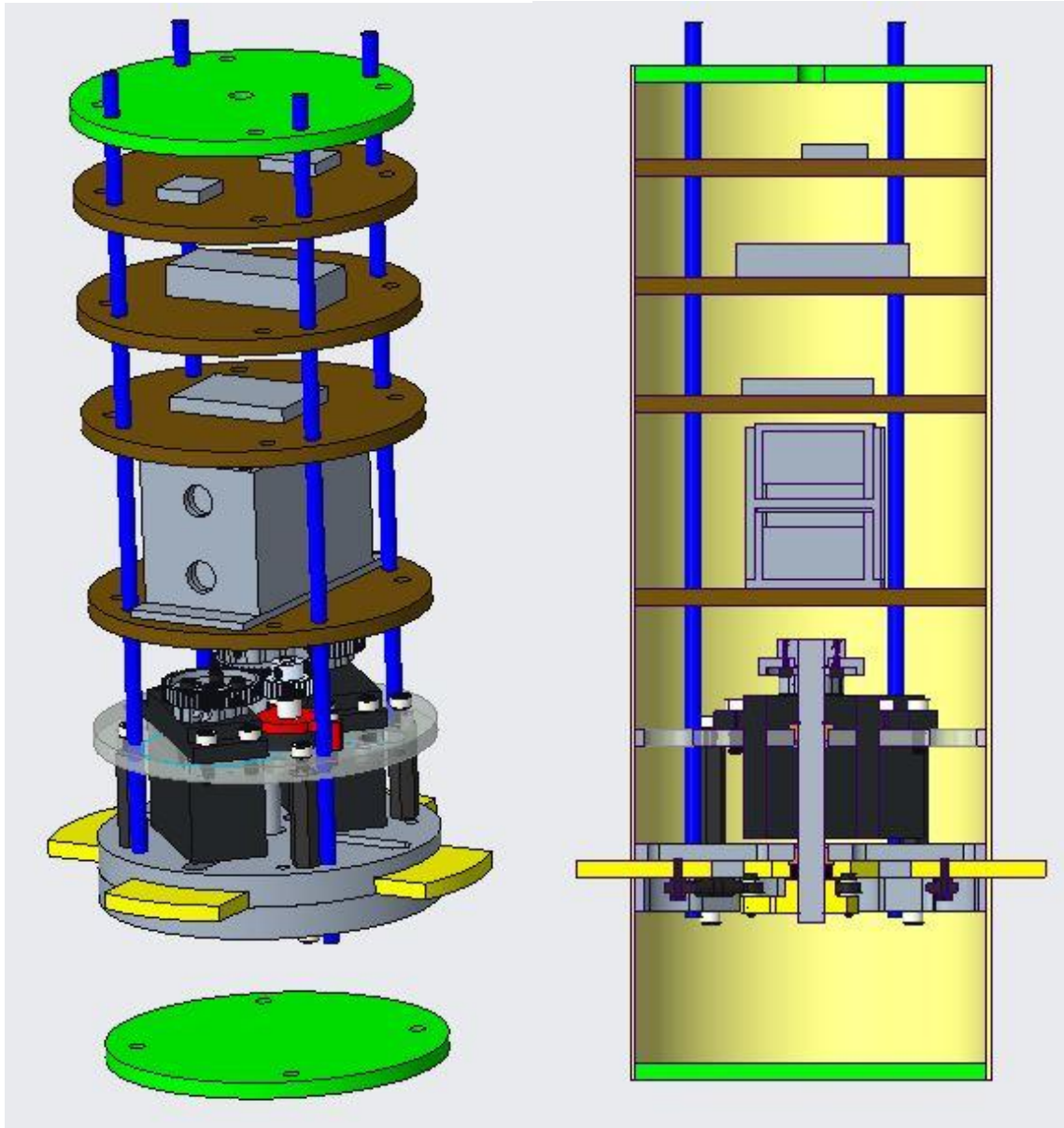
Figure 59. Overall design of the air braking system.

5.2.1.2 Success Criteria

The success of the air braking system will be determined in four stages. Stage 1 success is to affect the flight of the rocket in a measurable way. This means the system must reduce the apogee of the rocket by an amount greater than weather and wind conditions already would. Achieving stage 1 would mean that the system works, but needs a lot of improvement in the design of all three major components. Stage 2 success is to bring the apogee to a height within the margin of error of the previous methods used, namely adding ballast to the rocket. Achieving

stage 2 success means the system not only works, but is a more effective method of apogee targeting than those previously used. Design changes would still need to be made, but the focus of these changes would be on the mechanical and electronic components of the system. Stage 3 success is to bring the apogee to a height that is the closest to 5280 feet in the competition. Achieving stage 3 success means that the design is very effective and robust, and only minor changes to the system would be needed to improve it. Stage 4 success is to bring the apogee to the target of exactly 5280 feet. Achieving stage 4 success means that the system has successfully accomplished its required task. Any improvements that would be made to the design would be needed only to improve the robustness and repeatability of the system. If none of these stages are achieved during the operation of the air braking system, the performance will be deemed a system failure.

5.2.2   System Design

5.2.2.1 Aerodynamic System

5.2.2.1.1   Drag Tab Shape

The area of each drag tab was determined to be 2 in^2. This tab area was calculated by assuming that the tabs would be fully extended right after motor burnout and for the duration of the flight. The tab area was calculated using a summation of forces for the rocket seen in Equation 2.

$$m_{rocket}a \ = \ F_{drag,rocket} \ + \ F_{gravity} \ + \ F_{drag,tabs} \qquad \text{Eq. 2}$$

In Equation 1, m_{rocket} is the mass of the rocket, a is the deceleration of the rocket required to reach an apogee of 5280 feet, $F_{drag,rocket}$ is the skin-friction drag of the rocket, $F_{gravity}$ is the total weight of the rocket, and $F_{drag,tabs}$ is the total drag of the tabs at full extension. The drag forces of the rocket and the tabs were calculated using Equation 3.

$$F_{drag} \ = \ \frac{1}{2}\rho v^2 A C_D \qquad \text{Eq. 3}$$

In Equation 3, ρ is the density of the fluid, which is air in this situation, A is the cross-sectional area, v is the velocity of the rocket, and C_D is the coefficient of drag. The drag tabs were approximated as a flat plate and the rocket was approximated as a bullet. According to NASA, these approximations provided drag coefficients of 1.28 and 0.295 for the drag tab and the rocket, respectively. Using the approximate drag coefficients and the assumption that the tabs are fully extended for the duration of the flight, the tab area was calculated to be 2 in^2. However, because of variations in air density and rocket velocity, the full extension of the tabs throughout the duration of the flight is not necessary. As such, a control system will be implemented to

continually calculate the drag needed to reach apogee and will vary the extension of the tabs into flow as necessary. The varying extension of the tabs allows for the manipulation of the cross-sectional area exposed to flow and, in turn, the manipulation of the drag force created by the tabs.

In the design process of the drag tab, the outer edge was designed to be curved so that the tab may sit flush with the outer surface of the rocket when not extended. Also, the back edges were designed to be angled inward so that the drag tabs may fit within the confines of the rocket when not extended.
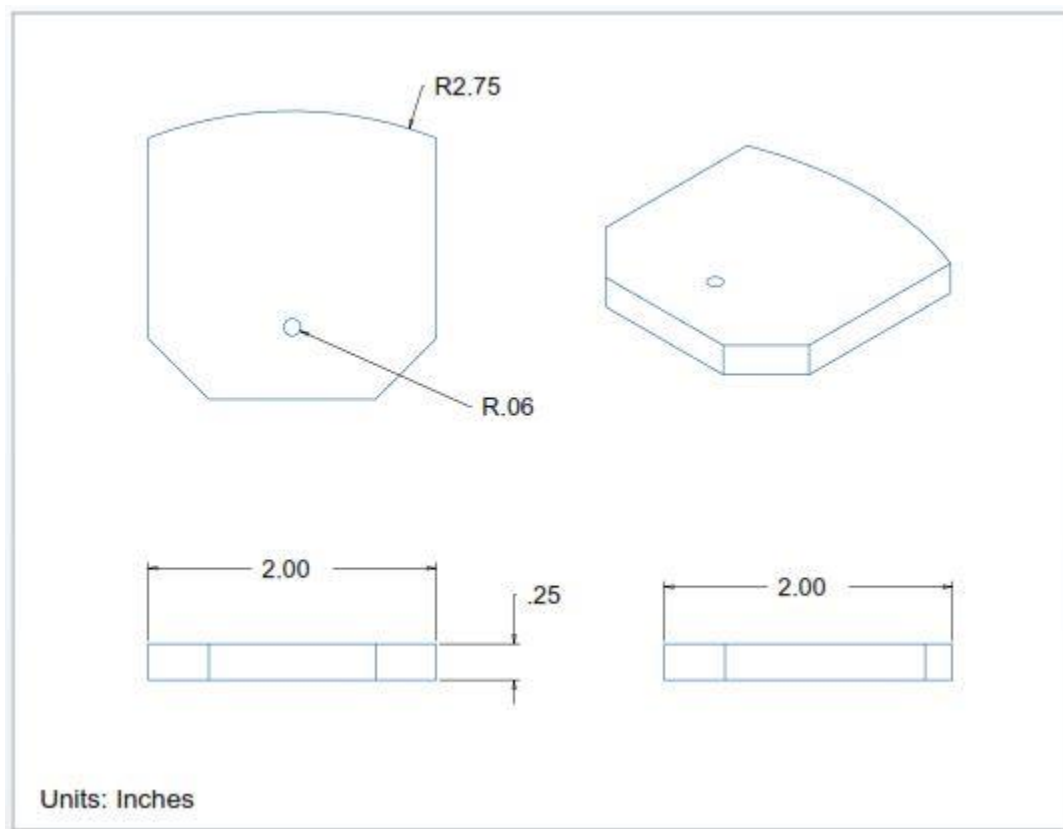
Figure 60. CAD drawing detailing the dimensions of a single drag tab.

5.2.2.1.2 Drag Tab Materials

The drag tabs will each be made of a single piece of Ultra High Molecular Weight Polyethylene (UHMWPE or UHMW). Although previous material considerations for drag tabs included High Density Polyethylene (HDPE), aluminum, or 3D printed carbon fiber, UHMW

was chosen for several reasons, including friction, cost, density, machinability, and wear resistance. For the same reasons, the slide plates that guide the tabs will also be made of UHMW. Several other types of high strength plastic were considered, primarily Delrin and PTFE, but a preliminary pricing check for the necessary amount showed them to be too expensive for further consideration.

While UHMW may not have a higher yield stress than aluminum or carbon fiber, it possesses more than sufficient strength for its application on this rocket and is superior to the other materials in almost every other area. UHMW on UHMW has a coefficient of friction that is lower than both aluminum and carbon fiber (but near HDPE), and is less dense, more machinable, and resists wear better than all other materials. HDPE is less costly and may have lower friction, but for the other added benefits of UHMW and the marginal cost difference, UHMW was chosen.

UHMW's wear resistance is so great that it is used as part of replacement joints and prosthetics, and this property is a key part of its selection for the tab material. Minimal wear means a more constant surface finish and friction coefficient, which allows the system to function predictably over long periods of time without tuning or adjustment.

All comparison data can be found in Table 25 below, and a stress strain curve for UHMW can be seen in Figure 61.

Table 25. Comparison of the possible drag tab materials.

Material	Yield Strength (psi)	Friction (static/ kinetic)	Cost (Equivalent Amounts, USD)	Density (g/cm³)	Machinability	Wear Resistance
UHMW	5000	0.2-0.3/0.2-0.3	$8.94	0.93	Excellent	Excellent
HDPE	4000	~0.25/~0.25	$7.21	0.93-0.97	Excellent	Good
Carbon Fiber	40000	0.65/~0.35	$60 (conservativ	~1.6	Poor, edits require an expensive	Moderate, but wear causes

			e)		reprint	hazard and increase in friction
Aluminum	40000	1.1/0.3	$14.54	2.7	Excellent	Moderate /Poor
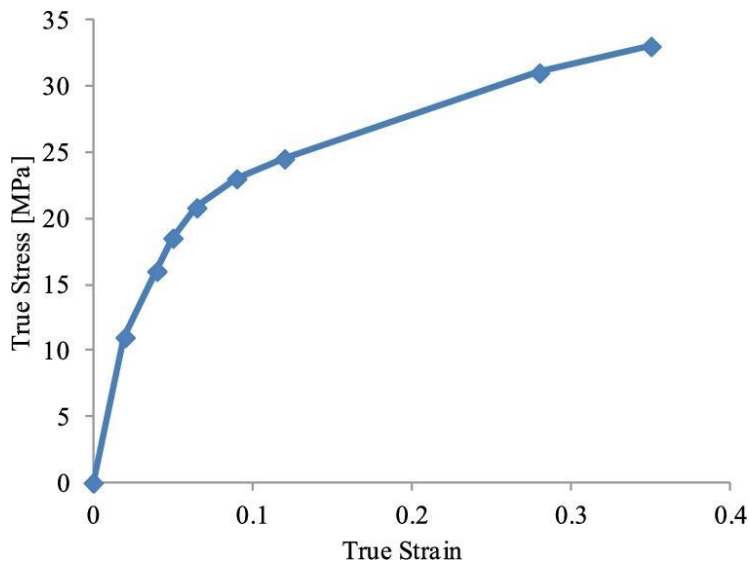
Figure 61. Stress-strain curve for UHMW.

5.2.2.2 Mechanical System

5.2.2.2.1 Mechanism Design

Mechanically, the air braking system will consist of four drag tabs deployed by a crank-slider type mechanism. Figure 62 shows the CAD model of the system, which was designed in Creo/Pro-E (Creo Parametric 4.0). The system is actuated by two PowerHD 1235MG High-Power servos, which power the central shaft via a 1:1 gear reduction. In order to transfer torque effectively, the gears are mounted to both the shaft and servo via clamping hubs. Since the cross piece that drives the tie rods uses a key to transfer torque, hubs were used at the gear end to ensure that the shaft could be adjusted such that the neutral position for the servos coincides with the retracted position for the tabs. Hubs are used to attach the servo gears because the servos use a non-standard servo spline, and so a clamping hub provides a more reliable solution

The tabs slide in slots in the upper plate. The lower plate is a ring around the exterior, because when the tabs are extended into the flow, they will rack in the slots, sliding on the exterior edge on the bottom of the tab, and the interior edge on the top. They are attached to the tie rods, which are attached to the cross piece, such that when the cross piece is rotated by the servos, the tie rods extend or retract the drag tabs.

The critical dimension for both the cross piece and the tie rods is the center-to-center distance between the holes, also called the link lengths. In this system, the link lengths were chosen based on a few factors. First, the chosen link lengths mechanically limit the system, such that the drag tabs can only extend 1 inch from the exterior of the rocket. Second, they are optimized to require the lowest theoretical maximum torque, which will be further discussed in the report. This second criterion is constrained by the fact that the links cannot interfere with each other when fully retracted. Furthermore, the payload needs to be able to retract the drag tabs to be inside of the slotted plates, not just flush with the rocket exterior, to allow the system to be assembled into the coupler and body tubes. Because of this geometry, the payload has no dead positions (configurations for which applying torque to the shaft physically cannot articulate the system) that are possible without the links interfering with each other. Similarly, at full extension, the system has an infinite mechanical advantage, since it is at a limit position.

There were also a few other design choices made that stand out. First, material selection was important throughout the design process, in addition to the choices described in section 5.2.2.1.2 to reduce friction in the system. Wherever there are non-shear, low-load applications, nylon fasteners will be used to reduce weight over steel and aluminum options. Aluminum bolts were also considered, but were too expensive for our budget. Nylon was also used for the hexagonal standoffs that support the servo plate, and for the shaft spacer near the cross piece. The drive shaft is aluminum to save weight, and rotates on oil-embedded, flanged, bronze bushings to reduce friction. A pair of retaining rings holds the shaft in place.

The servos are mounted in a custom polycarbonate plate. This mount plate also holds the upper bushing for the drive shaft. A potentiometer is mounted on this plate to give position feedback to the control system. It is held on by a custom 3D-printed mount and driven by a 3D-printed gear, again made of plastic to reduce weight in a low-strength application. Finally, the plate also has pass-through holes for the potentiometer and servo wires, with accompanying smaller holes so that the wires can be zip-tied in place to make sure they don't get caught in the mechanism.
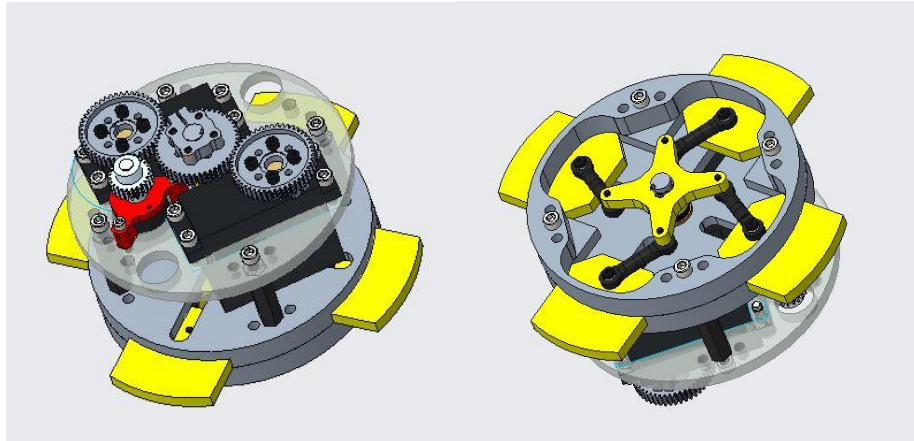
Figure 62. Isometric views of the drag tab mechanism.

5.2.2.2.2　Mechanism Components

The mechanism controlling the motion of the drag tabs will consist of several components, including the servo motor mount and gears that connect the servo motor to the crosspiece. The cross piece rotates to displace and turn 4 tie rods consisting of a shaft and two ends. The tie rods are connected to the drag tabs, which extend and retract based on the clockwise and counterclockwise motion of the crosspiece. The drag tabs rest upon slotted support plates which guide the tabs in the direction normal to the surface of the rocket.

The servo motor mount, which will hold the servo motors in place, will be made from polycarbonate. The polycarbonate will undergo shear forces as the rocket is accelerated upwards while gravity is pulling the servo motor down. Polycarbonate has a shear strength of 64 MPa, and will be more than enough to support the motor. Polycarbonate was chosen over other plastics because it is rigid and clear while being easy to machine and relatively cheap. A clear mount is desired so that those constructing the mechanism can see through it easily.

Both the servo gears and the driven gears will be aluminum. The gears will be forced to transmit the torque from the motors to the crosspiece. Each gear will both receive transmit forces on its perimeter as their teeth interlock and force the motion of the subsequent piece, meaning the yield strength of the gears must be strong so that they will not be deformed during operation. Aluminum has a yield strength of about 40000 psi.

The central crosspiece will be made from Ultra High Molecular Weight Polyethylene, (UHMW). The crosspiece will be under torsional forces. As the crosspiece translates the force generated by the motor to the tire rods, there will be shear forces present at the base of each arm as the forces from the tie rods act at an angle at the end of each arm. With a shear strength of 33.1 MPa, the UHMW won't break as a result of the shear forces at the base of each arm. A 4

view CAD drawing of the crosspiece is seen below. Each arm has a length of 1.05 inch. UHMW was chosen over other materials like carbon fiber and due to its low weight, low friction coefficient, and durability.
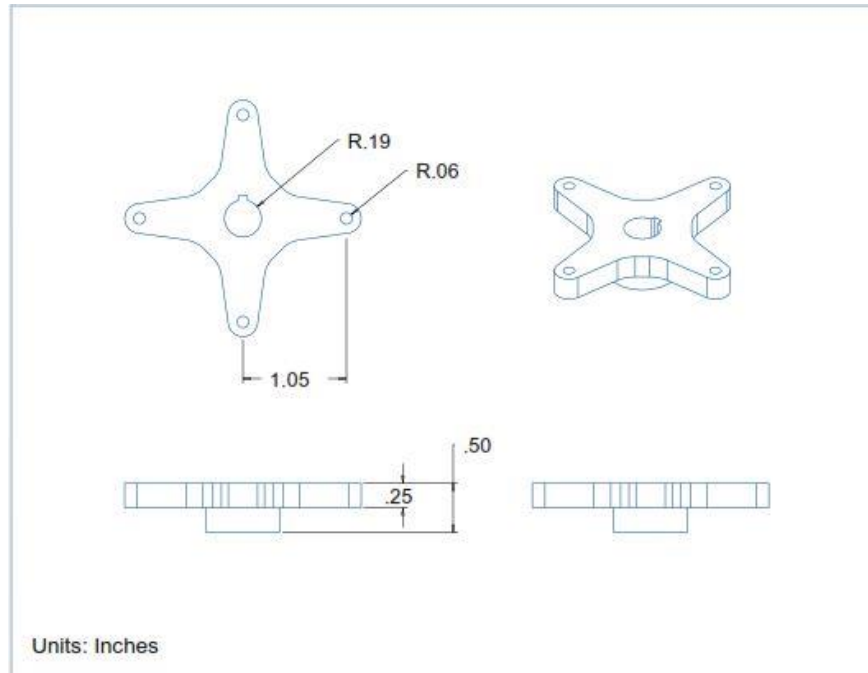
Figure 63. 4 View CAD model of the cross piece.

Tie rods connecting the cross arm to the drag tabs will be constructed using two rod ends with a fixed distance shaft. Aluminum was determined to be the best material to use due to its low density and affordable price. With a center-center (major) length of 1.20 inches, the tie rods will be under compressive and tensile forces as the cross piece rotates to extend and retract the tabs, respectively. Aluminum's typical tensile strength, being greater than 10152.6 psi, is more than adequate for the forces the tie rods will face.
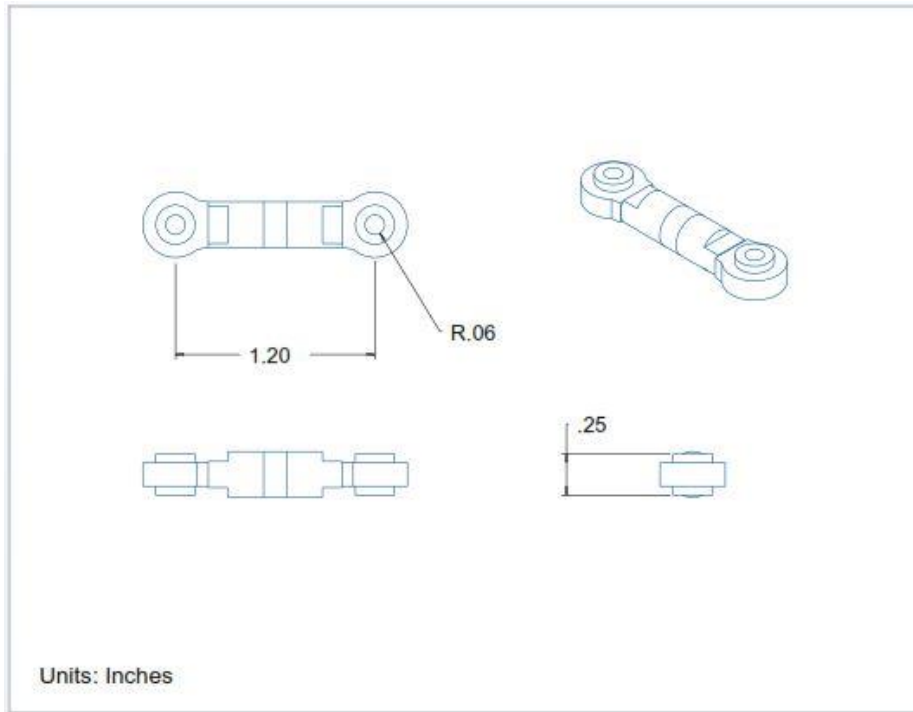
Figure 64. 4 View CAD model of the tie rods.

The drag tabs extending from the body of the rocket will be constructed using UHMW. UHMW was also chosen to be used for the slotted support plates, which guide the drag tabs out normal to the surface of the rocket body. The primary force on the support plates is friction from the drag tabs, while the drag tabs will undergo both friction and shear forces due to the support plates and drag that acts on the exposed area of the tabs. The low coefficient of friction allows the tabs to slide past the plates with ease, while a high yield strength will prevent the tabs from plastic deformation under the shear forces as a result of the drag force from the air and normal force from the support plates acting in opposite directions. Other materials such as aluminum and carbon fiber were also considered for the tabs due to their very high strength, however UHMW is more machinable and has greater wear resistance. Aluminum and carbon fiber are also much more expensive.

5.2.2.2.3   Torque, Servos, and Gearing

The PowerHD 1235MG Servos can each provide up to 35 in-lb of torque. According to our friction model, which is described in the Appendix I of this report, the system will require a maximum torque of 21.6 in-lb to articulate in the worst case scenario (almost-full tab extension, immediate post-burnout velocity). In order to ensure a factor of safety of at least 2, the servos need to combine to provide at least 43.2 in-lb. However, it would be easiest to control if the full

range of motion for the servos could be restricted to at most 90 degrees, since that is how much the servo can move in either direction from its neutral position. The shaft needs to rotate roughly 75 degrees to fully articulate the drag tabs, so for simplicity a 1:1 gear ratio was chosen between the servos and the drive shaft. This supplies a maximum 70 in-lb of torque at stall, providing a factor of safety of 3.24. This is important for control, since the excess of power from the servos ensures that the mechanism will never stall, and even at the worst case, it will be able to move quickly to any desired position at any time during flight.

The gears used are 48 tooth, 32 diametric pitch, aluminum gears pictured in Figure 65. The diametric pitch was chosen because it is a common pitch for systems of this scale, and so there are plenty of gearing options available, and using aluminum ensures that the gears will be more than strong enough. Aluminum was chosen over other metals because the gears available are compatible with the selected clamping hubs as well. Ideally, the gears would have a 14.5 degree pressure angle to reduce backlash, but the aluminum gears selected were only available in 20 degree pressure angle. Backlash still should be minimal since there is only one stage of reduction, and tight manufacturing tolerances will help to mitigate backlash as well. The selected gears are 48 tooth, which helps with packaging the servos in the payload. However, any combination of gears that have a total of 96 teeth will work without modifying the servo mount plate, meaning that the gear ratio can be changed later if necessary without requiring other design changes, though this seems unlikely.

Figure 65. Image of 48 Tooth, 32 DP, ½" Bore Hub Mount Gear.

The potentiometer will be driven by a 1:2 reduction (technically an overdrive), which will increase the accuracy of the sensor, since it has a larger range of motion than the mechanism. The potentiometer gear will be 3D-printer plastic to save weight, and it will be held on with a set screw to allow for adjustment in a low-load application.

5.2.2.3 Electronic System

5.2.2.3.1 Servomotors

The primary concerns in selecting a servo motor were torque output, power needs, operating speed, and price. The maximum torque required is approximately 1000 oz-in. The purchase of a single motor capable of meeting this requirement was financially prohibitive. Therefore, the team decided to use two servos, each capable of producing more than 500 oz-in of torque and operating in tandem to meet the 1000 oz-in requirement. The drawback of using two servos is the increased complexity, however it is the best option within the team's budgetary constraints.

The team selected the Power HD 1235MG as the best option. This model features an all-metal gear train, which offers more durability than the plastic gears often found in small servos. In addition, the output shaft is supported by ball bearings, which offer increased performance over the bushings found in similar servos. The 1235MG has an operating voltage range of 6 V – 7.4 V. To obtain maximum operating speed, we will be running the motors with a 7.4 V supply. At this voltage, the 1235MG has a speed of 0.18 sec/60°, a stall torque of 560 oz-in, and a stall current of 9 Amps. However, under expected conditions the servos will not reach stall torque (the combined 1120 oz-in stall torque that the servos provide is well above the maximum 1000 oz-in needed to move the system). Expected current draw is around 2-4 Amps, depending on friction in the mechanism. Table 26 lists the relevant specifications of the 1235MG.

Table 26. Specifications of the PowerHD 1235 MG servomotor.

Motor	Stall Torque (oz-in)	Operating Voltage (V)	Current at Stall Torque (A)	Speed (sec/60°)	Size (in)	Weight (g)	Cost ($)
Power HD 1235MG (use 2)	560	7.4	9	0.18	2.34 x 1.16 x 2.14	170	$60

While operation at stall torque is not expected, there is the concern of the mechanism jamming. In this scenario, the servos would be forced to operate at stall torque until a team member shut down the system. Although there are no manufacturer specifications on maximum duration of stall torque operation for the 1235MG, most small servos can be damaged by excessive operation at stall torque. For this reason, the control code will include lines to shut down the servos if a jam is detected.

5.2.2.3.2   Microcontroller

An Arduino MKR Zero will be used to control the air braking system. The Arduino MKR Zero has multiple advantages over other controllers considered. In the preliminary design phase, a Teensy 2.0 or Arduino Uno were the preferred options. However, the Arduino MKR Zero was chosen as a better option given its technical specifications and low cost.

The Arduino MKR Zero has multiple advantages over other options. It has faster clock speeds, more memory, and more flash storage than other boards considered such as the Arduino Uno. It has a built in SD card reader that will be utilized to store data on the performance of the system. The MKR Zero also runs on 3.3 V logic, which will allow for less power used by the controller.

While the Arduino Uno would be sufficient for this system and the specifications for the MKR Zero are better than needed, it was decided that the MKR Zero is a better investment due to its similar cost to the Arduino Uno for the higher specifications. The Arduino MKR Zero costs $21.90 as opposed to $15.00 for the Arduino Uno. The improvement in specifications for only about $7 difference in cost was decided to be valuable for long term usage of the microcontroller. For full specifications of the Arduino MKR Zero, refer to Table 27 below.

Table 27. Technical Specifications for the Arduino MKR Zero.

Microcontroller	SAMD21 Cortex-M0+ 32bit low power ARM MCU
Operating Voltage	3.3 V
Digital I/O Pins	22
PWM Pins	12
Analog Input Pins	7
Analog Output Pins	1
Flash Memory	256 KB
SRAM	32 KB
Clock Speed	48 MHz
Dimensions	65 mm x 25 mm
Cost	$21.90

5.2.2.3.3 PCB

The team elected to utilize a printed circuit board (PCB) to control and organize the logic of the payload. It is advantageous to wire all components to a PCB because it combines the strength and stability of soldered joints with the organization and modularity of Molex connectors. When all of the components are connected to the PCB, we can be confident in the reliability of the connections. However, we can also swap or remove components with a simple click of the Molex connectors. If the components were only wired together, without a PCB, it would be more difficult to connect components such as resistors, there would be greater difficulty in identifying the correct connections through the tangled mass of wires, and any connections that required replacement would need to be cut or de-soldered.

Two primary disadvantages of the PCB are space and cost. Adding an entire circuit board and connectors undoubtedly takes up more room inside of the rocket body tube than a collection of wires would. There is also the increased cost associated with ordering a custom printed circuit board and the required connectors. In the case of this project, it was determined that we had sufficient space within the rocket and in the budget to use a PCB, which is the superior option in most other respects.

When designing the PCB, it was important to keep in mind how the board will be used. In this case, wires are run between a motor and microcontroller. The motor can sometimes pull a relatively large current, so the trace width was made as large as reasonably possible while still not overlapping and short circuiting anywhere on the board. We settled on a trace width of 0.05 mm, which is larger than the default width on the EAGLE CAD program, but still allows for all of the traces to be printed on a single layer, resulting in the lowest cost and greatest simplicity of design. It is unnecessary to increase the trace width any further because the wire running from the PCB to the other parts of the rocket is 22 gauge, or 0.02540 mm.
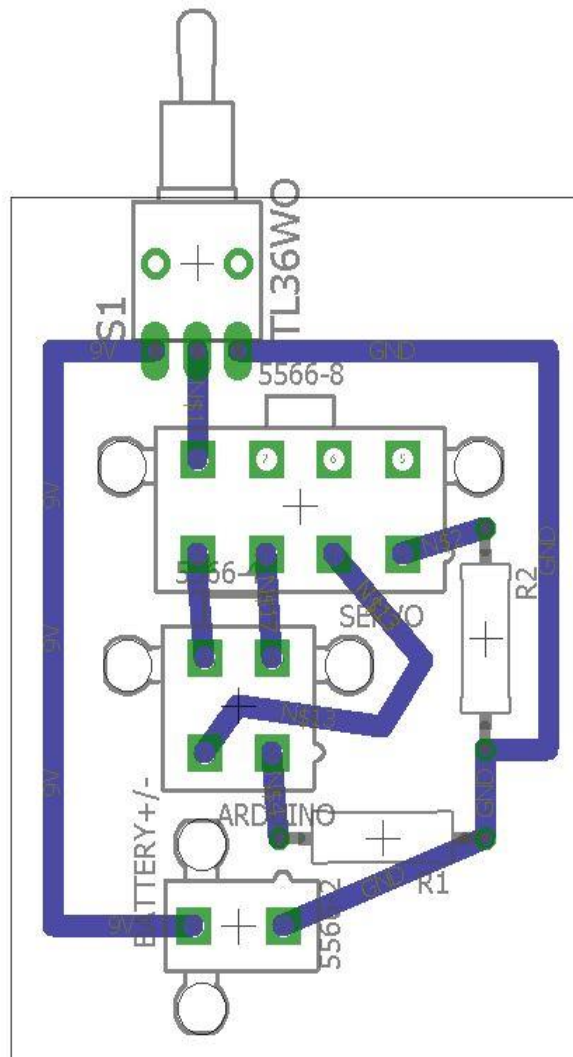
Figure 66. Board drawing of the PCB designed in EAGLE CAD.
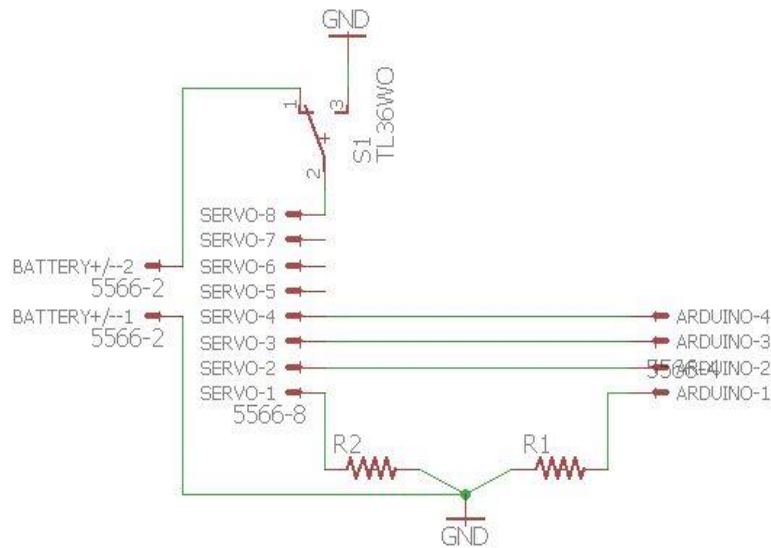
Figure 67. Schematic of the PCB designed in EAGLE CAD.

5.2.2.3.4 Power System

The batteries used to power the servo motors in the air braking system will be two 7.4 V Tenergy lithium ion batteries, shown below in Figures 69. Tenergy batteries were deemed to be a reliable supplier for the purpose of powering the servos. Limited by size, weight and price, the battery chosen has a capacity of 2600 mAh which was deemed acceptable for the payload, as it should provide enough capacity for the idle system before launch and the short term usage during the flight, and is also at an acceptable price point. Full specifications for the 7.4 Tenergy battery are listed in Table 28 below. The batteries will be secured within the system using a custom 3D printed battery case shown in Figure 68.
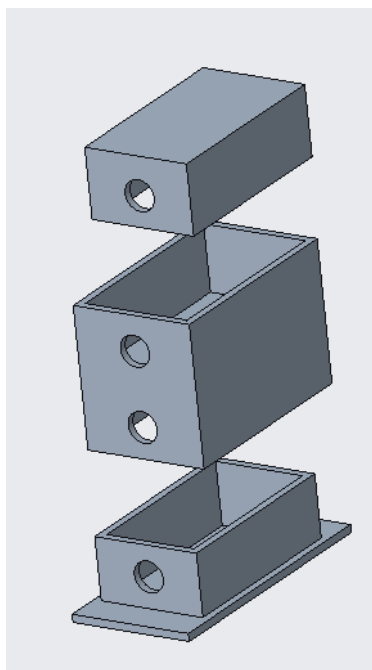
Figure 68. An exploded view of the battery case used to secure the servo batteries.

A 3.7 V Adafruit lithium ion battery, shown below in Figure 70, will be used to power the Arduino MKR Zero used to control the system. The official Arduino MKR Zero website recommends this Adafruit lithium ion battery, which is why it was chosen. The battery has a capacity of 2000 mAh which can power the Arduino MKR Zero for roughly four days, providing plenty of battery life for the run time of the air braking system, which is essential to ensure the whole system can reliably be controlled whenever necessary. Full specifications for the 3.7 V Adafruit battery are listed in Table 28 below.

Table 28. Technical Specifications for the air braking system power sources.

Battery Brand	Tenergy	Adafruit
Intended Use in System	Servomotor	Arduino
Chemistry	Lithium Ion	Lithium Ion
Size (mm)	72 x 38 x 19.5	60 x 36 x 7

Capacity (mAh)	2600	2000
Max Discharge Current (A)	5	0.5
Nominal Voltage (V)	7.4	3.7
Weight (g)	99	34
Cost per Battery ($)	19.99	12.50

Figure 69. A single Tenergy lithium ion battery pack.

Figure 70. An Adafruit lithium ion battery.

5.2.2.3.5   Sensors

The primary sensors utilized in the air breaking payload will be a barometer, the BMP280, and an accelerometer, the ADXL345. The BMP280 was chosen over the MPL3115A2 due to its much greater precision and accuracy, for a comparable measurement range, cost, and weight. The ADXL345 was chosen over the ADXL377 for its significantly greater precision and output rate. While the ADXL377 had a much greater measurement range, previous years' flight data and this year's simulation results indicate that the ADXL345's measurement range of ±16g is more than sufficient to accurately capture the rocket's behavior throughout its flight. The relevant technical specifications for both sensors can be found in Table 29, and images of the barometer and accelerometer are located in Figures 71 and 72, respectively.

Table 29. Accelerometer and Barometer Specifications.

Sensor	Resolution	Noise Level	Output Rate	Weight	Size	Cost
BMP280	1.3 cm	11 cm	157 Hz	1.3 g	19.2x18 mm	$9.95
ADXL345	0.004g	0.015g	3200 Hz	1.27 g	25x19 mm	$17.50
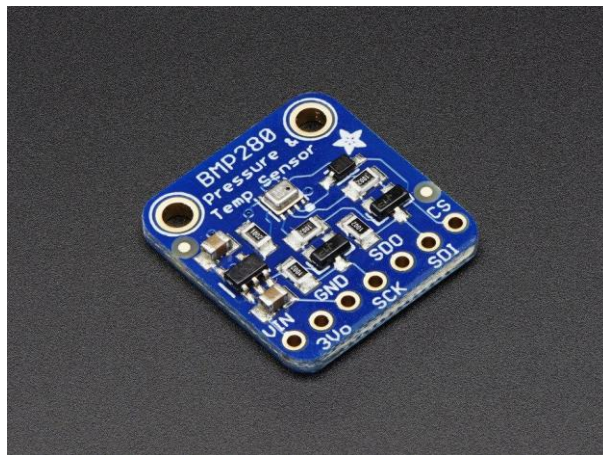
Figure 71. Image of the BMP280.

Figure 72. Image of the ADXL345.

Both the accelerometer and barometer will be powered via an I2C bus connected to the Arduino MKR Zero board. Both sensors are necessary to track the rocket's flight progress: the accelerometer can more accurately and rapidly detect liftoff and burnout since both events are marked by rapid changes in acceleration, while the barometer can more precisely detect apogee because that event is marked by a decreasing altitude. The barometer is also utilized to track the rocket's altitude during the coast phase, since velocity at a given altitude is used by the control algorithm as a prediction of apogee. Furthermore, both sensors are used to calculate the rocket's velocity at different points during flight, which is explained in more detail further in the report. In addition to the accelerometer and barometer, the control code will receive data from a R25W R10K L1% potentiometer attached to the servo gearbox, pictured below in Figure 73. This sensor will allow the control code to compare the servos' intended position to their actual position, indicating whether or not the gearbox or mechanism has jammed.

Figure 73. Image of the R25W R10K L1% Potentiometer.

5.2.2.4   Control Code

5.2.2.4.1   Code Architecture

The general code architecture begins with a startup sequence, which occurs on the launch pad immediately after the payload is powered on. Once all of the sensors are initialized and the ideal flight path data is loaded from the onboard SD card, the code sends a signal to the servos to fully extend and fully retract the drag tabs, providing a visual confirmation for the setup team that both the control code and the tab mechanism are functioning. Then, the code begins to check whether liftoff has occurred, based on an accelerometer threshold of more than 8 g. Once liftoff is detected, the code begins to calculate the rocket's velocity using a linear regression of a 10-point running buffer of barometer data. Additionally, it begins to monitor for burnout based on an accelerometer threshold of less than -1 g.

Once burnout is detected, the drag tab system activates. The control algorithm begins calculating velocity by performing a running Riemann sum of accelerometer data, and compares that velocity to a pre-calculated ideal velocity at the given altitude. This error information is then fed to a PID controller which continuously modifies the servos' position to change the extension of the drag tabs and achieve the desired change in velocity. This process is continued until apogee, detected via a decrease in barometer readings, at which point the drag tab system deactivates and the tabs are fully retracted into the rocket body. Throughout this process, data from a potentiometer mounted to the gearbox is monitored to check whether the mechanism has jammed, and data from all sensors is saved to the onboard SD card for post-flight review. A flowchart summarizing this process can be found in Figure 74 below.
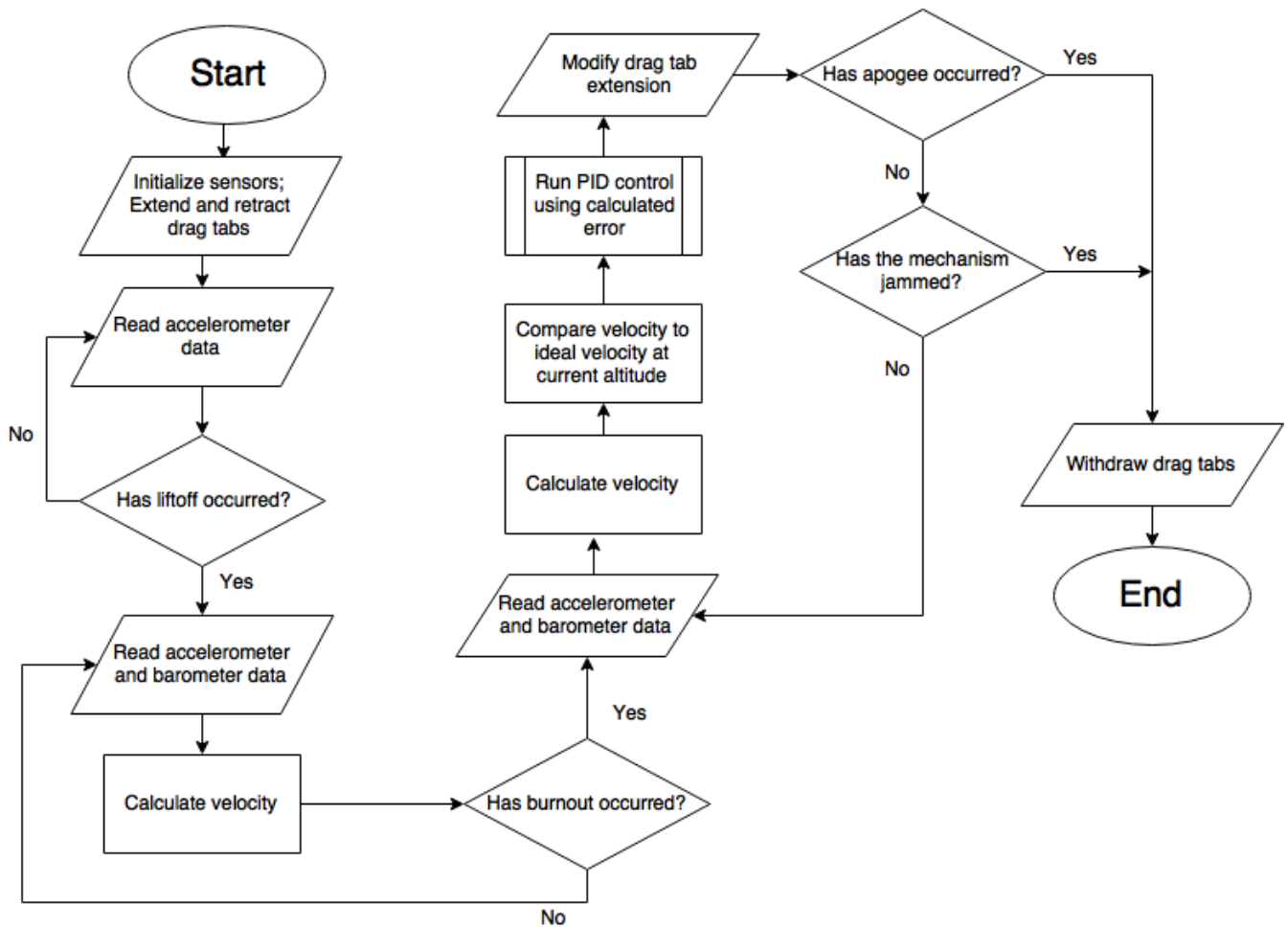
Figure 74. Flowchart of the primary control algorithm.

5.2.2.4.2   Flight Path Monitoring

The control algorithm will monitor the rocket's flight path using a combination of barometer and accelerometer data. During engine burn, a running linear regression will be performed on samples of barometer data to establish a fairly reliable baseline velocity. Once burnout is detected, accelerometer data will be integrated using a Riemann sum to calculate the rocket's velocity for the rest of flight. This "hand-off" method has been demonstrated by our control code simulations to be the most reliable method of obtaining accurate velocity information. Given reasonable sensor noise distributions and a variable launch angle, integrating accelerometer data more closely corresponds to the rocket's actual velocity than differentiating barometer data, and has the added benefit of being less computationally intensive. However, accelerometer-calculated velocity is prone to error during the initial phase of launch- if the integration does not begin precisely at liftoff, or if there is too much vibration-induced noise in the vertical axis during engine burn, then the resulting velocity calculations become highly

unreliable as each data point is dependent on the accuracy of the previous data point. Therefore, the barometer will be used to calculate data during engine burn in order to provide a fairly accurate baseline for the accelerometer data to be built upon during coast phase. In order to track the rocket's flight path, the control algorithm will use this calculated velocity and altitude data from the barometer. The rocket's vertical velocity at a given altitude will be compared to an ideal vertical velocity at that altitude, wherein the ideal velocity will be loaded from a pre-calculated dataset with an apogee of precisely 5280 ft. The difference between the rocket's current velocity and the ideal velocity serves as an indirect prediction of whether, and to what degree, the rocket will overshoot or undershoot its target apogee.

5.2.2.4.3   PID Control

The difference mentioned previously between current and ideal velocity will be fed into a PID (Proportional, Integral, and Derivative) controller, which will multiply the error, the derivative of the error, and the integral of the error by separate constants to generate a value for the servo's position. These constants have already undergone an initial calibration using the control algorithm simulation, and will be further calibrated once the air braking system's electronic subsystems have been constructed; currently, a C_p of 1.9, a C_i of 0.00001, and a C_d of 0.1 have been the most effective. The simulation involves the PID controller directly modifying the product of several terms in the drag force equation, specifically $\frac{1}{2}C_D A$, between a value of 0.1 and 1.5; velocity and air pressure are incorporated separately because both terms vary throughout flight independent of the system's control.

However, in the payload's actual control algorithm the PID controller will direct two servos, outputting a value between 0 (full retraction) and 90 (full extension). Since the cross-sectional area of the rocket varies approximately linearly with tab extension and the other terms modified by the simulation PID controller remain constant, the starting controller coefficients for our real-world tests will simply be the simulated values scaled linearly by a factor of 60, giving a C_p of 114, a C_i of 0.0006, and a C_d of 6. However, drag tab extension does not vary linearly with servo rotation, instead being proportional to the cosine of the servo's displacement angle. Therefore, the simulation-calculated constants will likely not be the most effective in the real world, necessitating further calibration once the physical system is complete.

5.2.2.4.4   Code Redundancy

The control code will serve as a redundancy and failsafe for the rest of the payload, primarily through its startup sequence and by monitoring the functionality of the gearbox via a shaft-mounted potentiometer. When the payload is first powered on, the control code enters a startup sequence which fully extends and then fully retracts the drag tabs. This will provide a

visual cue to the team setting up the rocket that the payload is functional, and if the startup sequence does not occur the payload can then be safely disabled before launch. Additionally, throughout the flight the code will compare the servos' intended position to data from a potentiometer mounted to the gearbox. Aside from quarter-second cooldown periods whenever an instruction is sent to allow the servo to reach its intended position, the control code will continuously check whether the potentiometer is reporting the same angular displacement as the code intends. If the reported data falls outside a pre-calculated margin of error (to be determined based on ground testing of the potentiometer and gearbox) for multiple comparisons, the control code will enter a "jammed mechanism" state, attempt to retract the tabs, and send no other instructions to the servo for the duration of the flight. It will, however, continue to log data and note at what point the mechanism jammed for post-flight diagnosis.

5.2.2.5 Integration

Each electronic component will be secured to a circular deck with a diameter of 5.255 inches made of HPDE plastic. The components will be screwed into the decks using 1 inch long, 10-32 threaded steel-alloy socket head screws and 10-32 low-strength steel lock nuts. There will be a total of four decks, one for each component. The battery will be secured in a 3D-printed fastener, which will include two holes that allow it to be secured to a deck in the same method described above.

The decks will be integrated into the coupler using four 13.25 inch long, 10-32 threaded steel rods, running the full length of the coupler. Each deck will include four holes for the threaded rods to go through and another four holes for the total system integration rods. Each deck will be secured to the rods by eight 10-32 low-strength steel lock nuts and #10 washers. The decks will be parallel to one another.

The same four steel threaded rods will be attached to the coupler through the forward bulkhead. Four holes will run through the bulkhead, which the tops of the steel rods will go through. Each rod will be secured to the bulkhead on both sides with 10-32 low-strength steel lock nuts and #10 washers.

The mechanism will be attached to the steel threaded rods near the aft bulkhead. The steel plates of the mechanism will each include four holes for the steel rods to run through. The mechanism will be secured to the rods using 10-32 low-strength steel lock nuts and #10 washers.

As mentioned previously, the gears will be attached to both the servos and the drive shaft using clamping hubs (ServoCity Part No's: 545592 and 545596) which will allow for adjustments to the angular alignment of the shaft and eliminate the need for additional spaces or retaining rings to position the gear on the shaft. The clamping hubs will also be able to transfer

the required torque, as verified through a phone conversation with ServoCity technicians (ServoCity does not list a torque rating on their product datasheet). The gear on the potentiometer will be held by a set screw, again to allow for adjustment. The set screw was chosen because of the low-load nature of the application.

5.2.2.6 Weight Statement

Component	Quantity	Weight per Part (oz)
Arduino MKR Zero	1	0.33
ADXL345	1	0.045
BMP280	1	0.046
Tenergy Battery Pack	2	3.5
Adafruit Battery	1	1.2
10-32 Low Strength Steel Threaded Rod	4	2.955
HDPE Electronics Deck	4	2.907
Printed Circuit Board	1	0.860
Custom Printed Battery Case	1	5.394
Top Slotted Plate	1	3.012
Other Sliding Plate	1	1.349
Drag Tab	4	0.501
Cross Piece	1	0.270

Drive Shaft	1	0.691
Servo Mount Plate	1	2.339
Tapped Servo Mount Standoff	4	0.097
Potentiometer Mount	1	0.127
32DP 24T Potentiometer Gear	1	0.079
Cross Piece Spacer	1	0.023
Tie Rod	4	0.080
PowerHD 1235MG Servo	2	5.82
0.3125" Clamping Hub	2	0.239
0.375" Clamping Hub	2	0.230
48T 32DP 20PA Gear	3	0.300
P3 R25W Potentiometer	1	0.710
3/8" ID Bronze Bushing	2	0.126
Retaining Ring for 3/8" Shaft	2	0.006
6-32x3/8" Steel Socket Head Screw	12	0.040
6-32x3/4" Nylon Socket Head Screw	2	0.008

M3x14mm Steel Low Profile Socket Head	8	0.033
10-32x1.5" Nylon Socket Head Screw	4	0.030
10-32x5/8" Nylon Socket Head Screw	12	0.017
6-32x1/4" Nylon Flat Tip Set Screw	1	0.002
3/32" Steel Square Key	1	0.020
Total Weight: 64.483 oz		

Note: A full Bill of Materials for the drag tab mechanism is available in Appendix K.

5.2.3 Simulation and Testing

5.2.3.1 Wind Tunnel Test Results

The wind tunnel testing did not yield any results. There was an instrumentation error in which the pitot probe was not operating properly, so the airspeed velocity data was not properly recorded. This was not discovered until the data processing was performed. Because the wind tunnel is now being used for research and for class experiments, the team no longer has access to the tunnel and cannot repeat the test with a properly functioning pitot probe. Therefore, no results from the wind tunnel tests could be obtained. The team will use test results from the subscale flights to confirm the efficacy of the tabs, and the researched drag coefficient of a flat plate in a flow will be used as the drag coefficient for the drag tabs in any calculations.

5.2.3.2 Subscale Flight Test Results

The purpose of the subscale flight was to confirm that the size of the drag tabs was appropriate relative to the size of the rocket. The drag tabs were intentionally sized larger than necessary, as they will not be extended fully throughout the operation of the system. This means that to be proven effective, the tabs at full extension throughout the duration of the entire flight should reduce the apogee of the rocket significantly more than necessary. The subscale flight test was performed using two flights, a control flight with the tabs absent from the body of the

rocket, and an experimental flight with the tabs attached to the rocket as shown in Figure 75. The tab body tube portion was modeled in Creo and was 3D printed using a Fortus 3D printer.

Figure 75. Image of the tab coupler used in the subscale flight test.

Because the subscale rocket was 40% of the size of the full scale rocket, so were the subscale tabs. The full scale tabs will have to reduce the apogee of the rocket by 120 ft, therefore the subscale tabs had to reduce the apogee of the subscale rocket by 40% of this, or 48 ft, if they were operating the same. But since the tabs are attached to the subscale rocket and are not able to be manipulated during flight, meaning they will be affecting the rocket for the whole flight, they will have to reduce the apogee by significantly more than this. The apogee of the control flight was 919 feet, and the apogee of the experimental flight was 858 feet. The difference between these two, and therefore the apogee reduction caused by the drag tabs, was 61 feet. This is 1.27 times the 48 ft predicted by a 40% size reduction. This reduction is proof that the size of the tabs relative to the rocket is large enough for the tabs to effectively alter the flight of the rocket. Therefore, the tabs do not need to be resized or otherwise altered and the air braking system will be aerodynamically effective.

5.2.3.3 Finite Element Method Simulation

Static analyses were performed on aluminum and Ultra-High-Molecular Weight Polyethylene (UHMW) tabs to confirm material strength. Three constraints were applied: one

displacement constraint to prevent movement in all directions on the hole inside of the tab and planar constraints on either side of the tab to prevent all but parallel motion, shown in Figure 76. Since the maximum expected load on each tab was 8.5 psi, a load of 34 psi was applied to obtain a factor of safety of four. This pressure was applied to the area of the tab that the flow will see when the tabs are fully extended. The maximum shear stress, or von Mises stress, shown in Figures 77 and 78, and the displacements, shown in Figure 79, were calculated. The maximum shear stresses calculated were 25 psi and 25.7 psi for the aluminum and UHMW, respectively. As the yield stress for aluminum and UHMW are 40,000 psi and 5,000 psi, there is virtually no concern of the tabs failing with either material. In addition, the maximum displacements calculated for the aluminum and UHMW were 6.4×10^{-6}in and 4.9×10^{-4}in, respectively. These displacements are four orders of magnitude smaller than the tab itself and are therefore negligible. It can be concluded from the static analyses that either tab material will be able to withstand the wind forces without breaking.
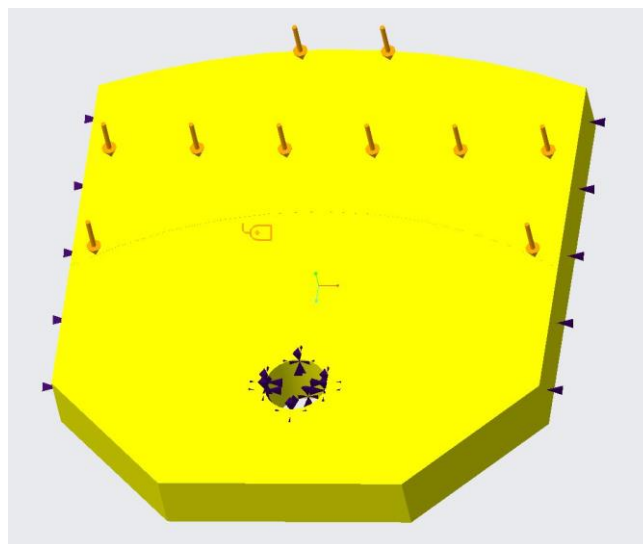
Figure 76. FEM analysis on drag tab. The purple arrows represent the constraints applied and the orange arrows represent the load applied.
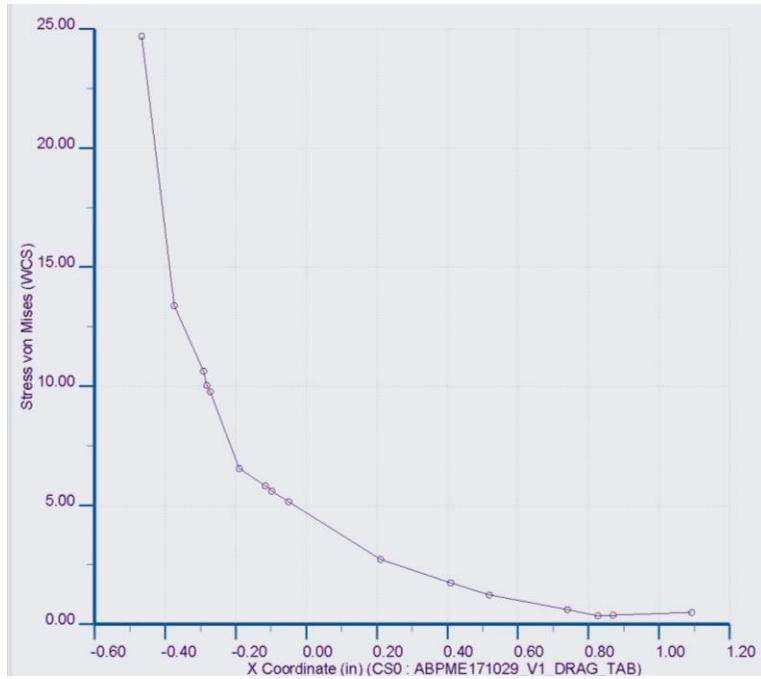
Figure 77. Plot of von Mises stress as a function of distance for the aluminum tab. The maximum von Mises stress observed was 25 psi.
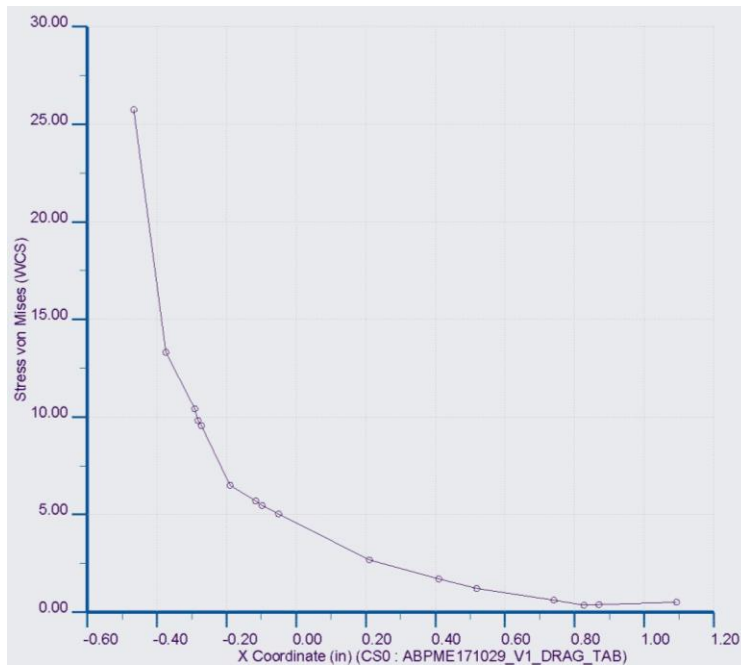
Figure 78. Plot of von Mises stress as a function of distance for the UHMW tab. The maximum von Mises stress observed was 25.7 psi.
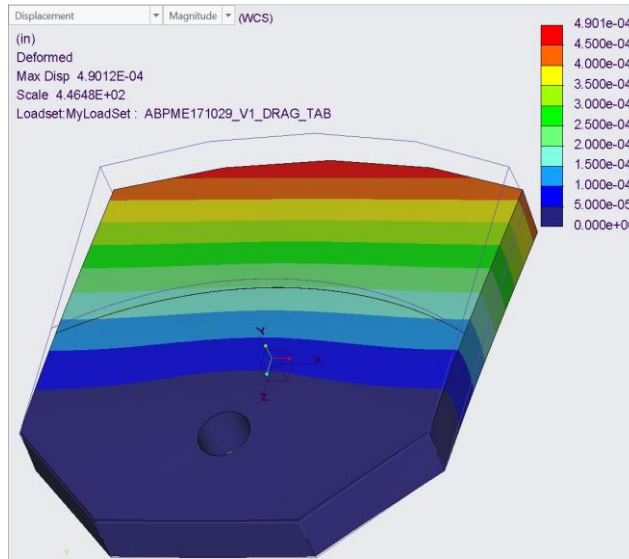
Figure 79. Schematic of the drag tab displacement. Maximum tab displacements were 6.4 × [10]^(-6)in for aluminum and 4.9 × [10]^(-4)in for UHMW.

5.2.3.4 Mechanical System Ground Testing

The coefficient of friction of Ultra High Molecular Weight Polyethylene (UHMW) will be measured against itself to confirm existing values. The setup for this experiment will be as follows: A surface will ensured to be level with a bubble level tool. A plate of UHMW will be attached to a device that lies flat on the table, and will allow the UHMW to be angled at any angle between 0 and 90 degrees. The angle will be verified through a protractor. Both sliding friction and static friction can be determined through this setup.

To calculate static friction (F_s), a second plate of UHMW will be placed on top of the original UHMW, and the angle will be slowly increased to find the maximum angle at which the UHMW does not slide down from its own weight. At this point, the force of static friction will equal the sine of the weight, and using known variables ($mass = m, gravitational\ acceleration\ = g, Normal\ force = N$), the coefficient of static friction can be solved for.

$$F_{weight} = mg$$

$$F_s = F_{weight}\ sin\theta$$

$$N = F_{weight}\ cos\theta$$

$$F_s = \mu_s N$$

$$\mu_s = tan\theta$$

Similarly, to calculate sliding friction (kinetic friction, F_k), a second plate of UHMW will be placed on top of the original UHMW, but the second plate will be given an initial push. When the second plate maintains its speed (the acceleration will be zero), the force of sliding friction will equal the sine of the weight. The angle at which the plate's acceleration most closely matches zero will be found. Using known variables ($mass = m, gravitational\ acceleration\ = g, Normal\ force = N$), the coefficient of sliding friction can be solved for.

$$F_{weight} = mg$$

$$F_k = F_{weight}\ sin\theta$$

$$N = F_{weight}\ cos\theta$$

$$F_k = \mu_k N$$

$$\mu_k = tan\theta$$

5.2.3.5 Power System Ground Testing

Batteries for the power system arrived after the start of the university's winter break, so testing will be performed in the near future, but unfortunately could not be conducted before this report.

Testing will be done to verify specifications for the Tenergy and Adafruit lithium ion batteries. A voltmeter will be used to verify the open circuit voltage for each of the batteries. A simple resistor circuit will be used to measure the effective voltage for the test circuit across the given resistor and then calculate the internal resistance of the battery to ensure it is not significant relative to other circuit components.

The capacity of the batteries will be tested through both measurement tests and full scale test flights to ensure the capacity actually lasts long enough for the flight. To test the capacity on the ground, a simple resistor circuit will be connected to the battery. Multimeters will be used to measure the voltage across the battery and current through the resistor over a testing time period. The circuit will be allowed to run until the measured voltage is below a specific tolerance. The length of time at which this occurs will be multiplied by the measured current value to provide an estimation of mAh for the battery. Due to variances of threshold voltages for estimating the capacity and not wanting the voltage to drop too low and cause damage to the battery, the test will likely need to be run multiple times to ensure a precise estimate.

The capacity of the batteries will also be deemed acceptable based on integrated system testing. Tests will be conducted with the motors before and after construction of the mechanism to ensure that the motor is properly powered by the chosen batteries. Additionally, a full scale test flight with successful payload operation without power loss will be used to verify the system before the final launch.

5.2.3.6 Printed Circuit Board Ground Testing

Most of the ground testing of the PCB will be covered by other tests verifying the ability of the microcontroller to control the motor because the required signal lines are all routed through the circuit board.

Additionally, an ohm meter will be used to verify connectivity between each of the signal inputs and outputs. The procedure for accomplishing this part of the test begins by comparing the schematic and board diagrams to the actual circuit board. Each connection made on paper should record an extremely low resistance value, indicating a strong wired connection in these places.

Finally, an LED will be placed across the switch to make sure voltage is going through the system. For this part of the test, the proper power supply would be connected to the board. An LED will be placed on the high and low poles on the switch. The switch should then be able to control LED on/off functionality.

5.2.3.7 Sensor Ground Testing

The chosen accelerometer and barometer models have both undergone initial performance testing to ensure they can fulfill the requirements of this payload. By wiring both sensors to an Arduino MKR Zero and running sample code, a large number of data points were obtained for both sensors. Since the surrounding environment was held constant and did not undergo any change in acceleration, pressure, or temperature during the testing period, an analysis of this data allowed the sensor's precision and sampling rate to be experimentally measured. Through the creation of histograms such as Figure 80 below, a standard deviation was obtained for each sensor.

Barometer Noise Histogram
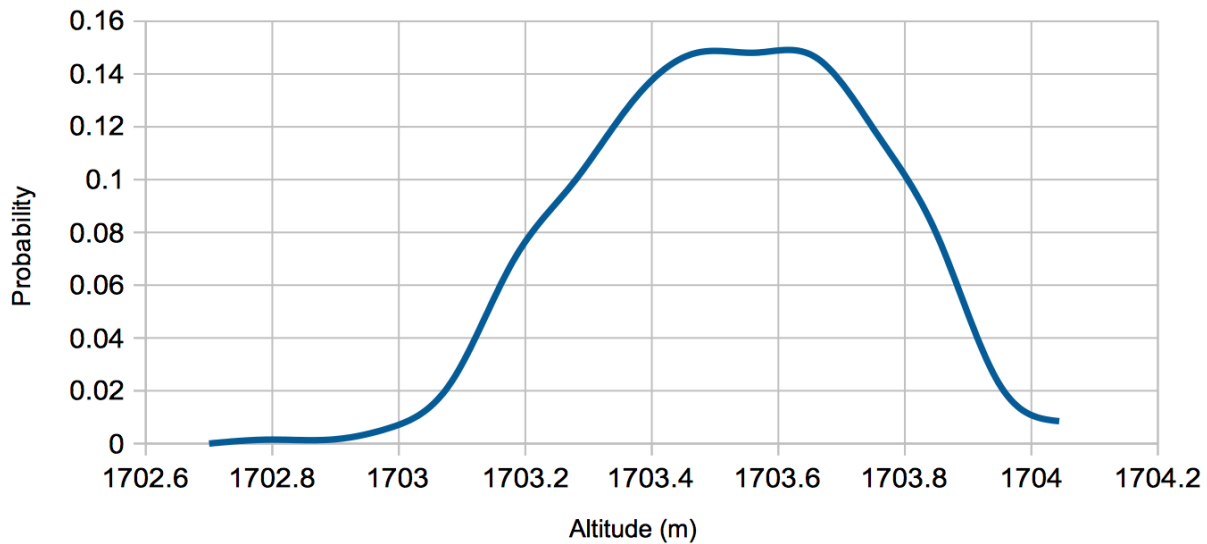
Figure 80. Histogram of the barometric altitude data generated from 5000 samples.

The BMP280 has a standard deviation of 0.22 meters (0.72 feet), and the ADXL345 has a standard deviation of 0.12 m/s (0.4 ft/s). Additionally, the barometer has an average update rate of 36 Hz, while the accelerometer has an average update rate of 122 Hz (running in 100 Hz mode instead of its maximum 3200 Hz). These specifications are in line with the manufacturer-provided information used in the control code simulation, so the algorithm's simulated performance should closely correspond to its real-world performance.

5.2.3.8   Control Code Ground Testing

The control code has undergone repeated and updated testing in a simulated flight environment, with improvements largely having been made in terms of more accurate information about the dimensions, mass, and aerodynamic profile of the rocket, along with more precise details regarding the performance of onboard sensors and the drag tab mechanism. This has allowed the team to verify that the control algorithm and air braking system will be effective in-flight, along with determining the limitations of both systems. For example, the system can reliably reduce a flight that would otherwise have an apogee as high as 5750 ft. to within ten feet of the one-mile target, even at a launch angle of up to 8 degrees. Furthermore, the method the simulation uses to deal with tab movement has been debugged and refined, indicating that average propagation times of up to 0.2 s will still allow the system to perform effectively.

In addition, simulated potentiometer data has been integrated into the control code, allowing it to monitor if the mechanism is jammed by comparing the servos' intended position to the position reported by the potentiometer. If a difference between these two values beyond the sensor's noise range is detected over multiple cycles, the control algorithm attempts to fully retract the tabs and then shuts down, to prevent any further damage to the mechanism or servomotors. Once the physical and electronic systems have been constructed, these tests will be repeated both on the ground and through test flights to ensure the results translate effectively from the control algorithm simulation to the completed payload, with particular focus on the anti-jamming failsafe subroutine.

5.2.3.9 Full Scale Flight Test

After the various ground tests confirm the functionality of each individual component and of the system as a whole, the air braking system will be placed in the rocket and operated during a launch. This will be done for two reasons. The first is to confirm that the payload operates safely throughout flight. This means that it must not cause any disruptions in the flight of the rocket that could cause a crash. Ground testing will have already provided strong evidence that the system operates safely by this point, but the only way to fully confirm this is to successfully operate the payload during an actual flight. The second reason to test the system during a full scale launch is to determine its effectiveness.

Ideally, the system reaches stage 4 of the success criteria explained previously. If this is accomplished, minor redundancies and changes may be added to the control code and electronic system as seen fit, but overall the design will be complete. The team expects to achieve stage 2 of the success criteria during the test launch (disclaimer: because the test flight is not part of the competition stage 3 success cannot be determined). This is expected because various natural factors like weather conditions and wind speed are difficult to reproduce in simulations and ground testing with our resources, and their effects can only be monitored during a full scale flight. Using the results of the full scale flight, different design changes and improvements will be made. If stage 2 success is reached, the primary improvements that can be made will be in the control code. These improvements will most likely consist of tuning the gains of the PID control algorithm and improving the method that is used to calculate the real flight path of the rocket. This is not certain, however, and any improvements that do need to be made can only be determined for certain after the test is performed and the results are analyzed. If only stage 1 success is accomplished during the full scale flight, significant changes in the design will need to be made. At this point in the process only code changes will be viable, including rewrites of large portions of the control code. If even stage 1 success is not achieved, this will be deemed a system failure.

If a system failure occurs, this will create the need for major changes in the electronic and mechanical systems. Because the vehicle construction will be completed by this point, altering the size of the drag tabs will not be a viable option. Changes made to the electronic system will most likely involve rewriting large portions of the control code and selecting new electronic components including power sources, sensors, and servomotors. Changes made to the mechanical system will most likely be an alteration in the link lengths of the crank-slider mechanism, a change in the gear ratio, or a different material selection for the drag tabs. Again, the changes that would need to be made to the system cannot be known for certain until the test is actually performed.

The full scale flight test will be performed the same way as the subscale flight test, with a control flight where the air braking system is not operating and then a second experimental flight with the system operating. The apogee results from each flight, along with data from the system itself, will be compared to determine which stage of success was accomplished.

5.2.4   Manufacturing and Assembly

5.2.4.1   Structural Components

There are a number of custom parts that are required for this payload. The drag tabs, sliding plates, servo mount plate, and cross piece will all be machined on a combination of a Techno CNC Router Table and a Bridgeport manual mill (equipped with digital readout and rotary table). However, many of the holes on these pieces are smaller than the smallest end mill the router can accommodate, so at a minimum these features will be done on the mill with appropriate drill bits. The potentiometer mount and gear will be 3D-printed on either a high-end Fortus machine or a new Makerbot, depending on machine availability. The shaft and its retaining ring grooves will be turned on a manual lathe. Finally, many of the parts will have the appropriate holes tapped by hand after machining, as is needed.

The tie rods will be made from purchased hobby rod ends connected by a length of threaded 4mm rod to produce a 1.20 inch long tie rod (center to center). For each tie rod, a spacer will also be made of an aluminum stock cylinder, which will cover any part of the threaded rod not inside the rod ends. This will ensure that all four rods are equal in length.

These tie rods will connect the servo cross-piece to the tabs and will be secured by 3mm bolts at each end. On the cross-piece side, the bolt will be threaded into a free nut, sandwiching both the cross-piece and the rod end between the two. On the tab side of the tie rod, the bolt will thread into a tapped hole on the tab.

The tie rods will be made from commercially available hobby rod ends. However, the available rod ends are too long, so they will be milled on one end to make them small enough to

fit together. Then, they will be joined by a length of M4 threaded rod. Once assembled, the rod ends will not be able to rotate and unscrew themselves, since they will be secured at both ends, so no thread locker or epoxy is necessary to secure them.

5.2.4.2 Electronic System Assembly

The system will be assembled using as many soldered components as possible. This offers a secure method of connection. 22 gauge wire will be soldered to the input/output pins of the microcontroller, motor, and switch. The corresponding Molex connectors will also be soldered to the PCB. The wires will then be integrated into the Molex connectors using the crimp terminals. For the removable parts of the system, the Molex header and receptacle snap into each other with a plastic tab.

6 Project Plan

6.1 Testing

The testing plans for each sub-team of the launch vehicle can be found in their respective sections as defined in the table of contents.

6.2 Requirements Compliance

Each sub-team has created a table with requirements and verifications that are specific to the system performance and how that performance affects the entire launch vehicle design.

6.3 Budgeting and Funding Plan

Detailed budgets for each of the four technical sub-teams can be found in Appendix K. Table 30 below summarizes the intended budget plan for the 2017 – 2018 competition year.

Table 30. Expected budget spending for the entire team.

Allocation Group	Budget Spent / Expected
Vehicle Design Sub-team	$ 3945.02
Recovery Systems Sub-team	$ 975
Deployable Rover Sub-team	$ 1,043
Air Braking System Sub-team	$ 299.81

Rocket Subtotal	$ 6,262.83
Educational Outreach Events	$ 300
Miscellaneous	$ 300
Competition Travel	$ 8,000
GRAND TOTAL	**$ 14,862.83**

The costs shown in Table 30 can be accounted toward the following items:

Vehicle Construction and Propulsion: These costs account for all materials that will be used to build the launch vehicle as well as for the motors used in all launches.

Recovery System: The recovery costs include all parachutes, altimeters, 3D printed materials and all items necessary for a safe and robust integration into the vehicle.

Deployable Rover Payload: The costs associated with the experimental payload include all materials, wheels, solar cells, rover motors, all electronics and items needed to ensure a safe and successful integration.

Air Braking System: The costs for the extra payload account for all materials, electronics, servo motors and 3D printed items needed.

Educational Outreach: These funds are set for use during educational and community engagement events, and are planned to be used to purchase Estes rockets with kids.

Miscellaneous: In this category are costs for posters and other items associated with a professional team image and presentation.

Travel: All costs associated with traveling are included in this number including transportation, food and lodging.

There has been an increase in the travel budget due to a new traveling policy implemented by the university this year. It has greatly increased the transportation budget, and the team is currently working with the university administration to account for this higher spending. The Notre Dame Rocketry Team draws funding from two main sources. The first is from a general account dedicated to aerospace design projects at the University. Support for this

fund comes from a wide variety of sources, including the College of Engineering, the Department of Aerospace and Mechanical Engineering and generous donors. The fund is replenished annually as deemed necessary by University faculty and staff.

The second source is from sponsorship by The Boeing Company. The team is working hard on securing corporate relations with different aerospace companies, and Boeing has been a pioneer with the Notre Dame Rocketry Team in this effort.

Appendix A: Launch Procedure Checklists

Prior to Departure for Launch Site: Vehicle Sub-team

Personnel Safety Components
Items to bring:
❏ Safety goggles
❏ Gloves

Vehicle Components
Items to bring:
❏ Nose cone
❏ Recovery body tube
❏ Fin can
❏ Communications coupler
❏ Shear pins
❏ Extra washers
❏ Extra nuts
❏ Extra screws
❏ Extra epoxy
    ❏ Inspect the body tubes and couplers to ensure they have not been damaged during storage.

Structural Integrity
❏ Ensure the items are stored in such manner as to not cause physical damage.
    ❏ Ensure the fin can is stored on the rocket holder so as not to damage the fins during transportation.
❏ Ensure lids to epoxy bottles are appropriately sealed

Subteam Member: _____ Date: _____
Signature: _____
Team Lead: _____ Date: _____
Signature: _____

Prior to Launch: Vehicles Sub-team

Personnel Safety Components
❏ Ensure everyone operating on the vehicle has proper safety equipment
❏ Safety goggles

Prepare the vehicle for launch
❏ Insert payloads into the top-most body tube
❏ Insert nose cone into the top-most body tube
❏ Ensure that the screws on the nose cone are not loose
❏ Friction fit the nose cone with masking tape or scotch tape if necessary
❏ Ensure CRAM core is inside the CRAM body
❏ Process performed by the Recovery Sub-team
❏ Ensure the CRAM can be armed directly from the rocket's rail position
❏ Attach rocket sections
❏ Check that all interfaces are aligned correctly
❏ Insert shear pins to secure each section
❏ Ensure the screws are tight
❏ Perform Cg test to ensure the center of gravity matches the simulated center of gravity.
❏ Ballast as necessary to keep the stability margin.
❏ Prepare and insert the motor (Process performed by Team Mentor Dave Brunsting)
❏ Remove motor from packaging
❏ Check that motor is properly assembled according to manufacturer's instructions
❏ Remove pre-installed ejection charge
❏ Properly dispose of black powder
❏ Insert motor into casing
❏ Ensure two spacers precede motor
❏ Screw on rear closure
❏ Insert motor into rocket
❏ Attach motor retainer
❏ Check for secure fit
❏ Check rocket stability (at least 1-2 calibers) and final weight
❏ Register with LCO and RSO at launch site.
❏ Ignite motor right before launch (Process performed by Team Mentor Dave Brunsting)
❏ Remove igniter clips from igniter
❏ Remove igniter from rocket
❏ Ensure igniter has properly exposed ends which are split apart
❏ Insert igniter into motor
❏ Attach clips to igniter, ensuring good contact

Payload Member: _____ Date: _____
Signature: _____
Payload Member: _____ Date: _____
Signature: _____
Payload Member: _____ Date: _____
Signature: _____
Team Lead: _____ Date: _____
Signature: _____
Team Mentor: _____ Date: _____
Signature: _____

After Launch: Vehicle Sub-team

Personnel Safety Components
❏ Instruct all personnel to get clearance before starting recovery process
❏ Assess there is no harmful physical damage before removal
❏ Ensure nothing is on fire
❏ Wait for at least 5 minutes before removing due to lingering motor heat
❏ Document state of rocket before removing

Structural Integrity
❏ Check the physical state of the overall body tube
❏ Check the physical state of each payload
❏ Did the communication payload suffer damages to the electronic components?
❏ Is the communication payload coupler structurally sound?
❏ Is the recovery body tube structurally sound?
❏ Ensure parachutes are re-usable

Subteam Member: _____ Date: _____
Signature: _____
Team Lead: _____ Date: _____
Signature: _____

Prior to Departure for Launch Site: Recovery

Personnel Safety Concerns
Items to bring:
❑ Safety goggles

Electronics
Items to bring:
❑ CRAM
❑ Main parachute
❑ Drogue Parachute
❑ Shock cords
❑ Shear pins
❑ Extra batteries
❑ Talcum powder

Structural Integrity
❑ Ensure the items are stored in safe boxes at a reasonable temperature.
❑ Ensure all applicable electronics are turned off.
❑ Ensure the recovery body tube has not been damaged during storage.
❑ Ensure the holes in the recovery body tube are the appropriate size
❑ Ensure the recovery body tube is clear of electronics before storage.

Squad Member: _____ Date: _____
Signature: _____
Team Lead: _____ Date: _____
Signature: _____

Prior to Launch: Recovery

Personnel Safety Components
❑ Ensure everyone operating on the payload has proper safety equipment
❑ Safety goggles

Prepare CRAM
❑ Insert fresh batteries into CRAM core
        ❑ Ensure batteries are connected to altimeters by listening for beeps from altimeters
❑ Insert CRAM core into CRAM body
❑ Put CRAM core cover on
❑ Tighten nuts down onto cover
❑ Insert long eyebolt through center of CRAM
❑ Place washer against both the bottom bulkhead and the CRAM cover
❑ Tighten nut against CRAM cover to hold bolt in place
❑ Connect the wires from CRAM core to screw terminals
❑ Attach short eyebolt to the long eyebolt with coupling nut
❑ Tighten nut on either side of coupling nut

Electronics
❑ Prepare Avionics
❑ Mark the Primary Raven as official contest altimeter
❑ Ensure arming switch is "safe"
❑ Properly secure altimeters and batteries
❑ Install the CRAM until it locks
❑ Ensure the CRAM can be armed directly from the rocket's rail position

Structural Integrity
❑ Prepare ejection charges
❑ Ensure personnel are wearing safety glasses
❑ Move all non-essential personnel away from rocket
❑ Connect electric matches/ejection charges to altimeter
❑ Properly load and prepare parachutes
❑ Check that shroud lines are not tangled
❑ Apply talcum powder to each parachute
❑ Ensure that shock cord is not tangled
❑ Insert parachutes, chute protector, and shock cord into rocket
❑ Attach rocket sections
❑ Check that all interfaces are aligned correctly
❑ Insert shear pins to secure each section

❏ Ensure tight fit of all components
❏ Leave hatched door open
❏ Check shock cord for brittleness
❏ Replace shock cord that appears brittle

Squad Member: _____ Date: _____

Signature: _____

Team Lead: _____ Date: _____

Signature: _____

After Launch: Recovery

Personnel Safety Components
❏ Instruct all personnel to get clearance before starting recovery process
❏ Assess there is no harmful physical damage before removal
❏ Ensure nothing is on fire
❏ Check that ejection charges have ignited
❏ Document state of rocket before removing

Electronics
❏ Disarm altimeters
❏ Disconnect batteries
❏ Structural Integrity
❏ Check the physical state of the recovery body tube
❏ Is it re-usable?
❏ Check that components are safely inside the payload

Squad Member: _____ Date: _____
Signature: _____
Team Lead: _____ Date: _____
Signature: _____

Prior to Departure for Launch Site: Various Payloads

Personnel Safety Components
Items to bring:
❏ Safety Goggles

Electronics
❏ Any Arduino connections must be soldered
❏ Any batteries must be unplugged to save power.

Items to bring (as applicable):
❏ Soldering iron, with extra solder
❏ Spare batteries
❏ Electric tape
❏ Extra wire
❏ Wire crimpers
❏ Wireless Data Receiver
❏ GPS Receiver
❏ Ground Station
❏ Voltage Dividers
❏ Microcontroller
❏ Sensor Bay
❏ Transmitter
❏ Ensure the items are stored in safe boxes at a reasonable temperature.
❏ Ensure all applicable electronics are turned off.

Structural Integrity
❏ Perform visual inspection to make sure outer surface has not been damaged during storage.
❏ Shake the fin can to ensure the payload components do not wiggle when shaken

Squad Member: _____ Date: _____
Signature: _____
Team Lead: _____ Date: _____
Signature: _____

Prior to Launch: Various Payloads

Personnel Safety Components
Items to bring:
❏ Safety goggles

Electronics (as applicable)
❏ Before activating electronics, ensure that the time until launch does not exceed battery life.
❏ Ensure all connections are correctly soldered.
❏ Test all connections to verify there are no short circuits or faulty wiring.
❏ Turn on wireless data receiver
❏ Turn on GPS receiver
❏ Check that all wire connections are according to design

Structural Integrity
❏ Perform visual inspection to make sure outer surface has not been damaged during transportation.
❏ Ensure all connections are tight and secure.
❏ Double-check that the drogue bulkhead is secure.
❏ Tighten the nuts on the parachute eye bolt
❏ Ensure there are no loose wires or solder
❏ Ensure all payload hardware components properly secured to sleds
❏ Ensure that the main parachute eyebolt is tight and the screws do not unscrew
❏ Perform a shake test to ensure that payload materials do not shift

Squad Member: _____ Date: _____
Signature: _____
Team Lead: _____ Date: _____
Signature: _____

After Launch: Various Payloads

Personnel Safety Components

❏ Instruct all personnel not let the fin can safely land before approaching.
  ❏ Instruct all personnel not begin recovering the payload until given clearance by ground personnel.
❏ Ensure the fin can has adequately cooled before handling.
❏ Document the state in which the system is before any tampering

Electronics

❏ Check that all electronics survived the flight intact.

Structural Integrity

❏ Perform visual inspection to make sure outer surface has not been damaged during flight.
❏ Assess any damages that may have occurred during operations.
❏ Determine if the damages are severe enough to prevent additional launches. Repair any minor damages, where possible.
❏ After recovery, re-perform component tests to ensure that operation has been uninhibited.

Squad Member: _____ Date: _____
Signature: _____
Team Lead: _____ Date: _____
Signature: _____

Appendix B: Safety Agreement

(The following is the safety agreement that all team members have signed)

By signing below, I agree to abide by all regulations, standards and guidelines set forth by the National Association of Rocketry. I have read and understand the High-Powered Rocketry Safety Code and will follow all rules outlined within the code. I am cognizant of all local, state, and federal laws regarding the regulation of airspace and handling of explosive or controlled materials.

I understand that the Huntsville Area Rocketry Association will oversee the contest launch, and I will abide by all club rules at the launch. I acknowledge that the Notre Dame rocket will be subject to range safety inspections before flight, and I will comply with the determination of the safety inspection. The Range Safety Officer has the final say on all rocket safety issues, and failure to comply with safety requirements will prohibit the team from launching its rocket.

I agree to abide by all procedures outlined by the Safety Officer of the Notre Dame Rocket Team, Team Leader, and Team Advisor when working on the NASA Student Launch project. I will use laboratory equipment and tools only when properly trained or under appropriate supervision. I will follow all Material Safety Data Sheets for materials used in design, construction, launch, and conclusion of the project.

I understand that failure to comply with anything in this safety agreement can result in my removal from the Notre Dame Rocketry Team.

_____

(Team Member Name Printed)

_____

(Team Member Signature)   (Date)

Appendix C: Personnel Hazard Analysis

Possible Failure	Failure Mode	Effect	Probability	Severity	Risk	Mitigations
Construction						
Hand and power tools	Improper use of tools due to lack of training; incorrect tool used for a job	Minor to severe injury to self and/or others	Remote	Critical	Moderate	Train all team members in proper tool use, ensure the proximity of assistance in case of injury
Flying sawdust chips or solder	Power tools kick up small pieces, solder can splash up	Eye injury	Remote	Critical	Moderate	Ensure all team members working with power tools or soldering have eye protection
Soldering iron	Physical contact with plugged in soldering iron	First- or second-degree burns	Remote	Marginal	Low	Avoid contact with soldering iron, tie back long hair
Epoxy hardener or resin	Physical contact with materials	Minor skin irritation	Remote	Marginal	Low	Rinse area immediately with soap and water
Ammonium Perchlorate	Physical contact with material	Irritation to skin or mucous membranes	Remote	Marginal	Low	Minimize handling of motor, rinse area immediately with soap and water
Lead	Ingesting solder	Lead poisoning	Improbable	Critical	Low	Wash hands after soldering, avoid eating or drinking while soldering
Electrical Shock	Touching exposed wiring	Low level shock to person handling payload	Remote	Negligible	Minimal	Cover up exposed wires

Fumes	Joining components with epoxy; soldering; spray-painting	Nausea, light-headedness	Occasional	Marginal	**Moderate**	Ensure adequate ventilation and air flow when working with solder and epoxy

Preparation and Launch					
Rocket launch ignition	Personnel being too close to rocket motor at ignition	Risk of burns	Improbable	Critical	**Low**	Ensure that personnel distance when launching rocket complies with NASA minimum distance table
Moving heavy objects	Transporting the ground station	Muscle strains; toe injury	Remote	Marginal	**Low**	Ensure the ground station is properly transported
Exposure to detonated black powder charges or residue	Packing, handling, or cleaning black powder charges before or after launch	Risk of fire, burns, or irritation of respiratory system	Probable	Marginal	**Moderate**	Ensure proximity of fire safety equipment; ensure that eye and skin protection is used; wash exposed area thoroughly with water

Ascent					
Rocket flight path	Rocket flies toward objects or people	Risk of blunt force trauma or lacerations	Improbable	Catastrophic	**Low**	Ensure rocket is pointing in safe direction at launch and launch stand is stable

Descent					
Rocket flight path	Parachute deployed: rocket falls predictively at moderate speeds	Risk of minor injuries	Frequent	Marginal	**High**	Point at rocket as it descends to ensure personnel are aware of rocket's position and out of harm's way

	Parachute not deployed: rocket falls unpredictably at high speeds	Risk of blunt force trauma or lacerations	Remote	Catastrophic	Moderate	Move out of the way of the rocket, alert others if they are in harm's way
Rocket motor	Motor can still be hot after flight	Minor burns	Remote	Marginal	Low	Only handle rocket after several minutes on the ground to allow to cool
Battery Acid	Battery overheating, event of crash	Potential chemical burns	Remote	Marginal	Low	Ensure batteries are properly maintained and operated, flush the affected area with either water or sodium bicarbonate solution, depending on specific acid

Appendix D: Failure Modes and Effects Analysis (FMEA)

Payload						
Possible Failure	Failure Mode	Effect	Probability	Severity	Risk	Mitigations
Solar Panel malfunction: Solar Panels are adjusted to incorrect and insufficient position	Arduino/Control code error, calibration failure in servo motor and adjustment within the adjustment mechanism	Increases/decreased amount of solar power to recharge battery; fail to meet rechargeable battery requirements	Remote	Marginal	Moderate	Simulate and test control algorithm code, ground test solar panel adjustment mechanism
Solar Panels breaking apart from rover body during flight and ground deployment	Excessive force applied on the sides of the rover during initial deployment or sustained pressure during flight	Uneven distribution of solar power on rover, loss of structural integrity, potential dead position into body of rover, loss of rover control	Remote	Critical	Moderate	Rover solar panels will be rigidly fixed to a desired orientation to provide more support and stability to the rover, solar panel deployment during ground testing
Power failure	Battery severely depleted during flight or on ground deployment due to temperature and pressure changes	Loss of controller function, no experimental data collected, underpowered servo motor	Remote	Critical	Moderate	Insure secondary batteries have sufficient charge to provide necessary power for the motor and sensors exceeding flight duration
Nose cone ejection malfunction	Design lacks necessary robustness and stability to release it off rocket with gunpowder charge	Payload will not exit the vehicle and will remain there indefinitely	Remote	Critical	Moderate	Nose Cone will be flexible and durably sufficient to withstand outside forces during flight, nose cone will be ground tested before flight to ensure

						proper ejection
Structural failure of polymers and aluminum metal during ground deployment	Design forcefully hits the ground at a very fast time response	Damage to payload, loss of data, failure of entire superstructure	Remote	Marginal	Moderate	Controller will be structurally and fully encased within the body of the rover, failure will not affect data, appropriate isolation from other payloads to be included in design

Air Braking System						
Possible Failure	Failure Mode	Effect	Probability	Severity	Risk	Mitigations
Structural failure or deformity of tab	Tab impact with airborne object mid flight	Unbalanced drag forces on rocket; possible inability to retract tabs	Improbable	Catastrophic	Low	Ensure that the flight path of the rocket is clear at launch
	Higher than expected stress forces from air flow	Unbalanced drag forces on rocket; possible inability to retract tabs	Remote	Catastrophic	Moderate	Run FEA simulations on models of the tabs at higher than expected stress forces
Loss of power to payload	Dead battery	Tabs lock in place, loss of control to the payload	Occasional	Marginal	Moderate	Mark dead batteries during competition, don't turn on battery unnecessarily, keep batteries charged.

	Defective solder joint	Tabs lock in place, loss of control to the payload	Occasional	Marginal	Moderate	Use PCBs to decrease the chance of a poor solder joint, have experienced members perform final solder
Jammed tab system	Fluid forces angle tabs, servo cannot contract tabs	Tabs lock in place, temporary loss of control to the payload	Remote	Marginal	Low	Test and verify coefficient of friction for HDPE, hang weights on tabs to create higher than expected forces
	Tabs retract too far inward, create dead position that motor is incapable of turning	Motor stalls, tabs lock in place, loss of control to the payload	Remote	Marginal	Low	Identify dead positions, code the microcontroller to not allow those positions
Structural Failure of Vertical Rail System	Payload experiences too much acceleration coupled with weight of subsystems	Loss of rigidity of system components, possible inability of subsystems to function	Improbable	Marginal	Low	Test rod threads for maximum force limits, ensure peak motor acceleration is not a threat
Non-optimal flight adjustments	Unexpected physical friction /resistance	Failure to meet precise apogee	Remote	Marginal	Low	Use PID controller to account for error, design code so that some variation is expected
	Weak control algorithm	Failure to meet precise apogee	Frequent	Marginal	High	High volume of simulation and testing of code with manipulation of variables, physical ground

						tests to ensure code functions as expected
					█	

Appendix E: Environmental Effects on Launch Vehicle

Possible Failure	Failure Mode	Effects	Probability	Severity	Risk	Mitigations
Bodies of Water	Launching near bodies of water	Landing in water can irrevocably damage electronics and the rocket can sink and become irretrievable	Remote	Catastrophic	Moderate	Being sure there are no bodies of water near the drift radius of the rocket
High Humidity	Launching in excessive humidity	The charges may become wet due to humidity and be unable to ignite	Improbable	Critical	Low	Motors and charges should be stored by certified personnel in a dry place
Lightning	Launching in a thunderstorm	Electrical shock to the rocket by lightning may ground the launch	Improbable	Catastrophic	Low	This will ground the launch; no rocket should be launched during a thunderstorm
Low Cloud Cover	Launching with low cloud cover	It can be difficult to keep track of the rocket and properly test rocket systems	Occasional	Critical	Moderate	Ow hanging clouds should be avoided during launch days, paying careful attention to the forecast
Low Temperature	Launching is extremely cold temperatures	Batteries can discharge at a faster rate and fiberglass parts can shrink	Occasional	Critical	Moderate	Battery levels will be monitored by the ground station and battery life will be conserved by turning systems on at designated times and turning them off when not in use
Rain	Launching with risk of rain	Rain may damage electrical systems and	Remote	Catastrophic	Moderate	This will ground the launch; rockets should not be

		ground the launch			 	launched in the rain
Trees	Launching near wooded areas	The rocket and parachute can be damaged if caught in a tree it may cause the rocket to be irretrievable	Occasional	Critical	Moderate	Ensuring that there are no trees near the drift radius of the rocket
UV Exposure	Rocket exposed to sun for long periods of time	This can weaken material adhesives if exposed for long durations of time	Improbable	Critical	Low	The rocket will not be exposed for a long period of time and extensive work on the rocket will be done indoors
High Winds	Launching in winds over 20mph	This can reduce altitude and send the rocket off course	Improbable	Catastrophic	Low	The launch will be grounded if the winds are too severe and there will be no obstructions in the estimate drift radius
Wildlife	Flying birds are large animals interfering with the launch	This can cause the rocket to be sent off course	Improbable	Catastrophic	Low	Ensuring the area is clear of wildlife

Appendix F: Safety Concerns for the Environment

Possible Failure	Failure Mode	Effects	Probability	Severity	Risk	Mitigations
Battery Leakage	Improper disposal of damaged or used batteries	Contaminate groundwater	Remote	Critical	Moderate	Using proper battery disposal methods and ensuring batteries are not damaged
Carbon Emissions	Using cars to travel to launch sites	Damage the ozone layer with emissions	Occasional	Marginal	Low	Using carpooling as much as possible to minimize the amount of vehicles used
Epoxy Leakage	Improper use or disposal of epoxy resin in an uncontrolled environment	Contaminate drinking water, be ingested by wildlife, or pollute as solid waste	Improbable	Critical	Low	Using proper techniques in application to ensure the resin is properly dried and disposing of the resin in designated areas
Field Fire	Igniting rockets near dry grass and shrubs or motor CATO	Set the launch site or other nearby objects on fire	Remote	Critical	Moderate	Making sure that any field in use is not near any shrubs and using the proper launching pad to ensure the ignition doesn't affect the surrounding area
Harmful Gas Emissions	Motors emitting gases upon ignition into the environment	Pollute the atmosphere with harmful substances	Remote	Critical	Moderate	There will not be many launches done by the team so the emissions will not be to a concerning level
Harm to Wildlife	Launching a vehicle in a non-designated area around an animal's natural habitat	Destroy animal habitat and result in loss of food source, water source, or life	Improbable	Critical	Low	Ensuring that we only launch in predesignated areas that will have minimal effect on surrounding wildlife
Plastic/Wire Waste	Improperly disposing of the waste of stripping wires	If not properly disposed of, can cause solid waste or be ingested by an animal	Improbable	Critical	Low	Ensuring that any stripped wires have the waste properly collected and disposed of

Spray Paint Fumes	Spray painting the rocket	Can contaminate the water supply or atmosphere	Remote	Critical	Moderate	Painting the rocket in a painting booth that properly disposes of waste
Waste	Improper disposal or storage of rocket components	Can result in pollution of environment if improperly disposed or stored.	Improbable	Critical	Low	Correctly storing any piece of the rocket that is still waste and disposing off the rest in the proper fashion
Water/Ground Pollution	Leakage of motor chemicals into the ground and water	Pollute the water system with improper disposal	Improbable	Critical	Low	Ensure that any hazardous material spilled is properly dealt with

Appendix G: Project Risks

Likelihood: Rare, Unlikely, Even, Probable, Extremely Likely

Impact: Negligible, Low, Moderate, High, Critical

Risk	Likelihood	Impact	Mitigation
Time Possibility of falling behind schedule and/or missing deadlines	Probable	Low	All aspects of the project will be divided up among team members to reduce the chances of falling behind in work. Additionally, multiple team members will coordinate together to ensure that deadlines are met and to keep each other accountable.
Budget Failure to have enough funds to purchase rocket materials, cover transportation costs, and pay for other expenses	Rare	High	All material costs will be determined prior to construction. The team will determine how much material must be ordered in order to prevent overspending. Similarly, travel/transportation expenses will be planned out. Overall budget and spending plans will help ensure that this constraint is met.
Equipment and Facility Physical injury associated with on- and off-campus facilities and the material/equipment used to build and operate the rocket	Unlikely	High	Dangerous materials and equipment, including power tools, machinery, and rocket engines, will be used. Every team member will have proper knowledge and training before using laboratories, workshops, materials, and/or equipment. In addition, team members will use personal protective equipment when working with the rocket. The team safety officer, and subteam safety liaisons will communicate proper safety practices.

Personnel Potential issues involving team members leaving, which may impact time and budget	Unlikely	Negligible	In the case of someone leaving the team, their responsibilities will be spread among other members.
Payload Possibility of malfunctioning or inoperative payload(s)	Unlikely	High	The payload subteams will ensure that work is split among members and adequate time is spent on each step of payload design, construction, and testing. Payload functionality will be verified at the full-scale test launch.
Launch Launch errors and hazards, including defective launch component(s)	Unlikely	Critical	Prior to launch, the rocket will be thoroughly inspected, and all the launch checklists and procedures will be reviewed. Additionally, the team mentor, David Brunsting, will assist the team at every launch.
Recovery Failure of planned rocket recovery, which may result in physical injury or more likely, damage to the rocket and its components	Unlikely	High	The recovery subteam will ensure that the recovery system functions properly by thoroughly designing, constructing, and testing the system. On launch day, following the pre-launch procedures and checklists will reduce recovery system issues. Recovery system functionality will be verified at the full-scale test launch.
Resources Risk of lacking materials, equipment, and facilities to construct and operate the rocket	Rare	High	Each subteam will outline necessary materials, equipment, and facilities prior to construction. Budget and spending plans will also help ensure that all necessary materials are purchased/obtained.

Appendix H: Electronic Control System Schematics
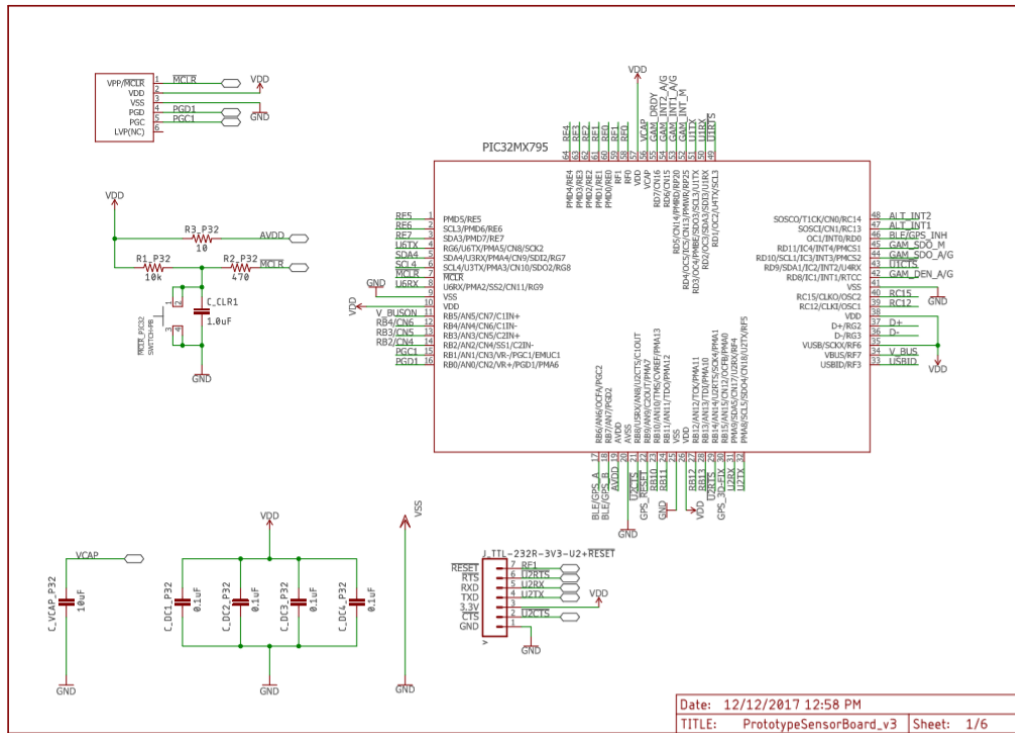
Figure 81. Pic32 power and output pins.
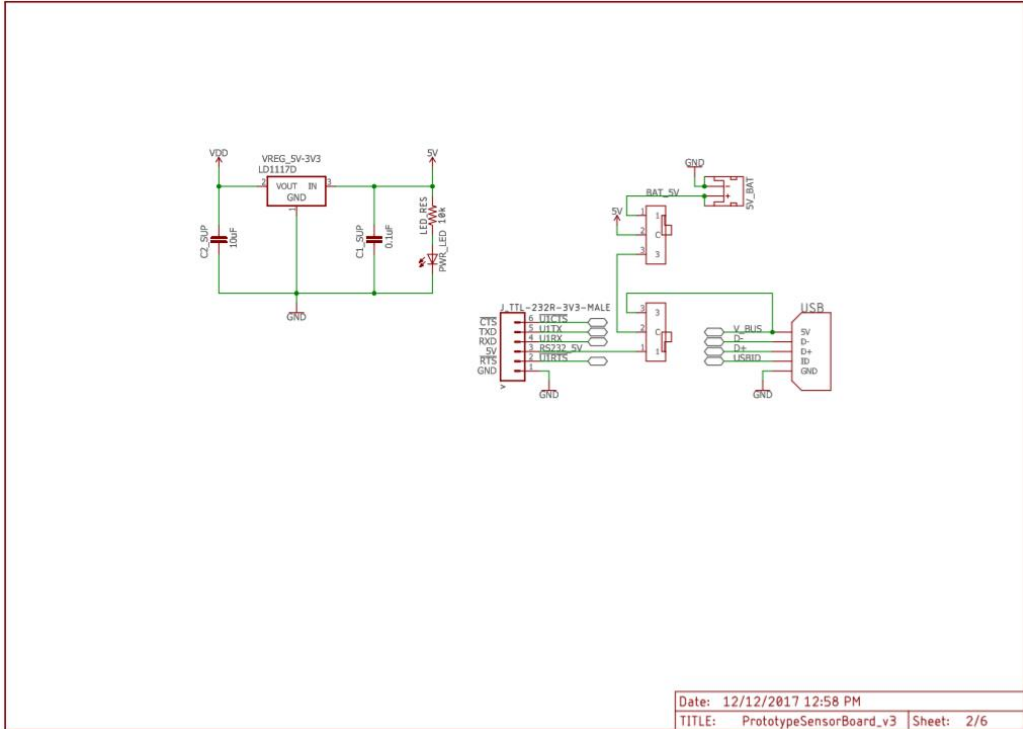
Figure 82, Power supply setup.
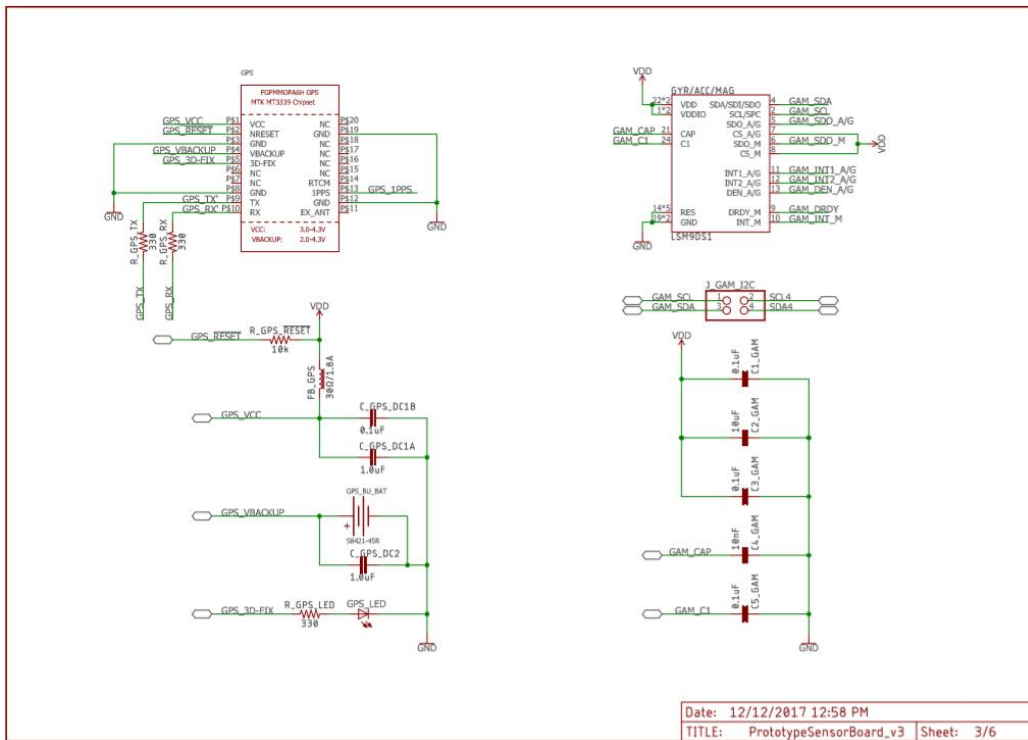
Figure 83. Gyroscope, accelerometer, magnetometer and GPS schematic.
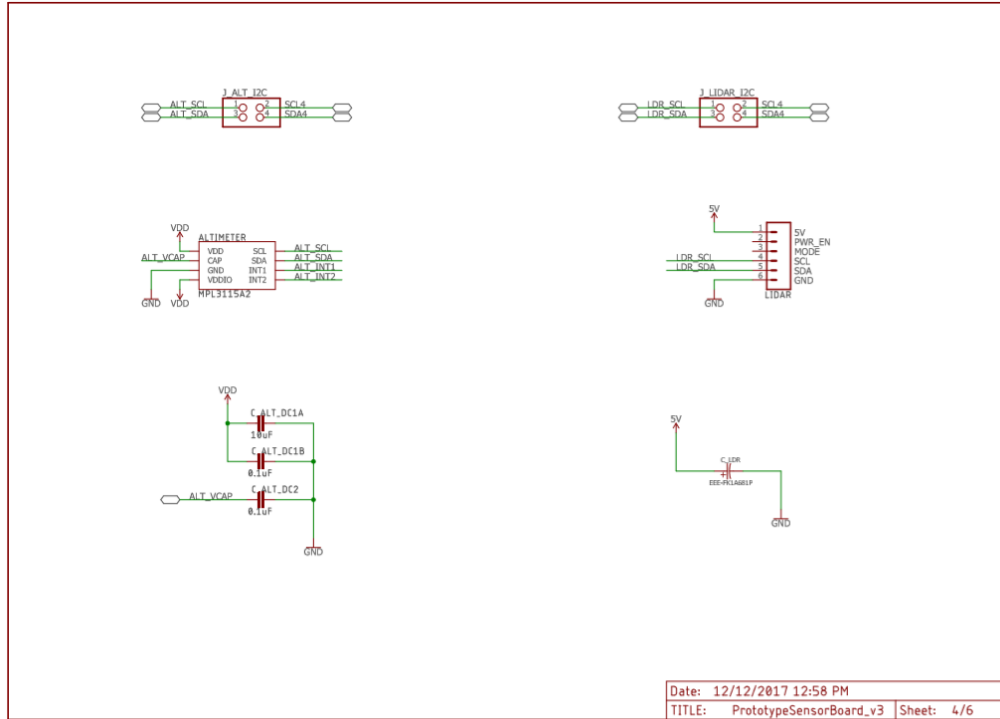
Figure 84. Altimeter and LIDAR modules.
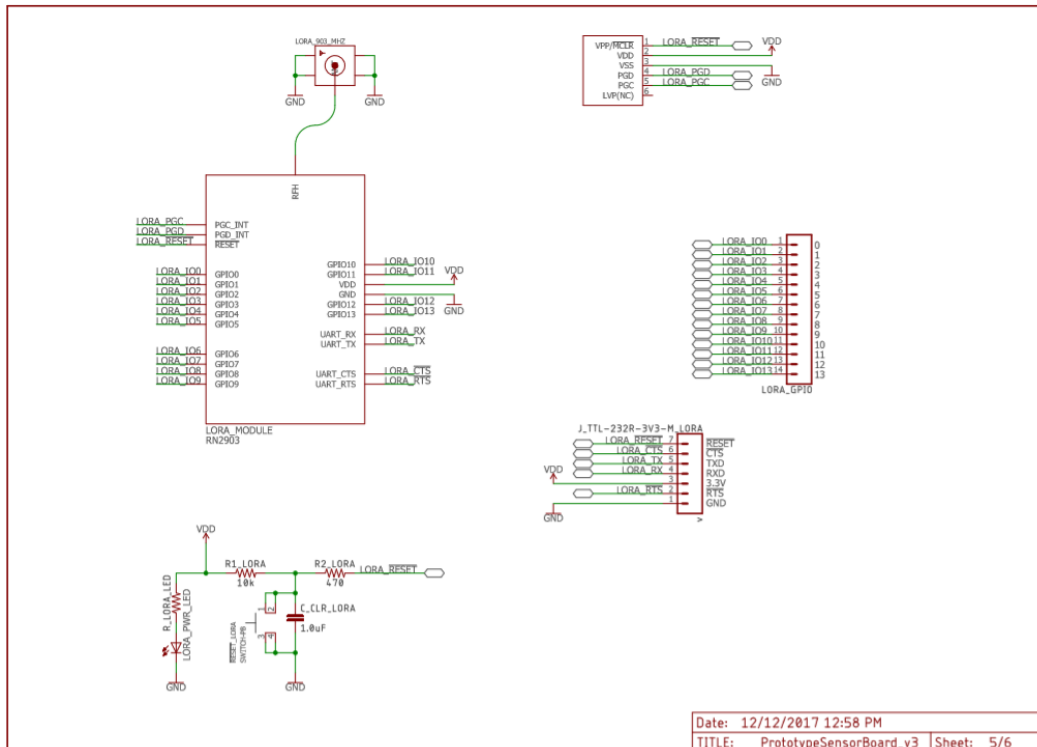
Figure 85. LoRa Module.
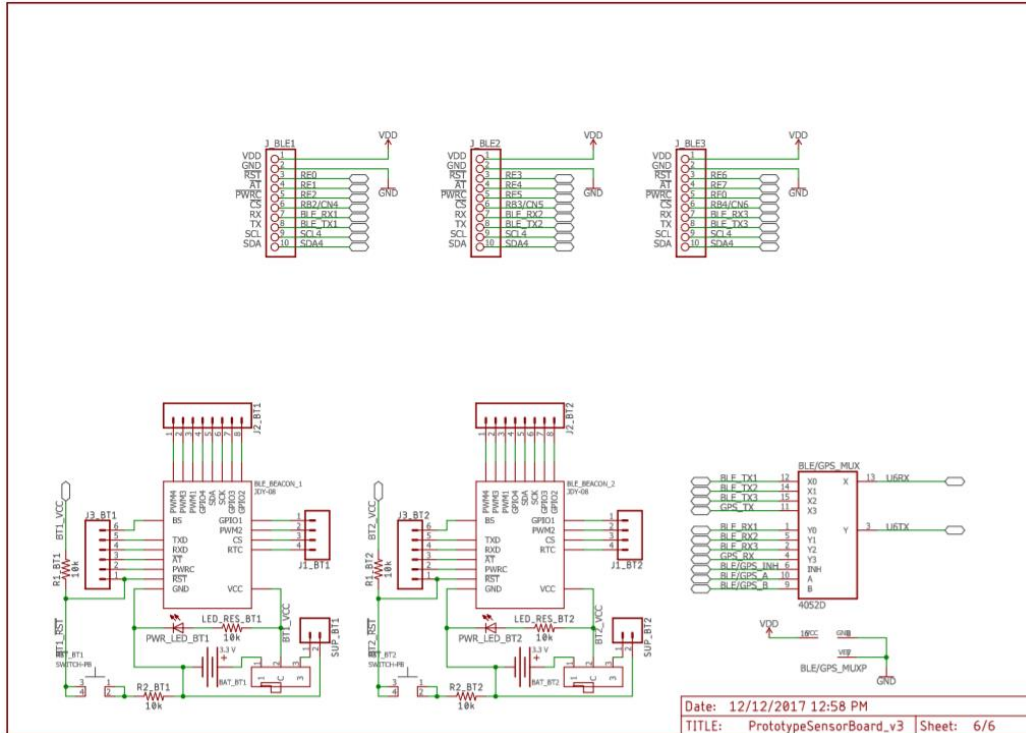
Figure 86. Bluetooth modules.

Appendix I: Calculation of Required Torque for ABP Mechanical System

The analysis of the crank-slider mechanical system is heavily based on the Vector Loop Method (VLM), as described in *Mechanisms and Machines: Kinematics, Dynamics, and Synthesis* by Michael M. Stanisic (Cengage, 2015). Using the VLM, a vector is assigned to each link in the mechanism, such that Vector 1 starts at the center of the cross piece and extends to the hole at the end of the crosspiece. Vector 2 starts at the same point but on the tie rod, and extends to the other hole in the tie rod, which is coincident with the bolt hole on the drag tab. These vectors have fixed length and a variable angle. Together, they sum to Vector 3, which points from the center of the cross piece to the bolt hole in the drag tab, such that changes in the direction of Vectors 1 and 2 (rotating the cross piece) result in a change in magnitude for Vector 3 (sliding the tab). Note that all three vectors have an angle measured counterclockwise from the positive x-axis, and that the vectors are depicted in Figure 87.
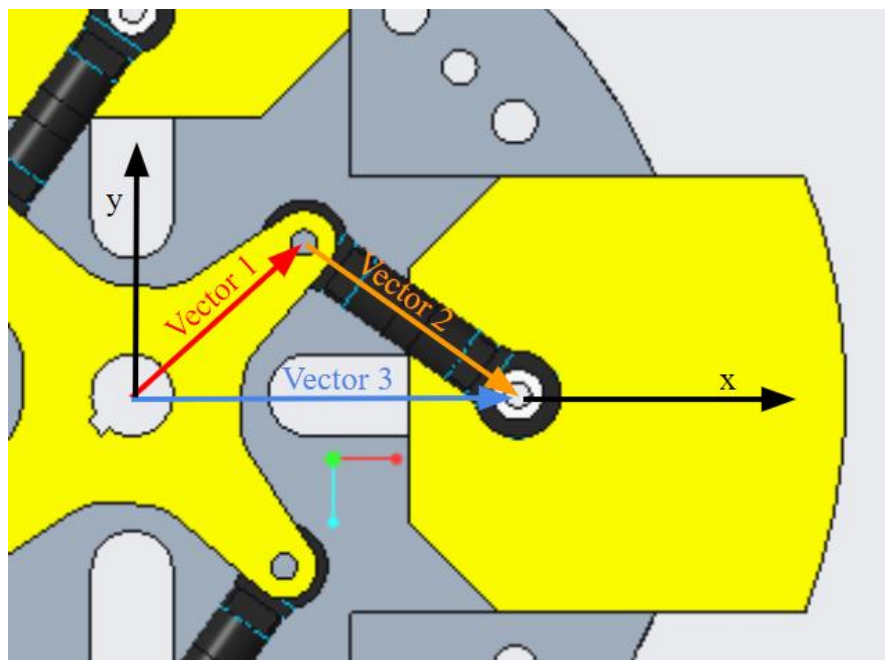
Figure 87. Assignment of vectors for application of the Vector Loop Method.

The mechanism is planar, so the summation of the vectors (note that the sum of all vectors in a loop is always zero) can be broken down into x and y components. For this document, r denotes the magnitude of each vector, while θ denotes its angle.

$$r_1 \cos(\theta_1) + r_2 \cos(\theta_2) + r_3 = 0$$
$$r_1 \sin(\theta_1) + r_2 \sin(\theta_2) = 0$$

By squaring and adding these two equations the value of the cross piece rotation can be solved for directly, as a function of only the drag tab extension.

$$\theta_1 = \arccos \frac{3_3^2 - r_2^2 - r_1^2}{2r_1 r_2}$$

This forms the beginning of the accompanying MATLAB code, provided in Appendix A.2, which is used to execute the model. The code is given a range of desired values for the tab extension, and then calculates the corresponding link angles. This section omits some calculations and parameters for brevity and clarity, but they are present in the code to adapt this theoretical model to the actual system.

There major force acting on the system is friction due to the drag force. A partial free-body diagram of the tab is shown in Figure 88. The tie rod force, however, does not act exclusively in the direction of sliding, and is only drawn this way for clarity. Because of this, there is a third friction component acting on the side of the tab, which is accounted for in the calculation. If Friction Forces 1 and 2 (caused by corresponding Normal Forces 1 and 2) as shown in Figure 88, are combined to f, and μ is the coefficient of friction, then the axial force in the tie rod (F_2) can be solved for.

$$f = \mu(N_1 + N_2)$$
$$F_2 = \frac{f}{\cos \theta_2 - \mu \sin \theta_2}$$

Then, the torque required is simply the magnitude of the cross product of Vector 1 and the tie rod axial force, which is in the opposite direction as Vector 2.

$$T = r_2 F_2(- \cos \theta_1 \sin \theta_2 + \sin \theta_1 \cos \theta_2)$$

This is the torque required for a single tab, so the whole system needs four times this torque to operate. The code does this calculation for every configuration of the system, scaling the drag force linearly with tab extension, and adjusting the dimensions as necessary to calculate the normal forces, before giving the maximum torque for a given dimension.
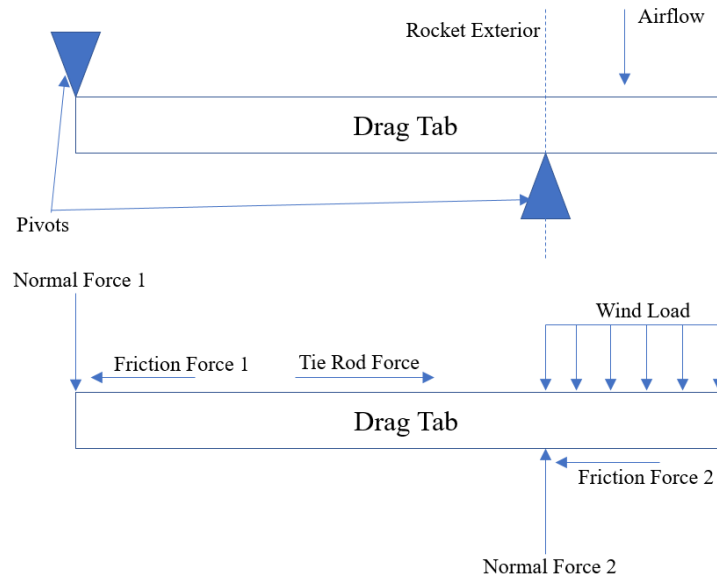
Figure 88. Drag tab free body diagram, side view.

Appendix J: MATLAB Code for performing Vector Loop Analysis

% This code simulates the ABP crank-slider mechanism using the

% vector loop method. This code uses theta_1 as the angle of the

% servo rotation, and theta_2 as the resulting angle of the

% tie rod. Link 1 is the servo horn, link 2 is the tie rod,

% and link 3 is the sliding drag tab.

% all units in inches, pounds, degrees unless otherwise noted


```
clear all;

close all;

clc


%% kinematics of motion

l_out_max = 1; % max extension of fin, inches

l_out = linspace(0,l_out_max,1000); % vector of extension lengths

l_tab = 2; % tab length

l_in = l_tab - l_out; % inner length


r_rocket = 5.5/2; % outer radius of rocket

inset = 0.5; % distance pin joint inset from interior tab edge

r3 = r_rocket - l_in + inset; % length used for vector loop


r1 = 1.05; % servo horn arm length

r2 = 2.25-r1; % tie rod length

test1=(-(r2.^2) + r1.^2 + r3.^2)./(2.*r1.*r3);

theta_1 = real((acosd((-(r2.^2) + r1.^2 + r3.^2)./(2.*r1.*r3))));
```

```matlab
% the theta_1 value is manipulated in the previous step to fit in the right
% quadrant and the correct direction of rotation
fig_num = 1;


% get a quick plot of theta_1 vs l_out for sanity check
figure(fig_num);
fig_num = fig_num + 1;
plot(theta_1, l_out);
xlabel('Servo Rotation [degrees]');
ylabel('Tab Extension [in]');
set(gca,'fontsize',12,'fontname','times new roman');
grid on


theta_2 = asind((-r1/r2)*sind(theta_1)) + 360;


% sanity check theta_2 plot
figure(fig_num);
fig_num = fig_num + 1;
plot(theta_1, theta_2);
xlabel('\Theta_1 [degrees]');
ylabel('\Theta_2 [degrees]');
set(gca,'fontsize',12,'fontname','times new roman');


%% forces time
f_drag_max = 15.5; % pounds, max force
f_drag = f_drag_max .* l_out ./ l_out_max;
```

```matlab
figure(fig_num);

fig_num = fig_num + 1;

plot(l_out, f_drag);

xlabel('l_{out}');

ylabel('f_{drag}');

set(gca,'fontsize',12,'fontname','times new roman');


% normal forces in z-direction

N_out = ((l_in + l_out ./ 2) ./ l_in) .* f_drag;

N_in = N_out - f_drag;


coeff_of_friction = 0.35; % UHMW


f_fric = coeff_of_friction .* (N_in + N_out);


f2 = f_fric ./ (cosd(theta_2) - coeff_of_friction...
    .* sind(theta_2));


figure(fig_num);

fig_num = fig_num + 1;

plot(l_out, N_out)

hold on

plot(l_out, N_in)

plot(l_out, f_drag)

plot(l_out, f_fric)

plot(l_out, f2, 'k-')

xlabel('l_{out}')
```

```matlab
h = legend('N_{out}','N_{in}','f_{drag}','friction',...
    'Tie Rod Force F2');


Torque = r1.*f2.*(-cosd(theta_1).*sind(theta_2)...
    + sind(theta_1).*cosd(theta_2));


figure(fig_num);
fig_num = fig_num + 1;
plot(l_out, Torque,'k-')
xlabel('Tab Extension [in]');
ylabel('Required Torque per Tab [in-lb]');
set(gca,'fontsize',12,'fontname','times new roman');
grid on


figure(fig_num);
fig_num = fig_num + 1;
hold on
plot(l_out, f_drag, 'k-.')
plot(l_out, f_fric, 'k--')
plot(l_out, f2, 'k-')
xlabel('Tab Extension [in]');
ylabel('Force [lb]');
h = legend('Drag','Friction',...
    'Tie Rod');
set(gca,'fontsize',12,'fontname','times new roman');
grid on
maxTorque = max(Torque)
```

Appendix K: Sub-team Budget Breakdowns

Table 31. Vehicles sub-team budget.

Vehicle Design Budget				
	Material	**Quantity**	**Per unit Price**	**Total Price**
Subscale	Polypropylene Nose Cone	1	$20.74	$20.74
	Phenolic Body Tube	1	$4.99	$4.99
	Bulkheads, Centering Rings, Fins (cut from same material)	1	$12.61	$12.61
	Couplers	1	$6.39	$6.39
	Motor Mount	1	$4.99	$4.99
	Transition Section Material	1	$5.98	$5.98
	Motors	2	$27.99	$55.98
	Motor Retention	1	$24.61	$24.61
	Subtotal			$136.29
Full Scale	Motor Casing	1	$331.65	$331.65
	PNC-7.51" Nose Cone	1	$87.95	$87.95
	Motor Retention	1	$47.08	$47.08
	Carbon Fiber Plates (Fins)	4	$71.99	$287.96
	Motor Mount	1	$200.97	$200.97
	Carbon Fiber Body Tube	7.5	$97.79	$733.425
	Carbon Fiber Coupler	1	$100	$100
	Fiberglass Transition Section	1	$150	$150
	Fiberglass Body Tube	2	$100	$200
	Fiberglass Plates	6	$28.99	$173.94
	Motors	5	$246.95	$1234.75
	Quick Links	6	$1.5	$9
	Eye Bolts	4	$1.5	$6
	Flat Head Wood Screws	10	$1.00	$10
	Hex Nuts and Bolts	10	$0.50	$5
	Subtotal:			$3577.725
Multi-Purpose Material	RocketPoxy	1	$65	$65
	JB Weld	1	$10	$10
	15 Minute Mid Cure Epoxy	6	$13	$78
	30 Minute Mid Cure Epoxy	6	$13	$78
	Subtotal:			$231
	TOTAL			**$3945.015**

Table 32. Recovery sub-team budget.

Recovery System Budget			
Material	**Quantity**	**Price per Unit**	**Total Cost**
Main parachute	1	$620	$620
Nomex (tubular)	2	$15	$30
Nomex (square)	4	$3.75	$15
PVC	1	$5	$5
Acrylic	1	$15	$15
Copper plating	1	$12	$12
Altimeter	1	$155	$155
Shock cords	1	$70	$70
9V battery boxes	3	$3	$9
9V batteries	3	$6	$18
Wire	1	$6	$6
Wire connectors	20	$1	$20
TOTAL			**$975**

Table 33. Deployable Rover sub-team budget.

Component	**Cost**
HDPE block	$15.00
Microcontroller	$10.00
Altimeter	$5.00
LoRa	$15.00
Gyroscope	$7.00
Lidar	$150.00
Batteries (2 sets of 4)	$80.00
PVC Boards (2 sets of 3)	$80.00
Wheels (2 sets of 2)	$32.00
Solar panels sheets	$30.00

Various Hardware	$100.00
Servomotor	$100.00
Brushless motors (4)	$80.00
Ejection System	$50.00
Gear Rack	$34.00
Gear	$15.00
3D printed components (tracks, securing cubes, covers)	$40.00
Miscellaneous	$200.00
TOTAL	**$1,043.00**

Table 34. Air-braking System sub-team budget.

Air-Braking System						Total Weight (oz)	Total Cost
For parts that come in larger quantities, cost per is omitted and total cost is overriden with total pack cost. Similarly, custom part costs are given as the total cost of the required stock. For these parts, per part cost is listed as zero. Total costs listed as zero come from stock also used by other parts.						**13.890**	**$299.81**
Component	**Supplier**	**Part No or CAD File**	**Qty.**	**Cost Per Part**	**Total Cost**	**Weight Per Part (oz)**	**Total Weight (oz)**
Top Slotted Plate	Custom	ABPME171227_V2_Channel_Base.prt	1	$0	$22.09	0.000	0.000
Other Sliding Plate	Custom	ABPME171227_V2_Channel_TopPlate.prt	1	$0	$0	0.000	0.000
Drag Tab	Custom	ABPME171227_V2_Drag_Tab.prt	4	$0	$13.61	0.000	0.000
Cross Piece	Custom	ABPME171227_V2_Crossarm.prt	1	$0	$0	0.000	0.000
Drive Shaft	Custom	ABPME171227_V1_Drive_Shaft.prt	1	$0	$11.94	0.000	0.000

Servo Mount Plate	Custom	ABPME180103_V1_Servo_Mount.prt	1	$0	$0	0.000	0.000
Tapped Servo Mount Standoff	Custom	ABPME180103_Servo_Mount_Spacer.prt	4	$0	$6.25	0.000	0.000
Potentiometer Mount	Custom	ABPME180103_Pot_Mount.prt	1	$0	$0	0.000	0.000
32DP 24T Potentiometer Gear	Custom	32DP_24Tooth_20PA_Gear.prt	1	$0	$0	0.000	0.000
Cross Piece Spacer	Custom	ABPME180103_V1_CrossarmSpacer.prt	1	$0	$1.71	0.000	0.000
Tie Rod	Tower Hobbies	LXGFVE	8	$0	$29.99	0.080	0.640
PowerHD 1235MG Servo	Banana Robotics	BR010234	2	$49.99	$99.98	5.820	11.640
0.3125" Clamping Hub	ServoCity	545592	2	$5.99	$11.98	0.000	0.000
0.375" Clamping Hub	ServoCity	545596	1	$5.99	$5.99	0.000	0.000
48T 32DP 20PA Gear	ServoCity	615190	3	$12.99	$38.97	0.300	0.900
P3 R25W Potentiometer	P3 America	R25W-C100-R10K	1	$6.00	$6.00	0.710	0.710
3/8" ID Bronze Bushing	McMaster-Carr	1677K4	2	$1.05	$2.10	0.000	0.000
Retaining Ring for 3/8" Shaft	McMaster-Carr	97633A170	2	$0	$8.74	0.000	0.000
6-32x3/8" Steel Socket Head Screw	McMaster-Carr	91251A146	12	$0	$8.42	0.000	0.000
6-32x3/4" Nylon Socket Head Screw	McMaster-Carr	95868A301	2	$0	$6.07	0.000	0.000
M3x14mm Steel Low Profile	McMaster-Carr	93070A071	8	$0	$6.14	0.000	0.000

Socket Head Screw							
10-32x1.5" Nylon Socket Head Screw	McMaster-Carr	95868A096	4	$0	$6.40	0.000	0.000
10-32x5/8" Nylon Socket Head Screw	McMaster-Carr	95868A090	12	$0	$6.71	0.000	0.000
6-32x1/4" Nylon Flat Tip Set Screw	McMaster-Carr	94564A023	1	$0	$5.48	0.000	0.000
3/32" Steel Square Key	McMaster-Carr	98830A050	1	$0	$1.24	0.000	0.000
Arduino MKR Zero	Arduino		1	$21.90	$21.90	0.332	0.332
ADXL345	Adafruit		1	$17.50	$17.50	0.045	0.045
BMP280	Adafruit		1	$9.95	$9.95	0.046	0.046
Adafruit Li-Ion Battery 3.7 V 2000 mAh	Adafruit	2011	1	$12.50	$12.50	1.199	1.199
Tenergy Li-Ion Battery 7.4 V 2600 mAh	All-Battery	31004	2	$19.99	$39.98	3.492	6.984

Appendix L: Timeline

NDRT 2017-2018 NSL Competition Plan

Legend: ■ Plan ■ Complete ■ In Progress ■ Beyond Plan

Mon Aug 14

ISO WEEK NUM	W33 W34 W35	W36 W37 W38 W39	W40 W41 W42 W43 W44	W45 W46 W47 W48	W49 W50 W51 W52	W1 W2 W3 W4 W5	W6 W7 W8 W9	W10 W11 W12 W13	W14 W15 W16 W17
MONTH	AUG	SEP	OCT	NOV	DEC	JAN	FEB	MAR	APR
(MON)DAY	14 21 28	04 11 18 25	02 09 16 23 30	06 13 20 27	04 11 18 25	01 08 15 22 29	05 12 19 26	05 12 19 26	02 09 16 23

Competition Milestones
- Proposal
- PDR
- PDR Presentation
- CDR
- CDR Presentation
- FRR
- FRR Presentation
- Leading to Competition
- Competition
- PLAR

Team Milestones
- Design Phase
- Construction Phase
- Testing, Integration, and Verification Phase

Test Launch Timeline
- Subscale Test Flight
- Full Scale Test Flight 1
- Full Scale Test Flight 2
- Full Scale Test Flight 3

Vehicle Milestones
- Subscale Design
- Subscale Construction
- Full Scale Design
- Full Scale Construction
- Full Scale Testing

Deployable Rover Payload Milestones
- Design
- Construction
- Testing

Air Braking System Milestones
- Design
- Construction